Title

Development of a Novel Olivetolic Acid Production Platform for the Further Study of the Therapeutic/Pharmacological Effects of Cannabinoids.

Author

Okorafor, Ikechukwu

Publication Date

2023

Peer reviewed|Thesis/dissertation

UNIVERSITY OF CALIFORNIA

Los Angeles

Development of a Novel Olivetolic Acid Production Platform for the Further Study of the Therapeutic/Pharmacological Effects of Cannabinoids.

A dissertation submitted in partial satisfaction of the requirements for the degree Doctor of Philosophy in Chemical and Biomolecular Engineering

by

Ikechukwu Chukwuemeka Okorafor

2023

ABSTRACT OF THE DISSERTATION

Development of a Novel Olivetolic Acid Production Platform for the Further Study of the Therapeutic/Pharmacological Effects of Cannabinoids

by

Ikechukwu Chukwuemeka Okorafor

Doctor of Philosophy in Chemical Engineering

University of California, Los Angeles, 2023

Professor Yi Tang, Chair

Cannabinoids are a large class of bioactive natural products originally derived from the *Cannabis sativa* plant that regulate the cannabinoid receptors CB_1 and CB_2 of the human endocannabinoid system[1]. Cannabinoid based medicines (CBMs) have shown promise as pharmacological agents, acting as antidepressants, analgesics, anticonvulsants, and antiemetics[2]. Cannabinoids have also shown to demonstrate preliminary beneficial therapeutic effects in the treatment of cancer cells[3]. In recent years, there has been significant interest from the synthetic biology community to produce these cannabinoids using microbial and cell-free strategies because of (i) the flexibilities in engineering the pathway to access rare or unnatural cannabinoids, (ii) the challenges associated with chemical synthesis, and (iii) the inconsistent and relatively low production of cannabinoids from plants with microbial production of naturally

occurring and new cannabinoids becoming a growing, disruptive technology to the ~$10 billion global cannabis industry.[4] However, the microbial synthesis of cannabinoids and related molecules requires access to the intermediate olivetolic acid (OA), a major bottleneck in the pathway due to its low production. Whereas plant enzymes have been expressed in *E.coli* and yeast biosynthesis, moderate yields and shunt product formation are major hurdles. Here in, I describe the elucidation of a non-plant biosynthetic pathway using genome mining consisting of fungal tandem polyketide synthases that produces olivetolic acid as well as the related octanoyl-primed derivative sphaerophorolcarboxylic acid (SA) in high titers using the model fungal organism *Aspergillus nidulans*. When compared with the plant pathway production of olivetolic acid, this biosynthetic pathway provides increased production, diversity, and selectivity. This platform can be groundbreaking for the production of cannabinoid-based medicines (CBMs). This platform has potential to not only produce common cannabinoids like Δ^9-tetrahydrocannabionol (Δ^9-THC) and cannabidiol (CBD), but also rare and potentially more potent cannabinoids such as tetrahydrocannabiphorol (THCP), the heptyl alkyl chain version of Δ^9-THC, due to the diversity of analog products produced. Here in, I also describe and detail the methods and results in increasing the titer of this production platform, the expansion of the diversity of products produced through the platform, and the attempt to go downstream to the final elaborated cannabinoid molecules in order to develop a de novo strain that produces a wide variety of cannabinoids. Therefore, in this work, I describe the development of an olivetolic acid platform that represents a new strategy to produce cannabinoid precursors in microbes without relying on plant enzymes, leading to higher titers and a flexible engineering pathway to access rare or unnatural cannabinoids.

The dissertation of Ikechukwu Chukwuemeka Okorafor is approved.

Harold Monbouquette

Neil K. Garg

Junyoung O. Park

Yi Tang, Committee Chair

University of California, Los Angeles

2023

Acknowledgements

I am greatly appreciative of my time here at UCLA and I have so many people to thank for making these past 4.5 years rewarding. First, I would like to thank my advisor Professor Tang for all his guidance and support. Professor Tang accepted me into his lab way past the application deadline and I am grateful that he took a chance on me. Professor Tang has helped me each step of the way along the path to achieve this PhD degree. Through his insight, constructive criticisms, and mentoring, I have become a much better scientist and researcher than when I started and I am truly grateful for that. The lab has very high standards which at first I was a little intimidated by but looking back I understand why the bar was set so high: to properly prepare me for the next phase of my scientific career. I am also grateful for lab dinners, cookouts, retreats, and other lab bonding experiences we have had under Professor Tang's guidance.

I would like to also thank my committee members Professors Harold Monbouquette, Neil Garg, and Junyoung Park and my former committee member Professor James Bowie for their feedback and advice starting from the prospectus through the thesis defense. I appreciated their insightful questions which caused me to think about my project in different ways than I would have originally thought.

Of course, I would like to thank my family, especially my parents who have supported me throughout. This hasn't been an easy 4.5 years, but I could always count on them. They have encouraged me and helped me keep a proper perspective when I felt truly discouraged whether it was through emails, text messages, and phone calls. I am grateful that my father was able to share his own experiences in getting a PhD so that I could better understand the process. I owe so much to them and I am grateful to be their son.

I would also like to acknowledge Professor Chaitan Khosla from Stanford University, my

undergraduate advisor. He played an integral role in my admission to the Tang Lab and UCLA and I am grateful that we still have a professional relationship throughout all these years. Truly a great person.

I am grateful to the Tang lab as a whole with a special shoutout to my mentors Dr. Nicholas Liu and Dr. Mengbin Chen. I learned so much about genome mining from Dr. Nicholas Liu and enjoyed watching Lakers games with him. Dr. Mengbin Chen introduced me to the olivetolic acid production platform project and I am very thankful for her mentorship. I would also like to acknowledge my fellow cohort member Dr. Joshua Misa. I have found the lab to be extremely helpful and a fun group to be around. Grateful for the hangouts, the conversations about science and life, etc.

I would also like to acknowledge my undergraduate Ashley Sun. Ashley Sun was great to be around and a huge help to me. In particular, I remember when I had Covid. Ashley adjusted her schedule to be able to spend more time in the lab and she helped keep things running. Without her, a good amount of work would not be able to be completed. It was great working with her in the lab.

I am grateful also for Dr. Michael Lake, director of the Living Biofoundry at the California NanoSystems Institute at UCLA. His help with regards the Biofoundry and with fluorescent microscopic imaging has been immense and I am truly grateful for our conversations as well.

Outside of the lab and family, a huge thanks goes to Chi Alpha Christian Fellowship and in particular, the pastor of the group, Rachelle Hamilton. Having such a support system has been vital for me here at UCLA and I am extremely grateful for the many people I've met and gotten to develop great friendships with in the fellowship. I would also like to acknowledge my good

friends Laqshya Taneja and Timothy Vernon, fellow engineering grad students. The laughs, great conversations, encouragement, and altogether our friendship has definitely added to my time here at UCLA.

Additionally, a huge thanks to Umu Igbo Unite, Los Angeles. Having a group here in the LA area that helps me connect more to my roots has been really special. I am grateful for all those who I've met and grateful to Amara Sheila Onyiah for introducing me to the group.

Lastly, and most importantly, I'd like to thank the Lord Jesus Christ for guiding my path throughout my time here at UCLA. It has not been easy but He has kept me in His hands the whole time and I praise Him for that. He is truly good all the time.

CV/Vita

Work Experience

University of California, Los Angeles January 2019-June 2023
Doctoral Research Assistant (Yi Tang Lab)

- Helped elucidate through genome mining a novel way to produce olivetolic acid, the first key intermediate in the cannabinoid biosynthetic pathway, from a fungal biosynthetic cluster at high titers providing an alternative way to produce cannabinoids.
- Engineered mutations in the keto-synthase region of the polyketide synthase to produce rare/novel olivetolic acid analogs
- Utilized genome mining to identify homologous fungal clusters that produce olivetolic acid as well as olivetolic acid analogs that can be further processed to form rare or new to nature cannabinoids
- Analyzed samples on single quadrupole LC-MS, triple quadrupole LC-MS, quadrupole time of flight LC-MS, and HPLC.
- Extracted, isolated and purified compounds from fungal cultures and characterized them with NMR to confirm the structure.
- Designed and executed protocols on the ThermoFisher Scientific Laboratory Automation System, a high throughput automation platform, PCR machines, incubators, centrifuge, plate washers, plate readers, etc., to generate plasmids in a highly programmable workflow
- Experience operating and executing protocols on Tecan Liquid Handling System
- Identified a new non plant prenyltransferase that can prenylate the resorcylic acid moiety to form cannabigerolic acid analogs, providing new IP in the field
- Utilized CRISPR tools to engineer a de novo *Saccharomyces cerevisiae* strain that produces rare cannabinoids at much higher titers than the plant.

enEvolv (now Ginkgo Bioworks) Medford, MA
Strain Engineer January 2016- August 2018

- Helped develop and implement a microfluidics-based approach to form emulsion droplets which serve as nanoliter reactors in order to characterize enzyme production. This approach has the ability to sort large library sizes in a short period of time.
- Developed and executed a design of experiments protocol using JMP software that increased transformation efficiency of a hard to transform proprietary gram-positive bacteria by 4 orders of magnitude (from 10^2 CFU/ug to 10^6 CFU/ug)
- Created new strains that improved transformation efficiency, introduced antibiotic resistant markers into strains, and made strains that expressed different genes by
  - Designing and cloning new plasmid vectors and transforming these plasmids into strains
  - Knocking out endonucleases using CRISPR RNA

Columbia University New York, NY
Graduate Research Assistant (Scott Banta Lab) Oct 2014- August 2015

- Worked on a novel way to further optimize an "electrofuels" production process utilizing the chemolithoautotroph bacterium *Acidithiobacillus ferrooxidans*
- Immobilized the bacterium onto three inert supports and grew biofilms. Theorized that by forming the biofilm, the bacteria would begin to use quorum sensing to induce production when nutrients were limited
- Designed own experiments to characterize and analyze electrofuel production by the biofilms.
- Ran experiments in batch and continuous cultures
- Quantified amount of isobutyric acid produced by individual cells

Skills: Plasmid Cloning | Cell Culturing | *E.coli*, Yeast, and Fungal Transformation | Heterologous expression | Genome Mining | Protein Purification | Compound extraction from Fungal and Yeast cultures | LC-MS | HPLC | Tecan Liquid Handling System | ThermoFisher Scientific Laboratory Automation System| JMP (DOE)

Education

UNIVERSITY OF CALIFORNIA, LOS ANGELES Los Angeles, CA
PhD in Chemical Engineering January 2019- June 2023

- NSF BioPacific Fellow
- UCLA Graduate Council Diversity Fellowship Recipient
- NIH Diversity Supplement Grant Recipient

COLUMBIA UNIVERSITY New York, NY
M.S in Chemical Engineering, **GPA: 3.63/4.0** September 2014-August 2015

- National Science Foundation S-STEM SEGUE Scholar

STANFORD UNIVERSITY Stanford, CA
B.S. in Chemical Engineering, **GPA: 3.34/4.0** September 2010-June 2014

- Dean's Award for Academic Excellence
- Co-founder of Stanford Women's Friends and Alumni Network (FAN) now called Stanford Alumni Women's Impact Network

Certifications: Certificate of Safety Achievement (Safety and Chemical Engineering Education (SAChE) and American Institute of Chemical Engineers (AIChE))
Publications: Okorafor, I., Chen, M., Tang, Y. “High-Titer Production of Olivetolic Acid and Analogs in Engineered Fungal Host Using a Nonplant Biosynthetic Pathway” 2021, *ACS Syn. Biology* 10, 2159-2166

Table of Contents

1. Introduction and History of Cannabinoids

Cultivation of the cannabis plant has been traced to around 10000 BC with the first evidence of the plant being found in China.[5] It is a plant long thought to have therapeutic properties and was used by the Chinese for medicinal purposes. Indians also attributed therapeutic properties to cannabis and greatly used it, dating back to 1000 BC, as an antispasmodic, appetite stimulant, antiparasitic, anesthetic, anticonvulsant, antibiotic, hypnotic, analgesic, diuretic, digestive, and aphrodisiac among even more other treatments.[6,7] The Sheng-nung Pen-Ts'ao Ching, known as the earliest Chinese materia medica book mentioned this about cannabis: *"ma-fen (the fruit of cannabis)... if taken in excess will produce visions of devils over a long term, it makes one communicate with spirits and lightens one's body*."[8] This was the first written record of cannabis having psychoactive activities. William B. O'Shaughnessy, a 19th century Irish physician used cannabis as a treatment for tetanus and various other convulsive diseases, introducing the plant to Western medicine.[9] Other physicians in that time period also tested the plant for the treatment of mental disorders. Therefore, interest in the therapeutic properties of cannabis has a long history. However, prohibition and federal legal restriction of the plant have greatly hindered the study of it therapeutic effects.

There are over 400 known compounds form the *Cannabis sativa* plant, with more than 104 of them labeled as cannabinoids.[10] The rest of the compounds include nitrogenous compounds, flavonoids, terpenoids, and other more common plant molecules. Cannabinoids from the *Cannabis sativa* plant are also known as phytocannabinoids. The cannabinoids act on cannabinoid receptors, part of the endocannabinoid system in the body that regulates the neurotransmitter release in the brain.[11] Of the cannabinoids, the most common are delta-9

tetrahydrocannabinol (Δ^9-THC) and cannabidiol (CBD). In the cannabis plant, the cannabinoids are mainly found as their carboxylic precursors which can then be decarboxylated in the presence of heat and light.[12] (Figure 1) Both CBD and Δ^9-THC are synthesized in the glandular trichomes of the plant. These glandular trichomes are only present in the female plant; therefore, cannabinoids can only be produced from the female *Cannabis sativa* plant.[13] The cannabis plant is classified into three categories, primarily based on the Δ^9-THC concentration: industrial hemp where Δ^9-THC does not exceed 15 percent dry weight, intermediate type with near equal amounts of both Δ^9-THC and CBD and the Δ^9-THC type also known as the drug type, having primarily Δ^9-THC.[14]

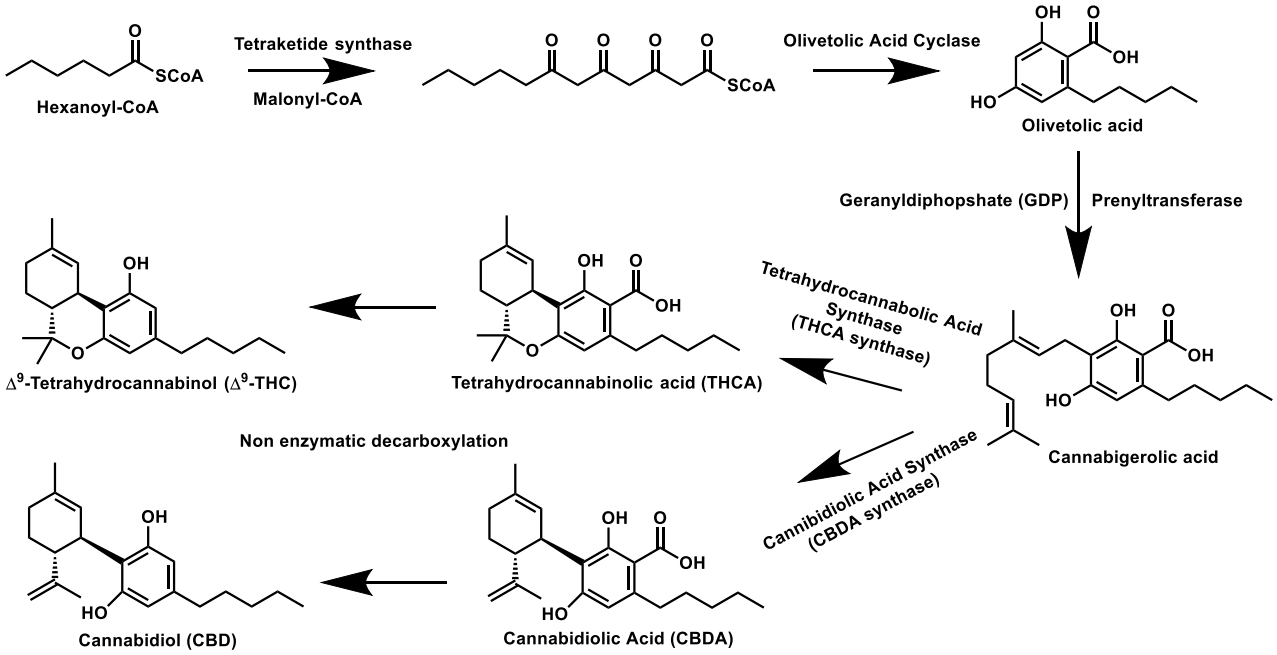

Figure 1. Cannabinoid biosynthetic pathway. Tetraketide synthase (TKS) and Olivetolic Acid Cyclase (OAC) convert the hexanoyl-CoA starter unit to olivetolic acid. A dedicated prenyltransferase then geranylates the C6 position of the olivetolic acid to form cannabigerolic acid (CBGA). Then, two dedicated oxidocyclase enzymes convert CBGA to THCA and CBDA. Non enzymatic decarboxylation removes the carboxyl groups from the cannabinoid acids to form the well-known cannabinoids Δ^9-THC and CBD.

1.1 Cannabinoid Receptors

Both Δ^9-THC and CBD act on cannabinoid receptors which were first elucidated in the 1980s by scientists William Devane and Allyn Howlett. They demonstrated that Δ^9-THC synthetic mimics were able to bind to a specific site in the membranes of the brain, inhibiting synthesis of cyclic adenosine monophosphate (cAMP) through a G-protein mediated mechanism. Furthermore, molecular cloning of the first cannabinoid receptor gene as well as brain mapping of the cannabinoid binding sites in rats confirmed the existence of the cannabinoid receptor in the brain, known as the CB_1 receptor.[15] The cannabinoid receptors are part of a larger family of receptors known as G-protein coupled receptors (GCPRs). G-protein coupled receptors total about 800 in number and are divided into five major families: secretin, frizzled/taste 2, adhesion, glutamate, and rhodopsin.[16] Majority of GCPRs including CB_1 and CB_2 belong to the rhodopsin-like family.[17] Rhodopsin is a pigment found in the rod photoreceptor cells of the retina and its role is to change photons into chemical signals, allowing vertebrate animals and humans to sense light by stimulating cellular biological processes in these organism's central nervous systems.[18] With regards to structure, GCPRs contain a transmembrane unit harboring seven alpha-helices conjoined with a G-protein that itself has three subunit proteins: $G\alpha$, β, and γ.[17] Once an agonist binds to the GCPR transmembrane domain, the G-protein subunits conjoin with another cellular protein such as a protein kinase or adenyl cyclase to catalyze downstream functions.[19] GCPRs role in regulating functions in the cells is so important that drugs targeting GCPRs make up 30-40% of all the drugs in the market.[20]

The CB_1 receptor's discovery was in 1984 through the observation that cannabinoid

binding to the receptors reduced cyclic adenine monophosphate (cAMP) concentrations in neuroblastoma cells.[21] Two years later, work was done to demonstrate that the cAMP concentration reduction by cannabinoid binding could be reversed through the exposing of the cells to the pertussis toxin, a Gαi protein inhibitor.[22] However, it wasn't until 1990 that the CB_1 receptor was cloned and elucidated from a cDNA library of cerebral cortex tissues with studies that same year demonstrating that CB_1 receptors in the brain were nearly as prevalent as gamma-aminobutyric acid (GABA) receptors and glutamate receptors.[23,24] The prevalence of CB_1 receptors and their localization in the brain allowed researchers to correlate their expression to the subsequent pharmacological effects. For example, localization and expression of CB_1 in the hippocampus and cerebral cortex correlated to memory and cognition effects whereas localization and expression of CB_1 in the cerebellum and basal ganglia was correlated to stride or gait effects.[17] Therefore, binding of the CB_1 receptors in the brain correlates to the psychoactive effects of cannabis. Although CB_1 receptors are prevalent in the brain, they also have been found to be located in the uterus, prostrate, adrenal glands, tonsils, gastrointestinal tract, spleen, and vascular smooth muscle cells.[25]

The discovery of the CB_2 receptor answered the question of why cannabis was reported to have immunomodulatory effects. The CB_2 receptor was discovered three years after the CB_1 receptor and was found in a human promyelocytic leukemia cell line.[26] Unlike the well characterized CB_1 receptor, CB_2 has not been as well as characterized due to numerous conflicting reports about the effects of its expression but one thing is known for sure: the CB_2 receptor plays a strong role in immunomodulatory effects with great implication for example, in Alzheimer's and Huntington's disease.[27,28] The CB_2 receptor is known as the peripheral receptor for cannabinoids and is primarily found and expressed in immune tissues.[26]

When these cannabinoid receptors are activated, as previously mentioned with regards to CB_1, there is a decrease in cAMP levels and there is also modulation of potassium and calcium levels in the cells.[11] When these receptors are stimulated, p38 mitogen activated protein kinases (MAPKs), c-Jun N-terminal kinases, and p42 and p44 MAPKs are activated. The p42/44 MAPKS are also referred to as extracellular signal regulated kinases 1 and 2 (ERK1 and ERK2) and they are involved in transcription regulation, cell differentiation, downstream regulation of genes, and cytokine synthesis regulation.[29,30] Both cannabinoid receptors (CB_1 and CB_2) utilize the transducing G proteins, G_1 and G_o, responsible for a wide range of cellular functions such as response to environmental stimuli and responses to hormonal signals.[31] Δ^9-THC binding to these receptors causes the opening of potassium channels, inhibition of adenylyl cyclase activity, closing of voltage gated calcium channels, and stimulation of mitogen-activated protein kinases, among other responses.[17]

The characterization of these cannabinoid receptors in human signaled to researchers that there are likely some endogenous ligands capable of binding to these receptors. These ligands are part of the endocannabinoid system and include anandamide (AEA) which was found to produce similar effects as the cannabinoids from *Cannabis sativa*, O-arachidonoyl ethanolamine, and 2-arachidonoylglycerol (2-AG), and 2-arachidonoyl glycerol ether.[17]

Additionally, reports have been made indicating that cannabinoids have been able to bind to other receptors in the body outside of CB_1 and CB_2. Cannabinoids have been found to be capable of binding to the transient receptor potential cation channel vanilloid type 1 (TRPV2), 5-hydroxytryptamine (5-HT)-3A ligand-gated ion channel, G-protein-coupled receptor 55 (GPR55), 5-hydroxytryptamine (5-HT)-3A ligand-gated ion channel, and transient receptor

potential cation channel Ankyrin type 1 (TRPA1).[32,33]

1.2 Therapeutic Potential of Cannabinoids

Both Δ^9-THC and CBD were isolated from the hemp oil plant in the 1940s[34,35]. Unlike Δ^9-THC, CBD has no psychoactive properties and has low affinity to both CB_1 and CB_2 receptors, whereas Δ^9-THC binds effectively to the CB_1 receptor. Although CBD has low binding affinity to the endocannabinoid receptors, there is some data that indicates that CBD has some beneficial properties in the treatment of seizures and epilepsy, movement disorder, psychosis, anxiety, multiple sclerosis, and Huntington's disease,[36] once again highlighting the therapeutic potential of cannabinoids.

The therapeutic potential of cannabinoids has led to the development of cannabinoid-based medicines (CBMs). Currently, in the United States, there are 3 licensed CBMs approved by the Food and Drug Administration: nabilone (cesamet®) , a synthetic analog of Δ^9-THC, used as an antiemetic, preventing vomiting and nausea caused by cancer medications, dronabinol, synthetic Δ^9-THC , used to treat lack of appetite leading to weight loss in AIDS victims as well as treat nausea and vomiting like nabilone, and a liquid formulation of dronabinol. (Figure 2) The FDA has also placed on the fast track a few more CBMs and has also approved investigational drug studies of CBD due to its ability to treat chronic pain and help prevent seizures in childhood epilepsy cases. All in all, the global pharma cannabinoid industry is projected to exceed $102 billion by 2030 indicating a significant interest in the development of CBMs[37]; therefore, methods for the efficient large-scale production of cannabinoids are necessary.

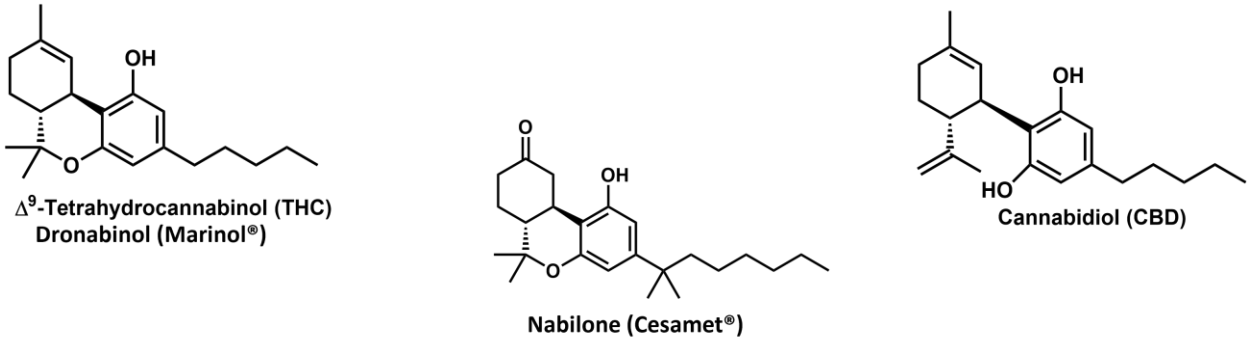

Figure 2. Cannabinoid based medicines (CBMs). Nabilone, an antiemetic and Dronabinol, used to treat lack of appetite in AIDs victims have been approved by the FDA while CBD has been fast tracked for further investigational studies.

1.3 Microbial Efforts to Produce Cannabinoids

In recent years, there has been significant interest from the synthetic biology community to produce cannabinoids using microbial and cell-free strategies because of (i) the flexibilities in engineering the pathway to access rare or unnatural cannabinoids, (ii) the challenges associated with chemical synthesis, and (iii) the inconsistent and relatively low production of cannabinoids from plants.[4] Owing to the identification of important enzymes in the cannabinoid biosynthesis pathway such as olivetolic acid synthase (OLS) and olivetolic acid cyclase (OAC), which converts hexanoyl-CoA to olivetolic acid, microbial hosts have been utilized to produce cannabinoids.[38] Another key finding was the discovery of the prenyltransferase responsible for prenylating olivetolic acid with geranyl to form cannabigerolic acid (CBGA).[39] (Figure 1)

With these key enzymes identified, different groups have attempted to microbial produce cannabinoids and their precursors. Tan et al., employing olivetolic acid synthase and olivetolic acid cyclase from the *Cannabis sativa* plant in addition to further engineering, were able to produce 80 mg/L of olivetolic acid from *E. coli.*[40] To date, that is the highest literature recorded

amount of olivetolic acid produced *in vivo* in any wild type or engineered organism. Additionally, Luo et al. were able to express the entire cannabinoid pathway in *Saccharomyces cerevisiae* and produce 8 mg/L of tetrahydrocannabinolic acid (THCA), the direct Δ^9-THC precursor, and 4.3 ug/L of cannabidiolic acid, the direct CBD precursor; this was the first time that Δ^9-THC and CBD were produced by yeast.[41] Furthermore, Valliere et al., utilizing commercial olivetolic acid and the synthetic biochemistry approach of cell-free systems, showed that they were able to produce 1.25 g/L of cannabigerolic acid (CBGA), by engineering an aromatic prenyltransferase from *Streptomyces sp*. CL190 to efficiently prenylate olivetolic acid, another important intermediate in the cannabinoid biosynthesis platform.[42] Additionally, Jimbo Ma et al engineered the yeast *Yarrowia lipolytica* to improve the biosynthesis of olivetolic acid and achieved an 83 fold titer increase giving a final titer of .11 mg/L.[43]

E.coli and yeast strains have not been the only microbial organisms utilized to produce olivetolic acid and cannabinoids. Two groups have demonstrated that amoeba can also be engineered for the production of olivetolic acid. Reimer et al. engineered *Dictyostelium discoideum*, due to its ability to produce polyketides and terpenoids, to ultimately produce olivetolic acid. By fusing the OLS to the C-terminal of the *D. discoideum* StII gene , they were able to engineer an amoeba/plant hybrid gene for the production of olivetolic acid. The group utilized the StII gene, an enzyme consisting of a type III PKS and FAS and swapped the type III PKS domain with OLS and overexpressed this fused hybrid gene to produce olivetolic acid.[44] Kufs et al also utilized *Dictyostelium discoideum* to produce olivetolic acid , developing a scaled approach in bioreactors able to achieve a titer of 4.8 µg/L.[45] Although novel with the use of *Dictoystelium discoideum* to produce this cannabinoid intermediate, such a result underscores the need to increase production of olivetolic acid. To date, these approaches for the production of

olivetolic acid and cannabinoids all rely on the plant pathway with the enzymes olivetolic acid synthase (OAS) and olivetolic acid cyclase (OAC) catalyzing the formation of olivetolic acid from hexanoic acid and have heavy intellectual property surrounding them so a novel way of producing olivetolic acid is preferred. We were able to discover a novel pathway to olivetolic acid by focusing on fungal natural product biosynthetic pathways, a vast field with promising capabilities.

2. Elucidation of a Novel Olivetolic Acid Platform Through Genome Mining

2.1 Fungal Natural Products and Genome Mining

Natural products from fungi have demonstrated great therapeutic and agricultural potential[46,47] with two of the currently used antifungal drugs being the natural products echinocandins and amphotericin[48]. Echinocandins, referred to as the "penicillin of antifungals"[49], and amphotericin are also included in the World Health Organization's List of Essential Medicines[50], showcasing the powerful potential of fungal natural products. Natural products, also referred to as secondary metabolites, are most times not essential for the organism's life but do still have important roles such as acting as metal-transporting agents, symbiosis facilitators, sexual and differentiation effectors, and metal-transporting agents, among other functions.[51] Fungi produce a vast variety of natural products that can be classified as terpenes, polyketides, sugars, and alkaloids.[52] There are 100,000 known fungal species, although upwards of one million fungal species are expected to be in existence.[53] Of the known 100,000 fungal species, only a fraction of their natural products and biosynthetic pathways have been elucidated.[54] Therefore, there is great potential to search for more fungal natural products with interesting

bioactivities, underscoring the importance of genome mining.

Genome mining is utilized to search for and identify biosynthetic gene clusters.[55] These biosynthetic pathways encode secondary metabolite genes that produce natural compounds. Genome mining has been used to search for biosynthetic pathways for known products as well as undiscovered biosynthetic pathways that can produce novel natural products. Genome mining answers the question of how natural products are formed. It describes the utilization of genomic information to search for biosynthetic gene clusters responsible for producing natural products. Over the years many different methods of genome mining have been developed. Among them include classical genome mining, comparative genome mining, phylogeny-based genome mining, and resistance gene/target directed genome mining.

Classical genome mining involves the search for genes involved in a biosynthetic pathway. Typically, the process consists of querying for a desired gene across many genomes and then querying for that gene in the context of a biosynthetic gene cluster. NCBI Basic Local Alignment Search Tool (BLAST) is widely utilized for classical genome mining.

Comparative genome mining involves comparing multiple genomes in different organisms to identify similar clusters.[56] It differs from classical genome mining in that instead of searching for single genes, one is searching for partial or whole gene clusters across various genomes. Gene clusters in a genome are then prioritized based on their homology to other clusters in other organisms' genomes.

Phylogeny-based genome mining is based on the understanding of the mostly modular structure of biosynthetic gene clusters.[53] It is theorized that this mostly modular structure comes from a quickly evolving defense system where new molecules are produced by randomly swapping and shuffling domains and modules.[57] As an example, the program Natural Product

Domain Seeker (NaPDoS), constructs a phylogenic tree based on ketosynthase (KS) domains and condensation (C) domains of PKS and NRPS genes, respectively[58]. KS and C domains are two of the enzyme families used to construct phylogenic trees in order to predict compound structures.[59,60] This phylogenic tree can be utilized to give information about the function of the PKS and NRPS gene searched for, its evolutionary history, and the novelty of products produced in the secondary metabolite cluster containing the gene.

Lastly, resistance gene directed genome mining and target directed genome mining involve identifying biosynthetic gene clusters that contain self-resistance genes. For organisms that produce antibiotics or antifungals, there needs to be a development of a self-resistance method to avoid suicide.[61] One self-resistance mechanism is the use of efflux pumps to transport the compounds to extracellular space.[62] Another self-resistance mechanism involves the inclusion of self-resistance enzymes (SREs) in biosynthetic gene clusters. These SREs are mutated copies of the housekeeping target that retain activity and are not inhibited by the natural product produced, thereby keeping the organism alive.[63] These SREs are typically found in secondary metabolite clusters. Therefore, an approach searching for these SREs can be developed to find biosynthetic gene clusters. Utilizing this knowledge, Moore et al. were one of the first groups to utilize a targeted genome mining approach. They screened for housekeeping copies of genes in 86 similar strains of *Salinospora* and screened for location near biosynthetic gene clusters. They identified the second copy of a bacterial fatty acid synthase colocalized within a cluster that contained a PKS-NRPS hybrid gene. They annotated the cluster, heterologously expressed the genes, and after chemical characterization, elucidated that the cluster produced thiolactomycin, which is a fatty acid synthase inhibitor.[64] To demonstrate its capabilities, target directed genome mining has been used to locate biosynthetic gene clusters

(BGCs) with known biomolecular targets[65], for (re)discovering natural products with desired biomolecular targets[66], and for discovering the biomolecular targets of known natural products.[67] Therefore, searching for resistance enzymes in a secondary metabolite cluster has become an increasingly appealing genome mining approach for finding new clusters and subsequently, novel natural products.

In recent years, tools and programs have been developed to search for new biosynthetic clusters more quickly. These programs have the ability to predict the entire secondary metabolite gene cluster. Antibiotics and Secondary Metabolite Analysis Shell (antiSMASH) is one of these programs. antiSMASH identifies polyketide synthase (PKS)and non-ribosomal peptide synthetase (NRPS) core genes in potential clusters and then outputs the cluster information in a user-friendly interface that can be readily searched through[68]. Secondary Metabolite Unknown Regions Finder (SMURF) is another one of these programs. SMURF evaluates secondary metabolite gene clusters by scoring the nearness of core genes with the different tailoring genes near the core gene.[69] Additionally, there is another program that is more specified in its search called Antibiotic Resistance Target Seeker (ARTS). ARTS specifically queries for antibiotic resistance genes in bacteria that can lead to biosynthetic gene clusters for possible novel drug targets.[70] We utilized antiSMASH to elucidate the non-plant olivetolic biosynthetic pathway.

2.2 Resorcylic Acid Lactones

Since its inception, the Tang lab has utilized various methods of genome mining to identify many natural products and novel enzymes, as well as elucidate the biosynthetic pathways of natural products in addition to the production of novel natural products through the engineering of biosynthetic genes. (Figure 3) One such example is the further characterization of

the biosynthetic pathway of zearalenone, a member of the resorcylic acid lactone family of products produced from the fungal species *Gibberella zeae,* and production of novel resorcylic acid lactones (RALs) achieved through the reconstitution of the polyketide synthase (PKS) involved in the biosynthesis of zearalenone.[71] RALs are polyketides, exclusively produced by fungi, consisting of a macrolactone ring with a 2,4-dihydroxybenzoic acid moiety embedded.[72] The first discovered RAL, radicicol was characterized from the fungal species *Monocillium nordinii* in 1953, with 200 more RALs having been identified from a variety of fungal species since then.[73,74]

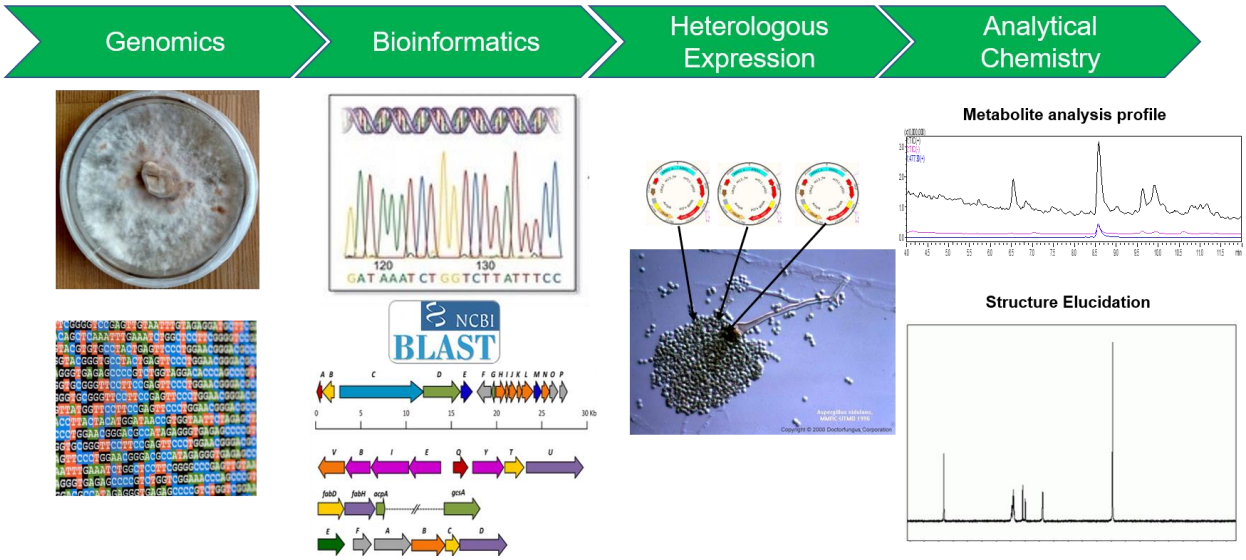

Figure 3. Pathway for Elucidation of Biosynthesis of Natural Products. The process for the elucidation of natural products and their biosynthetic pathway in the Tang lab. Starts from genomics, proceeds to bioinformatics, then to heterologous expression, and finally to analytical chemistry.

RALs are potent molecules that exhibit of variety of biological activities including having antimalarial, anti-cancer, anti-microbial, mitogen activating protein (MAP)-kinase inhibitor, TAK1 inhibitor, heat shock protein inhibitor, and estrogen receptor against properties.[71,75] (Figure 4) Many RALs consist of 14 membered lactone rings, although there also exists RALs

consisting of 10, 12, and 16 membered lactone rings.[69] The RAL biosynthetic gene cluster typically consists of two polyketide synthases: a highly reducing polyketide synthase (HRPKS) and a non-reducing polyketide synthase (NRPKS). Regarding the biosynthetic pathway of RALs, the HRPKS generates the terminal hydroxyl group that becomes the macrocyclizing nucleophile. The chain is then transferred to the NRPKS where it is further elongated and then goes through aldol cyclization to form the enzyme bound resorcylic thioester. A fused thioesterase (TE) domain in the NRPKS then performs macrocyclization to release the final RAL product. Furthermore, considerable structural diversity at the C_6 position of the RAL can be generated by utilizing different HRPKSs that are able to synthesize a variety of reduced products.[76,77,78]

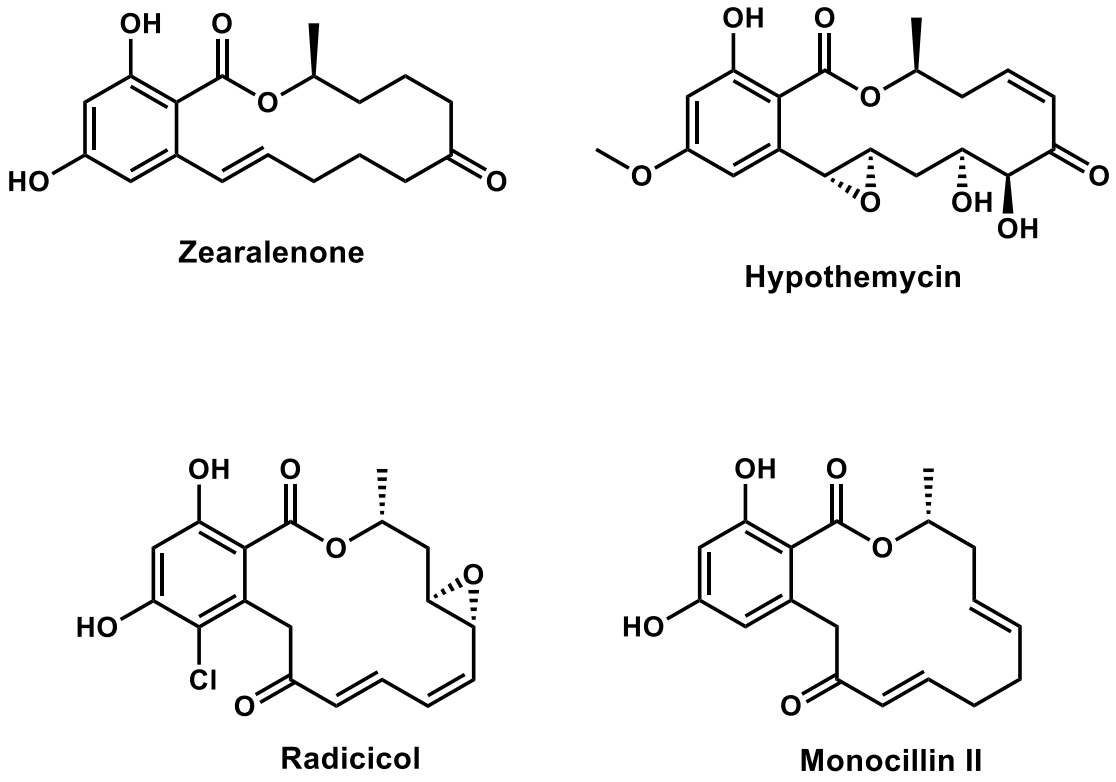

Figure 4. Examples of Resorcylic Acid Lactones. These polyketides consist of a 12, 14, or 16-membered macrolactone ring with a β-resorcylic acid embedded.

2.3 Polyketide Synthases

Taking it a step back, fungal polyketide synthases are enzymes designed to synthesize polyketides through the interactive condensation of malonyl coenzyme A (malonyl-CoA) building blocks.[79] Fungal polyketide synthases are type I polyketides synthases. These interactive polyketide synthases are large and contain multiple domains. There are three categories of polyketide synthases: type I, type II and type III.

2.3.1 Type I Polyketide Synthases

Type I polyketide synthases contain multiple functional and catalytic domains, generating most of the polyketides that have been characterized.[80] Furthermore, type I polyketide synthases are divided into two separate categories: iterative type I and modular type I. Modular type I polyketide synthases are more commonly found in bacteria. They are large multimodular enzymes having assembly line like characteristics, condensing acyl substrates module by module, where the order of the module defines the order of the functional groups of the final elaborated compound.[81] Iterative type I polyketide synthases, more commonly found in fungi, contain a single multidomain, and iteratively use the domain, similarly to fatty acid synthases (FASs) operate, to generate the programmed polyketide product.[82]

2.3.2 Type II Polyketide Synthases

Type II polyketide synthases are similar in operation to type I iterative polyketide synthases; however, instead of being a megasynthase like type I PKSs, type II PKSs are separate enzymes that are monofunctional. Aromatic bacterial polyketides are typically synthesized by type II PKSs.[83] Whereas type I PKSs use acetyl-CoA and malonyl-CoA as starter units, type II PKSs typically utilize acetate as their starter unit. Minimally, type II PKS contain a KS_{α} subunit,

a chain length factor (CLF or KS_β) subunit, and an ACP subunit.[84] Type II PKSs are the least characterized PKSs of the three.

2.3.3 Type III Polyketide Synthases

Type III polyketide synthases are found in plants , although a few have been elucidated from microbes, and are much smaller than type I and type II PKSs.[85] They are homodimers of ketosynthases; therefore, they extend chain length through iterative decarboxylative Claisen condensation and are responsible for producing compounds such as stilbene, flavonoids, and alkylresorcinols from plants.[86] Type III PKSs release their products to either the active site cysteine of the enzyme or the carrier molecule, coenzyme A. There have also been reports of Type III PKSs utilizing an acyl carrier protein bound substrate as the starter substrate, similar to type I and type II PKSs.[87]

Since our platform utilizes two type I iterative polyketide synthases, it is appropriate to go into more detail concerning these megasynthase enzymes. Fungal PKSs resemble bacterial type II PKSs in that the catalytic domains of both classes of enzymes are iteratively utilized during polyketide synthesis and resemble bacterially type I modular PKSs in that the catalytic domains of both fungal PKSs and bacterial type I modular PKSs are linearly arranged.[88] However, fungal PKSs differ from bacterial type I modular PKSs in rules dedicated to chain elongation, regioselective cyclization, and starter-unit selection[89,90,91,92] There are three types of fungal polyketide synthases: highly reducing polyketide synthases (HRPKS), partial reducing polyketide synthases (PRPKS), and nonreducing polyketide synthases (NRPKS)

2.3.4 Highly Reducing Polyketide Synthases

HRPKSs generate highly reduced compounds that can be furthered modified to produce compounds such as lovastatin. Fungal HRPKS domains contain, minimally, a ketosynthase (KS) domain, a malonyl-CoA: acyl carrier protein transacylase (MAT) domain, and an acyl carrier protein (ACP) domain. These HRPKSs also contain tailoring domains such as an enoyl reductase (ER) domain, a dehydratase (DH) domain, a methyltransferase (MT) domain, and a ketoreductase (KR) domain. These domains are interactively utilized to produce the reduced polyketide product, with the HRPKS employing the tailoring domains in different arrangements for each extension cycle.[76]

2.3.5 Partially Reducing Polyketide Synthases

PRPKSs typically synthesize phenolic aromatic compounds such as 2,4-dihydroxybenzene and 6-methylsalicylic acid (6-MSA). As their name implies, these enzymes utilize their iterative domains to generate partially reduced polyketide compounds. The ketoreductase domain is the key domain controlling the reductive programming in PRPKSs, through judicious reduction of the polyketide compounds.[93] 6-MSA is a perfect example of this, with the PRPKS responsible for producing 6-MSA undergoing just one round of reduction by the KR domain and one round of dehydration by the DH domain.[94]

2.3.6 Nonreducing Polyketide Synthases

NRPKSs, similar to HRPKSs and PRPKSs, minimally contain KS, AT, and ACP domains. Separate from the other two polyketide synthase types, however, NRPKSs also harbor a starter unit: acyl carrier protein transacylase (SAT) domain that takes up the starter unit, and a product template (PT) domain which acts as an aldol cyclase. They also may contain a methyltransferase domain and usually contain a domain for product release such as a thioesterase (TE) domain. The

SAT domain's role is to take up the starter unit, and to transfer the starter unit onto the ACP domain where it is moved to the KS domain, undergoing decarboxylative Claisen condensation with an extender unit transferred from the AT domain[95]. An example of a starter unit would be a malonyl-CoA unit or if in conjunction with a HRPKS, the product produced from the HRPKS. Iterative use of these domains of the NRPKS extend the chain and the PT domain cyclizes the product and then the product is programmed for release by the releasing domain.

2.4 Comparison Between Resorcylic Acid Lactones and Cannabinoids

All the RALs elucidated contain the 2,4-dihydroxybenzoic acid moiety otherwise known as the β-resorcylic acid moiety, the same moiety comprising the core of tetrahydrocannabinol, cannabidiol, cannabigerol, and the rest of the cannabinoids from the *Cannabis sativa* plant. (Figure 5) Furthermore, the first key intermediate in the cannabinoid biosynthetic pathway is olivetolic acid, a β-resorcylic acid with a pentyl alkyl chain at the C_6 position. Olivetolic acid is found in small quantities in *Cannabis sativa* extracts; therefore, this key intermediate is expensive. Additionally, although not fully studied for its biological activity, it is proposed to have antimicrobial, photoprotective, and cytotoxic activities.[96] Due to the similarities between olivetolic acids and RALs which the Tang lab is quite familiar with, we hypothesized that fungal biosynthetic pathways containing a tandem PKS pair may be able to produce olivetolic acid or related molecules that vary in the C_6 position chain length and saturation. Therefore, we hypothesized that, by using genome mining to look for tandem fungal polyketide synthases, we could find a biosynthetic gene cluster in fungi that produces olivetolic acid.

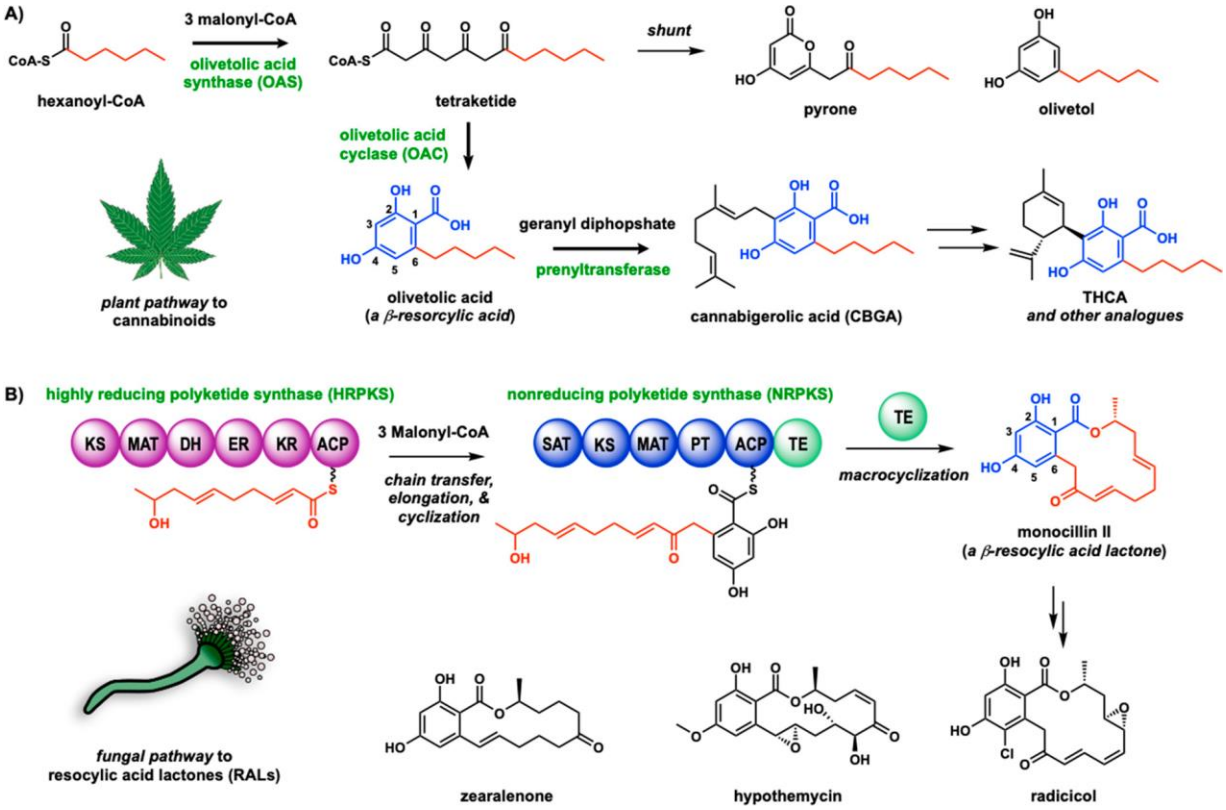

Figure 5. Resorcylic Acid Natural Products Produced from *Cannabis sativa* and from Fungi. (A) *C. sativa* cannabinoid biosynthetic pathway. The β-resorcylic acid, olivetolic acid (OA), is produced from the olivetolic acid synthase (OAS) and olivetolic acid cyclase (OAC). OA is processed to the final products THCA and analogues. In the absence of OAC, side products (pyrone and olivetol) emerge. (B) Tandem fungal iterative polyketide synthases produce resorcylic acid lactones.

2.5 Identification of Potential OA Producing Pathways in Fungi.

The terminal TE domains in the NRPKSs that produce RALs are responsible for the macrocyclization reaction. In order to produce resorcylic acid instead of RALs, the releasing enzyme must catalyze a hydrolysis reaction instead of esterification. In fungal PKSs, TEs that catalyze hydrolytic release have been characterized and are typically free-standing enzymes.[97] With this in mind, we performed genome mining of sequenced fungal genomes for biosynthetic gene clusters that encode a HRPKS, a NRPKS, and a standalone TE. Among the

clusters identified by antiSMASH,[98] one set of homologous clusters satisfied this particular criterion (Figure 6A).

The *ova* cluster from *Metarhizium anisopliae* encodes a typical HRPKS (Ma_OvaA) and a NRPKS (Ma_OvaB) that is not fused to a terminal TE domain. Instead, a didomain enzyme Ma_OvaC containing an *N*-terminal ACP and a *C*-terminal TE is present in the cluster. Further sequence analysis of the ACP domain showed the well-conserved DSL triad in all functional ACPs, in which the serine is post-translationally phosphopantetheinylated, is mutated to NQI.[99,100,101] This suggests the ACP domain is unlikely to carry out the canonical function of acyl chain shuttling, thus the enzyme is designated as a ψACP-TE. Previously, a ψACP-methyltransferase (MT) fusion enzyme was found in a fungal PKS pathway, in which the ψACP facilitates protein-protein interactions between the NRPKS and the ψACP- MT to enable methylation of the growing polyketide intermediate.[102] Hence, we hypothesize the ψACP domain in Ma_OvaC may have a similar role in facilitating the catalytic function of the TE domain on a PKS-bound intermediate. The *M. anisopliae* cluster contains additional genes encoding a transcriptional factor and a flavin-dependent monooxygenase. Alignment of homologous clusters from various fungal species (*Metarhizium rileyi*, *Talaromyces islandicus*, and *Tolypocladium inflatum*) showed that HRPKS, NRPKS, and ψACP-TE are conserved (Figure S1), including the inactivated ACP triad (Figure 6A). None of these clusters have been characterized and no product has been reported in the literature. Based on these analyses, we predict that the trio of HRPKS, NRPKS, and ψACP-TE will make resorcylic acids that are structurally related to OA.

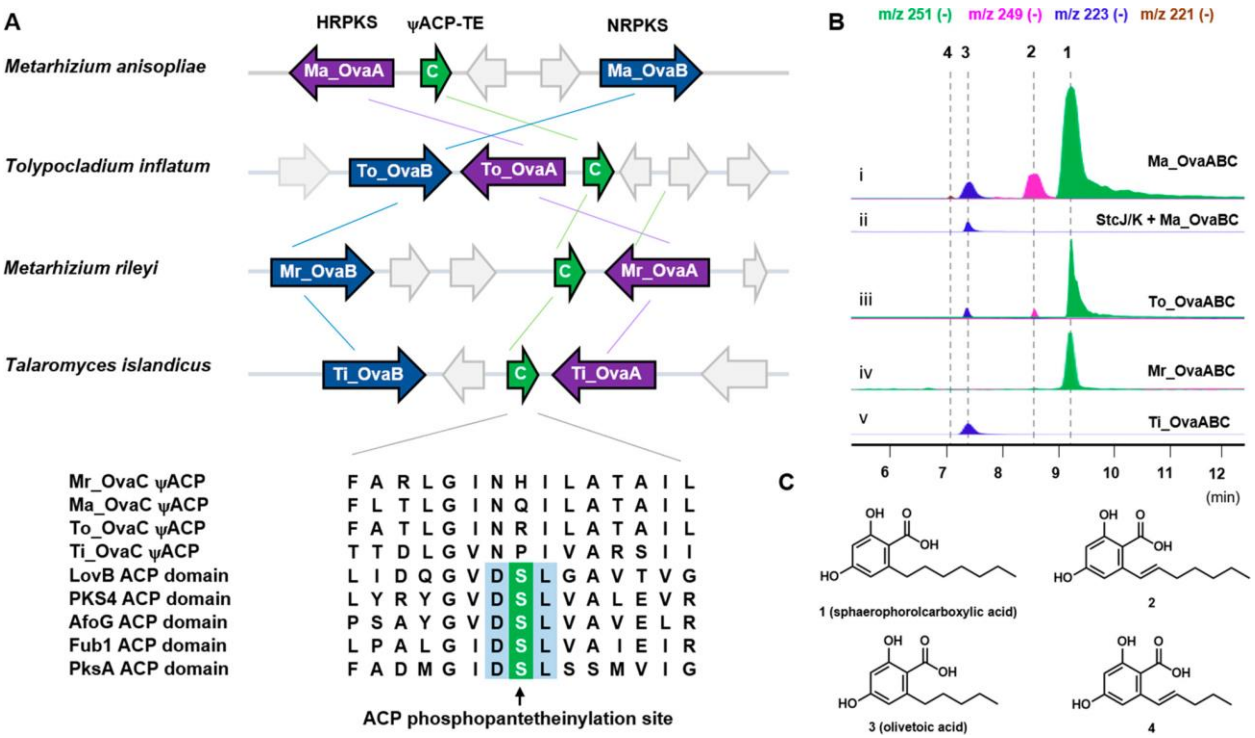

Figure 6. **Genome Mining of Microbial Clusters that can Synthesize Olivetolic Acid and Related Compounds.** (A) Homologous clusters were elucidated through genome mining of the ψACP-TE gene. All of the homologous clusters found contained an HRPKS, an NRPKS, and a ψACP-TE. Functional ACPs contain the hallmark DSL sequence, where the serine is post-translationally modified with phosphopantetheine (pPant) and is therefore activated to shuttle the acyl chain. Because the ψACP sequences do not have that serine residue, they cannot be post-translationally modified with pPant and are therefore proposed to be inactive. (B) LC-MS traces of *Aspergillus nidulans* expressing different biosynthetic clusters and combinations of genes. (i) Heterologous expression of Ma_OvaABC from *M. anisopliae* produced compounds **1**–**4**. (ii) Combinatorial biosynthesis of OvaBC with StcJ and StcK fatty acid synthase from *A. nidulans* selectively produced OA. (iii) Heterologous expression of To_OvaABC from *T. inflatum* produced compounds **1**–**3**. (iv) Heterologous expression of Mr_OvaABC from *M. rileyi* primarily produced compound **1**. (v) Heterologous expression of Ti_OvaABC from *T. islandicus* selectively produced compound **3**. (C) Structures of compounds **1**–**4**.

To examine the product profile of the *ψ*ACP-TE containing pathways, we heterologously expressed Ma_OvaA, B, and C in the model fungus *Aspergillus nidulans* A1145 ΔSTΔEM strain.[103] This strain has been used in reconstitution of fungal biosynthetic pathways, and contains genetic deletions that inactivated biosynthesis of endogenous metabolites sterigmatocystin and emericellamide B.[102] Each of the three genes was cloned into separate

episomal vectors, transformed into *A. nidulans*, and the resulting transformants were grown on CD-ST agar plates (see Methods). Following 5 days of growth in CD-ST, the sample media were extracted and analyzed by liquid chromatography-mass spectrometry (LC-MS).

Coexpression of Ma_OvaA-C in *A. nidulans* produced four metabolites **1**-**4** (Figure 6B). The molecular weights (MWTs) as indicated by LC-MS for these compounds are **1**: 252; **2**: 250; **3**: 224; and **4**: 222. The MWT, retention time and UV absorption of **3** all matched to those of OA. To obtain compounds for structural determination, we first optimized the culturing conditions to get high titers from shake flask culture. By examining the organic extracts from cells and media separately, we determined that most of the compounds were secreted into the media. We also observed that a spore inoculum size of 10^4 spores/mL led to the highest titers of the four compounds whereas inoculum sizes of 10^8 spores/mL and higher gave low production of target compounds (Figure S4). Notably, when the molecules were produced at high titers, *A. nidulans* adopted a morphology of globular pellets. As the titer drops upon increased inoculum size, *A. nidulans* grew as dispersed filaments (Figure S4). This is in agreement with previous reports that *Aspergillus niger* accumulated a high titer of citric acid when the fungus grew as globular pellets.[104]

From this simple optimization, these metabolites were purified from a large-scale culture and characterized by NMR (Supporting Figures S11–S25 and Tables S3–S5). Compound **3** (80 mg/L) was confirmed to be OA, while **1** (~ 1400 mg/L) was determined to be the C6-heptyl substituted 2,4-dihydroxybenzoic acid, i.e. sphaerophorolcarboxylic acid (SA) (Figure 6, Table 1). Compounds **2** (140 mg/L) showed a slightly red-shifted $\lambda_{max,}$ together with a decrease in MWT of 2 mu compared to **1**, indicating there is an extra degree of unsaturation that is conjugated with the aromatic ring. NMR analysis confirmed the presence of an olefin in the C6

alkyl substitution (Figure 6C). While **4** was not isolated due to its lower titer (estimated to be 300 μg/L), based on the UV absorption and −2 mu decrease in MWT compared to **3**, we propose the structure to be olefin-containing version of **3** (Figure 6C). Significantly, formation of **3** unveils a new microbial pathway to the cannabinoid precursor. The most abundantly produced SA (**1**) is a precursor to the octanoyl-primed, rare analog of cannabinoids, such as tetrahydrocannabiphorol (THCP). THCP represents the most potent natural CB1 and CB2 modulators isolated to date, with K_i of 1.2 nM and 6.2 nM, respectively.[105] Hence the *M. anisopliae* pathway provides a facile route to access SA that can be further elaborated to the rare THCP and related molecules.

The biosynthesis of **1**-**4** confirms the hypothesis that a freestanding TE enzyme in a HRPKS/NRPKS-containing biosynthetic gene cluster is indicative of a resorcylic acid pathway. The biosynthesis of **1**-**4** requires all three enzymes, as we observed that omitting any of the three in *A. nidulans* completely abolished the biosynthesis of **1**-**4** (Supporting Figure S5). Based on the mechanism of dual PKS pathways, we assigned the functions of the enzymes as shown in Figure 7A. HRPKS Ma_OvaA can produce a mixture of four different starter units, octanoyl-, 2-octenoyl-, hexanoyl-, and 2-hexenoyl-thioester, with octanoyl-thioester being the most abundant. The α,β-unsaturated starter units result from the enoylreductase (ER) domain of Ma_OvaA not functioning in the last iteration prior to the chain transfer to Ma_OvaB. Transfer of any of these four starter units to Ma_OvaB, facilitated by the SAT domain, is followed by three additional rounds of chain elongation and aldol cyclization by the product template (PT) domain to yield the resorcylyl-thioester attached to the ACP domain of Ma_OvaB. *ψ*ACP-TE Ma_OvaC then performs thioester hydrolysis to give **1**-**4**. The interaction between Ma_OvaB and Ma_OvaC may be enhanced by the *ψ*ACP domain as previously described for the *ψ*ACP-MT system,[101] although this requires more detailed biochemical characterization.

Table 1. Summary of Titers of Olivetolic Acid and Analogues from Heterologous Expression in *A. nidulans*

	1 (mg/L)[a]	**2 (mg/L)**	**3 (mg/L)**	**4 (mg/L)**
Ma_OvaA-C	1400 (±80)	140 (±20)	80 (±10)	0.3
StcJ/K + Ma_OvaB-C	0	0	5 (±1)	0
To_OvaA-C	750 (±20)	75 (±10)	40 (±10)	2 (±1)
Mr_OvaA-C	600 (±10)	60 (±10)	30 (±5)	0.5 (±1)
Ti_OvaA-C	0	0	60 (±10)	0
Ma_OvaA + Ti_OvaB-C	75	0	4	0
Ti_OvaA + Ma_OvaB-C	0	0	0	0

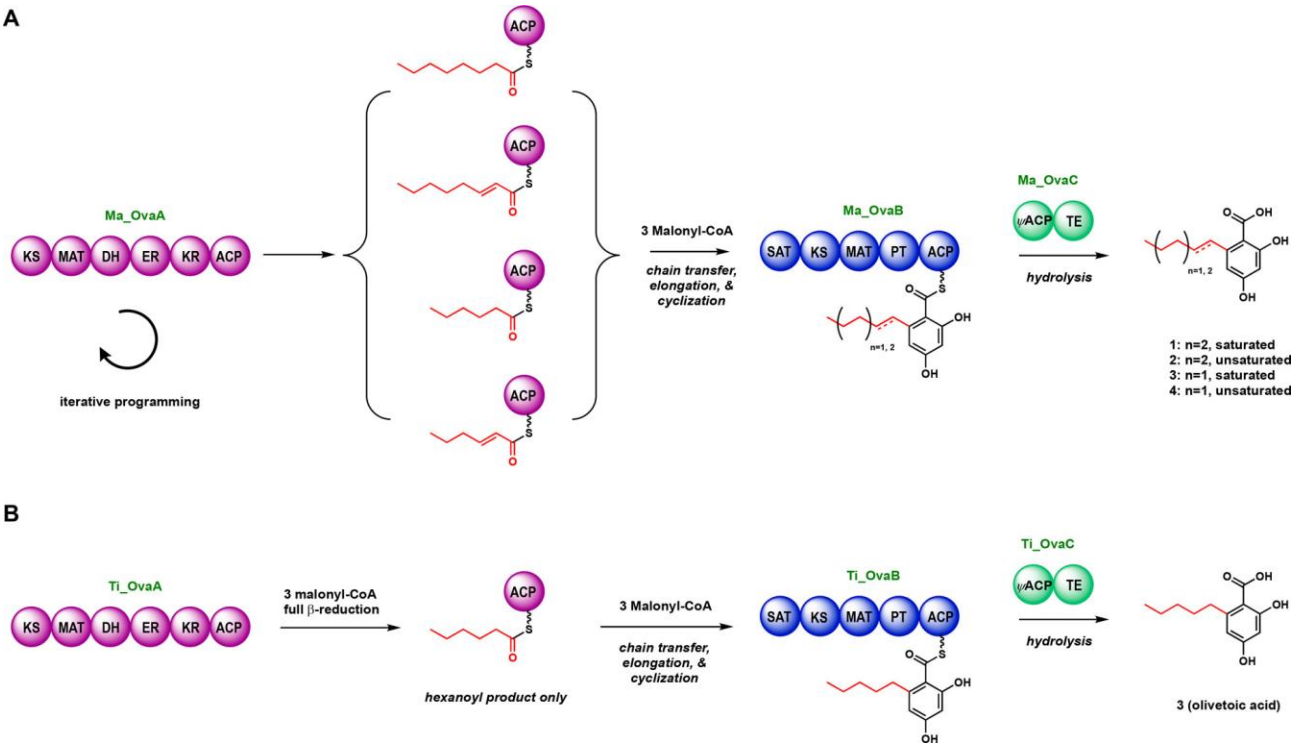

Figure 7. Proposed Biosynthetic Pathway of Olivetolic Acid and its Analogues from *M. anisopliae* ARSEF23 and Proposed Olivetolic Acid Biosynthesis Pathway of the Homologous Pair from *T. islandicus*. (A) HRPKS, Ma_OvaA, produces an ACP-bound starter unit that is promiscuous in alkyl chain length and saturation degree. NRPKS, Ma_OvaB, accepts any of the four starter units and further processes each into a resorcylyl-thioester. This is followed by hydrolysis of the thioester by Ma_OvaC to generate olivetolic acid 3 and its analogues (1, 2, and 4). (B) *T. islandicus* Ti_OvaA homologue produces only an ACP-bound hexanoyl that is accepted by the SAT domain of the Ti_OvaB to exclusively form olivetolic acid 3.

2.6 Strategies Towards Finding an Exclusive OA-Producing Pathway.

While the *M. anisopliae* cluster is able to make an abundant amount of SA, OA, the precursor to common cannabinoids, is produced as a minor product. It is desirable to obtain a pathway that can produce OA exclusively for further optimization. Since removing HRPKS Ma_OvaA abolished the production of all related compounds, we reasoned that supplying a strain expressing Ma_OvaB and OvaC with a hexanoyl starter unit could lead to exclusive OA production. First, 1 mM *N*-acetylcysteamine thioester (SNAC) of hexanoate was supplied to a

25-mL *A. nidulans* culture on day 2 and cultured for 5 days to test if the KS-domain of OvaB can directly capture it as the starter unit. However, when analyzing the sample on days 3, 4, and 5, no product could be detected from the culture, indicating hexanoyl-SNAC was either not taken up by the cell or was not accepted (Figure S6). Next, we attempted to directly generate hexanoyl-CoA as a primer for Ma_OvaB by feeding 1 mM hexanoic acid and coexpressing the *Cannabis sativa* acyl activating enzyme (CsAAE1) in combination with Ma_OvaB and Ma_OvaC. CsAAE1 was previously expressed in yeast to generate the hexanoyl-CoA for OAS incorporation.[38] We cultured the transformed strain in 25 mL of CD-ST media in a 125-mL flask for 5 days following feeding with 1 mM of hexanoic acid on day 2. However, no OA or related product was observed (Figure S6), suggesting Ma_OvaB requires a hexanoyl starter unit attached to an upstream ACP, and small molecule mimics are not compatible.

To pair Ma_OvaB with a HRPKS-like enzyme that can supply an ACP-bound hexanoyl starter unit, we turned to the related biosynthetic pathways of aflatoxin B1 and sterigmatocystin. Both utilize a pair of fatty acid synthase-like enzymes to synthesize a hexanoyl starter unit, which is then transferred by the SAT domain of the NRPKS for elongation and cyclization to yield the intermediate norsolorinic acid.[106,107] In the *A. nidulans* sterigmatocystin pathway, the StcK/StcJ enzymes have been paired with an NRPKS from asperfuranone pathway to afford hexanoyl-primed hybrid products.[108] To test if crosstalk between StcJ/StcK and Ma_OvaB can take place, we coexpressed these enzymes with Ma_OvaC in the engineered *A. nidulans* ΔSTΔEM strain. Metabolic analysis showed that only OA is produced by this host at a titer of 5 mg/L. The lowered titer of OA using this combinatorial biosynthetic approach is likely due to nonnative and suboptimal protein-protein interactions between the ACP domain of StcJ/StcK and the SAT domain of Ma_OvaB. Nevertheless, this simple mix-and-match attempt

showed that the product profile can indeed be manipulated by using different acyl donors.

Homologous clusters to the *M. anisopliae* cluster were discovered in *T. inflatum*, *M. rileyi*, and *T. islandicus* through bioinformatic analysis (Figure 6A). Although the clusters all share OvaA, B and C, their sequence identities are different (Supplementary Figure S1), indicating the potential to generate resorcylic acids with different C6 substituents. While OvaA, B, and C from *T. inflatum* (To_OvaABC) and *M. rileyi* share high homology (~84%−89%) with the *M. anisopliae* cluster, those from *T. islandicus* (Ti_OvaABC) share low homology (~46–52%). Heterologous expression of To_OvaABC in *A. nidulans* cultured in CD-ST revealed a similar product profile to Ma_OvaABC, albeit with lower titer (750 mg/L for **1** and 40 mg/L for **3**) (Figure 6B, Table 1). Similarly, heterologous expression of Mr_OvaABC showed that **1**-**4** can be detected from *A. nidulans* extract at lower titer (600 mg/L for **1** and 30 mg/L for **3**) (Table 1). Interestingly, when we heterologously expressed Ti_OvaABC genes from *T. islandicus*, **3** was exclusively produced at ~ 60 mg/L, which is ~12 fold higher than that from the StcJ/StcK and Ma_OvaBC combination (Figure 6B, trace ii; Table 1). Therefore, we propose that Ti_OvaA, differentiated from Ma_OvaA, selectively produces an ACP-bound hexanoyl starter unit, which leads to the exclusive formation of **3** (Figure 7B). Ti_OvaABC therefore represents a new pathway to produce olivetolic acid in microbial hosts.

Next, we explored combinatorial mix-and-match of OvaA-C from *M. anisopliae* and *T. islandicus* to determine if an exclusive **3**-producing strain can be attained. We generated strains that coexpressed Ma_OvaA with Ti_OvaBC, as well as Ti_OvaA with Ma_OvaBC. Heterologous expression of Ma_OvaA with Ti_OvaBC produced **1** and **3** at 75 mg/L and 4 mg/L, respectively (Table 1). This is almost 19-fold less than heterologously expressing Ma_OvaABC. This result indicates that NRPKS does not have selectivity towards different C8

or C6 starter units. On the other hand, pairing of Ti_OvaA with Ma_OvaB-C led to abolishment of **1**-**4** production, suggesting the unnatural pair is not compatible.

There might be two factors contributing to the low titer (Ma_OvaA + Ti_OvaBC) and abolishment of production (Ti_OvaA + Ma_OvaBC): i) The most plausible cause is the disruption of specific protein-protein interactions between the domains participating in acyl chain transfer; and ii) rates of intermediates and final product formation by different clusters are different, in that each has been evolutionarily optimized to serve their respective biological hosts. The unnatural pairing can compromise the performance of overall biosynthesis by a "rate-limiting" component such as Ti_OvaBC. Aside from the molecular recognition of the acyl chain by the SAT domain active site, a successful acyl chain transfer also requires complementary protein-protein interactions between HRPKS ACP domain and NRPKS SAT domain.[109,110] Previous studies have shown that although for some non-cognate HRPKS-NRPKS pairs, acyl chain could occur and new products emerged without any protein engineering efforts,[111] for others replacement of SAT domain is necessary to compensate for the otherwise undermined inter-domain communication.[105,112] While the sequence identity between ACPs of Ti_OvaA and Ma_OvaA is 62%, the identities between NRPKS SAT of Ti_OvaB and Ma_OvaB is lowered to 48%. Such moderate sequence identity between the SAT domains implies that the recognition sites between ACP from noncognate HRPKS and SAT can be weakened or even abolished. Therefore, to generate a combination that exclusively produces **3** at a higher titer, protein engineering endeavors that improve the compatibility between unnatural HRPKS and NRPKS enzymes are necessary. Alternatively, further genome mining of related clusters may lead to one that can produce olivetolic acid robustly in a heterologous host.

In summary, we have discovered a novel platform to produce OA and its analogs from

filamentous fungi. The platform consists of an HRPKS and an NRPKS, known to produce resorcylic acid moieties in tandem, and a separate TE enzyme. This platform represents a new strategy to produce these cannabinoid precursors in microbes without relying on the OAS and OAC found in *Cannabis sativa*

3. Methods to Increase Titer of Platform

3.1 Design of Experiments

Small quantities of olivetolic acid are produced in *Cannabis sativa* and chemical synthesis of the compound has proven to be difficult.[113] Therefore, we hypothesized utilizing a Design of Experiments (DOE) approach on our novel platform can further increase titer and thereby effectively solve the issue of low production. With regards to increasing production of fungal secondary metabolites and enzyme expression, DOE has proven to be an effective tool. DOE has been used for increased secondary metabolite production in bacteria[114], increased lipase production in fungi[115], increased xylanase production in fungi [116], and increased lignocellulolytic production in fungi[117], amongst other uses. We therefore sought to utilize a DOE approach to optimize the olivetolic acid and olivetolic acid analogs' titer produced by our novel platform.

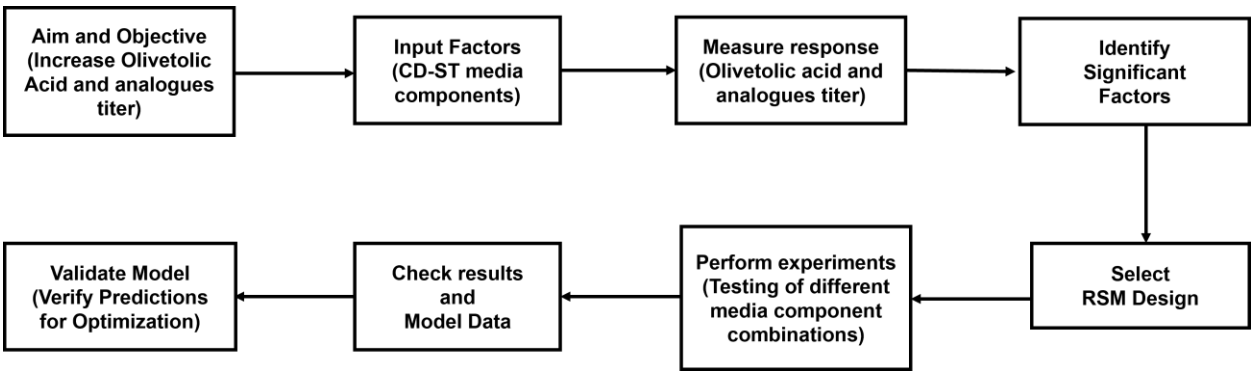

Figure 8. Design of Experiments Process Flow Diagram. DOE begins with screening and ends with optimization using predictive modeling.

Design of Experiments is a systematic method of evaluating factors and their effect on parameters.[118] DOE has proven to be more effective than one-factor at a time analysis because it greatly reduces the number of experiments needed and considers the interactive effects that factors can have with each other.[119] The DOE approach begins at screening and ends at optimization and predictive modeling. (Figure 8) First, screening is done to identify the factors that are most significant in the parameter response. We decided to focus our DOE approach on the media that our *A. nidulans* strain producing olivetolic acid and its analogs is cultured in. Since our DOE approach is focused on media, we tested the effects that nine different components (temperature, pH, NaCl, addition of other carbon sources such as dextrose, addition of other nitrogen sources such as yeast extract, casein acidic digest, starch, trace elements, and 20x nitrate salts) have on the production of sphaerophorolcarboxylic acid, olivetolic acid, and the analogs. Utilizing JMP statistical software, we performed an initial screening run of 24 experiments in order to identify the 3-5 most significant facts. To perform the screening experiments, we had to decide between a variety of screening platforms provided by JMP.

JMP offers two types of screening designs: classical screening designs which include fractional, factorial, Plackett-Burman, regular fractional factorial, Cotter, and mixed-level designs and main effects screening designs: screening designs focused on measuring main effects with negligible interactions between the factors. We opted for a classical screen design because we wanted to include the interactions between factors and considered the different types from there.

Two-level full fractional factorial design

Two-level full fractional factorial designs account for all the combination of the factor levels. Two-level refers to a high value (level) and a low value (level) for the factor tested. The total number of runs for this design is the product of the factor levels. For example, for a two-level full fractional design, the total number of runs would be 2^n where n is the number of factors tested. The design also estimates that all of the effects are uncorrelated and that there are no interactions between the factors, i.e., the factors are orthogonal to each other.[120] From a screening point of view, we determined the full fractional factorial design to be inefficient and cumbersome to do since it would require us to generate 2^9 (512) types of media to test. The next classical screening design to consider was two-level regular fractional factorial.

Two-level regular fractional factorial

Two-level regular fractional factorial designs are similar to full fraction factorial designs; however, instead of the number of runs being equal to 2^n where n is the number of factors tested, regular fractional factorial design runs are equal to 2^{n-k} where k<n. In other words, a two-level regular fractional factorial is just a fraction (k) of the full two-level fractional factorial design and therefore like the full factorial design, considers all the factors to be orthogonal to each other.[121] Since we could determine the fraction we would use, this was seen as an adequate design to choose; however, we wanted to consider some interactions between factors we determined to not follow through with this design and next looked at Cotter designs.

Cotter designs

Cotter designs are useful due to the ability to test a large number of factors in a small number of runs and are also useful if one is interested in the interaction between factors. Cotter designs are upheld by what is known as the principle of effect sparsity. These designs operate

under the assumption that if one of the components of the sum of factors has an active effect (whether negative or positive), the sum of the factors will display the response.[122] However, this can be potentially misleading and lead to false negatives if for example, one factor has a positive effect on the response, while the other factor has a negative effect, therefore totaling the sum of the factors to be zero/near zero, and therefore failing to show an effect. We determined not to go through with this design due to the false negative risks. We proceeded then briefly to mixed level designs.

Mixed level designs

Mixed level designs are typically used when screening categorical or discrete factors containing varied factor levels.[123] For example, one can be screening for the effect that light (measured on/off) and a four-level media component have on the titer of a metabolite. Since we desired to keep the screen simple with just two levels for our factors since and we did not have any qualitative factors, we proceeded to our last design, the Plackett-Burman design.

Plackett-Burman designs

Plackett-Burman designs are somewhat like regular fractional factorial designs except the total number of runs are a multiple of four rather than a power of two. Additionally, interactive effects between factors in a Plackett-Burman design are only partially confounded by the main effects which differs from regular fractional factorial where the interactive effects are completely confounded by the main effects and are therefore indistinguishable from each other.[124] Plackett Burman designs are typically utilized when testing for the main effects among a variety of factors and so with this in mind, we chose to utilize the Plackett-Burman design as our screening design.

We implemented the two-level Plackett-Burman design and generated 24 runs to test, with each run being a different media composition. For the two levels (low and high value marks), we determined these values to input: temperature (25 C, 37 C), pH (4, 7), starch (10 mg/ml, 30 mg/ml), NaCl (0 mg/ml, 10 mg/ml), dextrose (0 mg/ml, 20 mg/ml), yeast extract (0 mg/ml, 20 mg/ml), casein acidic digest (10 mg/ml, 30 mg/ml), trace elements (.5 ml/L, 2 ml/L), and 20x nitrate salts (10 ml/L, 90 ml/L). We cultured the strain in these different medias, assaying the titer in media sets of 4 with CD-ST (20 g/L starch, 20 g/L casein acidic digest, 50 mL/L 20x nitrate salts, 1 mL/L trace elements) as the control media in each run. We inputted the data into the JMP software and performed analysis of variance (ANOVA) and generated a Pareto chart from ANOVA and noted the results. (Figure 9)

ANOVA is a widely used tool to determine if there are statistical differences between means of different groups. It is a collection of different statistical models and is used to determine whether the variance of a specific effect or factor interaction is statistically significant.[125] The Pareto chart puts the ANOVA data in a simple to understand form, displaying whether the factor or factor interaction has exceeded the t- value limit and Bonferroni limit. The t-value refers to the value of the difference relative to the variation of the data tested. It is a value that represents the ratio of the difference between the estimated value of factor and its hypothesized value to its standard error.[126] The Bonferroni limit is the value from the Bonferroni method that answers which factors means are significantly different from each other. Factors and factor interactions above the Bonferroni limit indicate that they are statistically significant and have a great effect on the parameter response, factors and interactions between the t-value limit and Bonferroni limit are indicated as potentially significant, and factors and interactions below the t-value limit are noted as insignificant.[127]

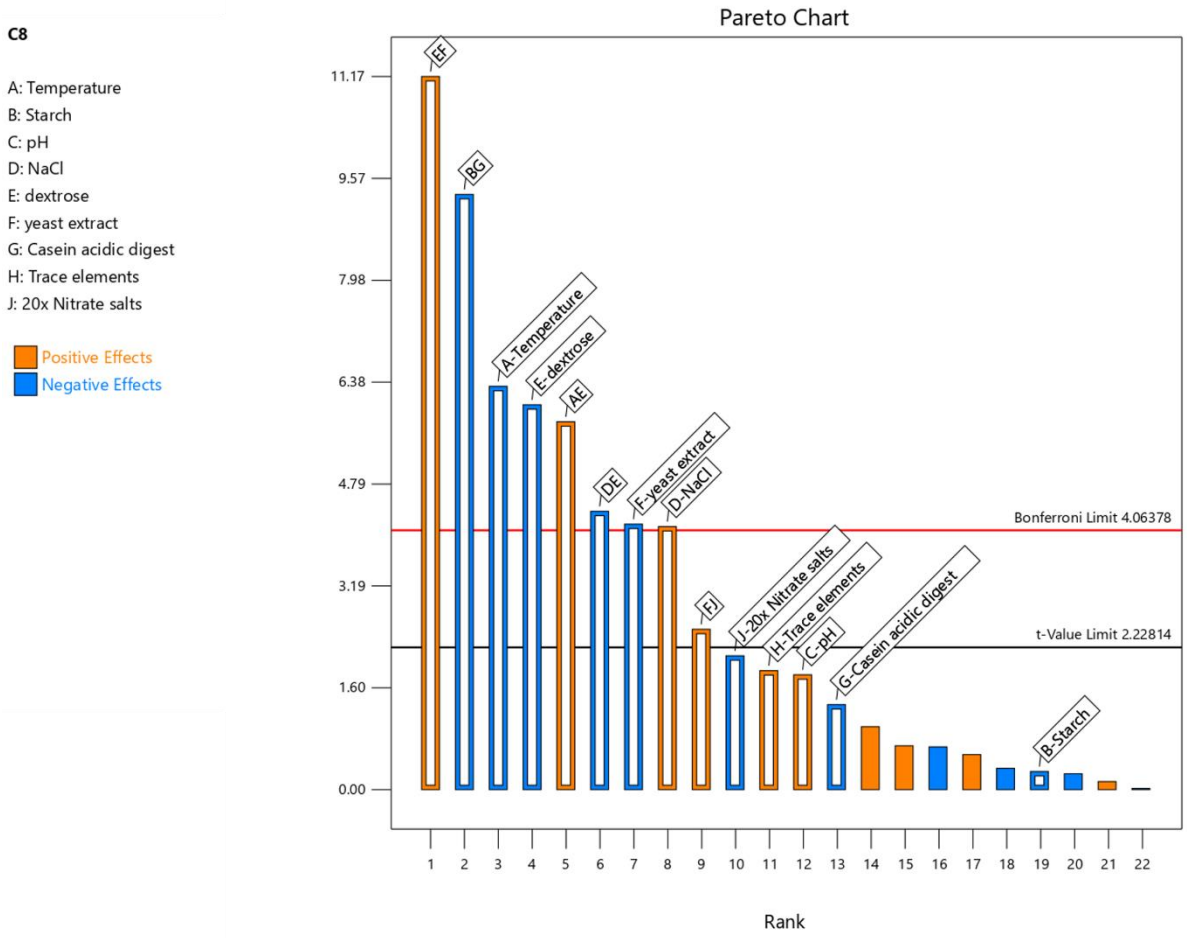

Figure 9. Pareto Chart Displaying the Results of the Screening Experiments. Sphaerophorolcarboxylic acid production is the response being measured. Temperature, dextrose, yeast extract, and NaCl were the main factors that all had the greatest effect on production (all above the Bonferroni Limit) whereas the interactions between dextrose and yeast extract, starch and casein acidic digest, temperature and dextrose, and NaCl and dextrose were the two factor interactions with the greatest effect on production.

Based on the Pareto chart, we noted that increased temperature, addition of dextrose, addition of yeast extract, and addition of NaCl all had values above the Bonferroni limit indicating that these factors significantly affected the titer. However, three of values were all labeled blue indicating a negative result. Increased nitrate salts which had a negative effect on the media based on its blue distinction had a t-value greater than the t-limit but lower than the Bonferroni limit whereas increased casein acidic digest and increased starch which were also

labeled blue had t-values lower than the t-limit indicating that these factors are not statistically significant. For factors having a positive effect on the titer labeled orange, NaCl salt had a t-value greater than the Bonferroni limit indicating its statistically significance and increased nitrate salts had a t-value lower than the t-limit indicating it is not significant. From the screening data, we proceeded with two factors for our optimization experiments: NaC1 and nitrate salts. Although it was tabulated as not significant, we chose to include nitrate salts mainly because we did not want to optimize just one factor and since nitrate salts were already included in the media. We also included addition of $MgSO_4$ since that was noted in the literature to increase metabolite production.[128]

Once we obtained the three factors, we utilized the response surface methodology (RSM) optimization approach for optimization of the media, seeking to add these factors to our CD-ST media containing starch, trace elements, and casein acidic digest as the base since these factors had no statistical significance towards the titer. RSM is a widely used method for modeling/predictive modeling.[129] RSM optimizes the factors correlating to a response with the inclusion of the effects interactions between the factors have. RSM has proven to be just as effective in modeling as a 3-level full factorial design[130], but its advantage is that RSM greatly reduces the number of experiments needed to form an accurate model. As an example, in a 3-level factorial design utilizing 3 factors, one would need to do 27 experiments to get an accurate model as opposed to the 15 experiments one would need for a central composite design RSM approach. As the number of factors increase, the difference between the number of experiments needed for a 3-level full factorial design vs a central composite design RSM approach greatly increases, which is why RSM is the advantageous approach.

Reports of the effectiveness of increasing secondary metabolite production in fungi with

the RSM approach have been recorded. Talukdar et al. observed a 7-fold increase in antibiotic production of *Penicillium verruculosum* MKH7 utilizing an RSM approach on the media used[131]. Additionally, Chaichanan et al. measured an 8-fold increase in zofimarin production by the endophytic fungus, *Xylaria* sp. Acra L38 utilizing a complete, from screening to optimization, design of experiments approach.[132] Therefore, we sought to implement this RSM approach to optimize the media for increased titer of olivetolic acid and its analogs. To do so, similar to the screening design, we had to determine which RSM design to use.

JMP software offers three methods of performing a response surface design experiment: custom design, central composite design, and Box-Benhten design.

Custom design

Custom designs are more flexible than the central composite and Box-Benhten classical designs. They can incorporate both categorical and numerical factors and up to eight of these factors. JMP touts that one can adjust these designs to accommodate for one's specific experimental conditions, including adding one's desired restrictions and specifying the number of runs.

Central composite design

Central composite design is one of two classical RSM designs that JMP offers. The central composite design coalesces the two-level fraction factorial design with center and axial points. The center point is the midrange of the two levels inputted for the factors and there are two axial points, a value higher than the high factor level and a value lower than the low factor level.[133] Therefore, a central composite design can have five levels.

Box-Behnken design

Box-Behnken designs are the second of the two RSM designs provided by JMP. Box-Behnken designs only contain three levels: low, midpoint, and high. There are no axial points. Due to its lack of axial points, Box-Behnken designs typically have higher prediction variance than central composite designs.[134] We ultimate decided to proceed with the central composite design due to its ability to incorporate these axial points. Since we did not know where the optimum of the factor values lied, we hypothesized that these axial points could prove closer to the optimum than the initially two-level factor values and so it was best to include them.

We implemented the central composite RSM design with our three factors, inputting values of 0 mg/ml (low axial point), 10 mg/ml (low level), 20 mg/ml (midpoint level), 30 mg/ml (high level), and 36.81 mg/ml (high axial point) for NaC1, values of 5 ml/L (low axial point), 10 ml/L (low level), 30 ml/L (midpoint level), 50 ml/L (high level), and 63.64 ml/L (high axial point) for 20x nitrate salts, and lastly inputted values of 0 mg/ml (low axial point), 1 mg/ml (low level), 2.5 mg/ml (midpoint level), 5 mg/ml (high level), and 7.5 mg/ml (high axial point) for $MgSO_4$. The JMP software generated 18 media compositions from the values outputted. We ran the assays in sets of 5, once again utilizing CD-ST as our control media for each run. We augmented the design, added 12 more runs (media compositions). We recorded the titers for each of the runs and graphed the data. (Figure 10) From the data, we observed that in 6 media formulations, our *A.nidulans* cultures producing olivetolic acid and its analogs produced these metabolites at higher titers than when cultured in CD-ST.

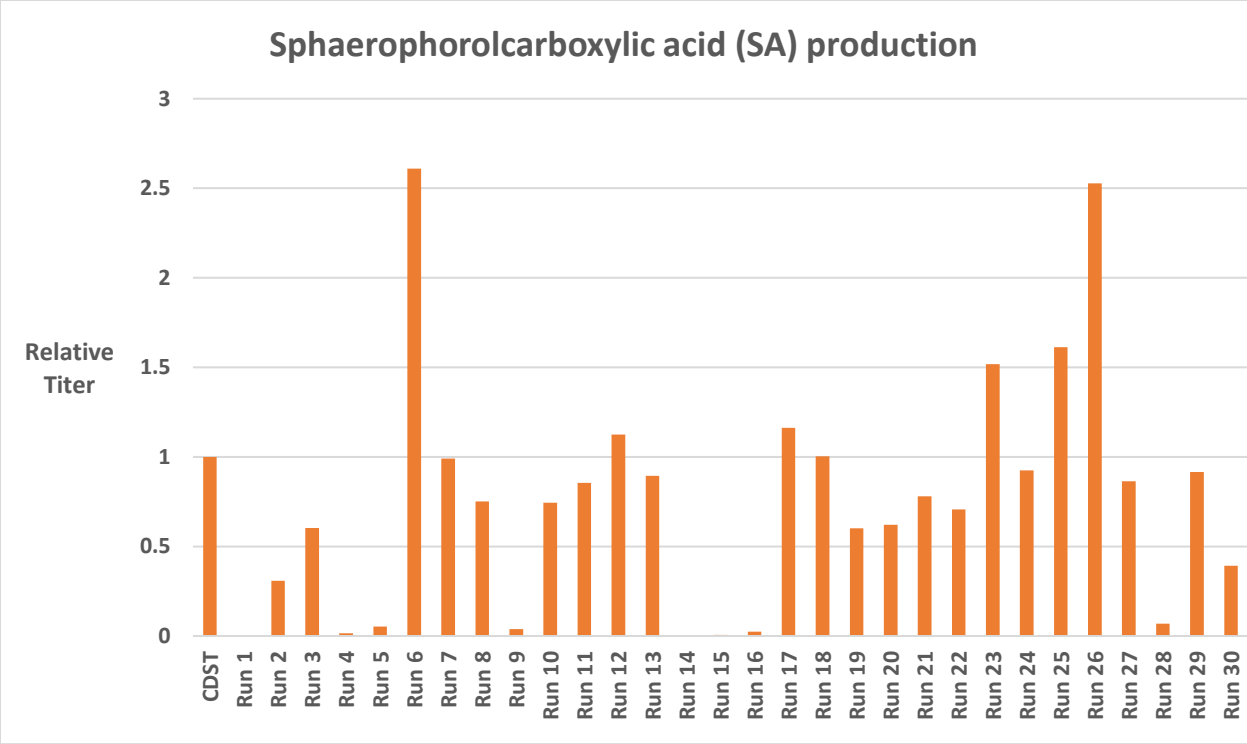

Figure 10. RSM Runs and Their Titers Relative to the Standard CDST Titer. *Aspergillus nidulans* strains expressing Ma_OvA, Ma_OvaB, and Ma_OvaC were culture in 10 ml of media in 50 ml falcon tubes and the titer was measured on day 5.

Both the screening design runs and the central composite design RSM set of experiments were done in 10 ml cultures in 50 ml falcon tubes. From there, we chose the three media formulations that outputted the greatest titers and cultured the *A. nidulans* strain in 25 ml of the respective medias in a 125 ml flask to test whether these results would hold. Titer measurement from the flasks confirmed that all three media formulations selection were able to produce higher titers than CDST with RSM run #6 containing 20g/L starch, 20g/L casein acidic digest, 1 mL/L trace elements, 10 mL/L 20x Nitrate salts, and 10 g/L NaCl and RSM run #25, containing 20 g/L starch, 20 g/L casein acidic digest, 1 mL/L trace elements, 5 ml/L 20x Nitrate salts, having the greatest improvement, improving titers of sphaerophorolcarboxylic acid and olivetolic acid almost 2-fold from CD-ST (20 g/L starch, 20 g/L casein acidic digest, 1mL/L trace elements, 50 ml/L 20x Nitrate Salts). The comparison between the components of RSM run #6 and CD-ST

media shows that a 10-fold decrease in 20x Nitrate salts volume with and without the addition of NaCl, leads to about a 1.75-fold increase in titer, a surprising result whereas comparison between RSM run #25 and CD-ST media shows that a 5-fold decrease in 20x Nitrate salts volume in addition to supplementation of 10 g/L NaC1 leads to about a 1.9 fold increase in titer. (Figure 11) RSM run #26 containing 20 g/L starch, 20 g/L casein acidic digest, 1mL/L trace elements, 20 mL/L 20x Nitrate salts, 2.5 g/L $MgSO_4$ had a 1.1-fold improvement in titer compared to CD-ST media. Therefore, RSM run #6 is the best option for improvement of olivetolic acid titer and analog. For further direction and next steps, we would need to determine if this new optimized titer is a local optimum or a global optimum. To do this, we would need to model this data using the JMP software and utilize the software's predictive modeling tool to predict whether or not we have reached the global optimum and if not, which values outside the 5 levels previously chosen that we need to input for the next series of runs.

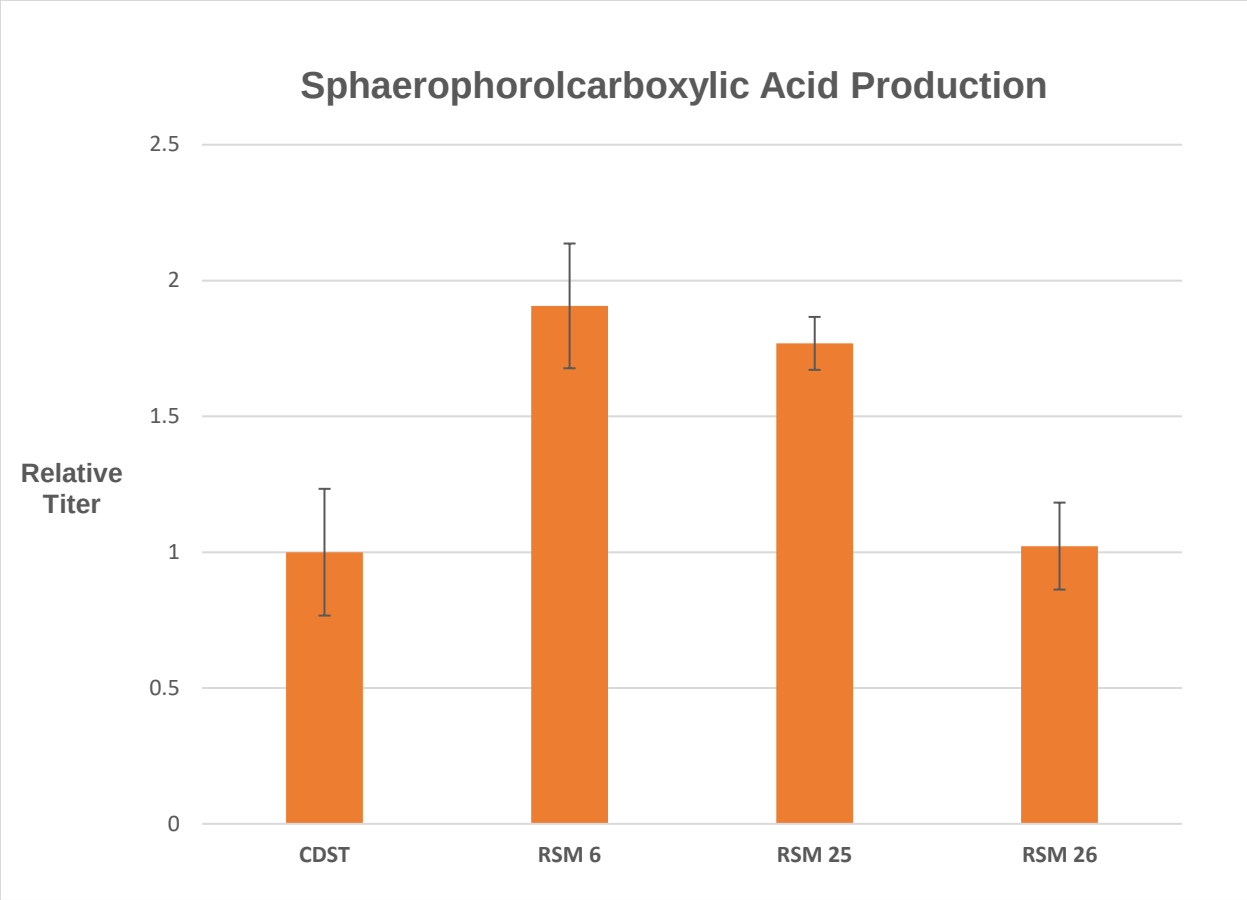

Figure 11. RSM Runs and Their Titers Relative to the Standard CDST Titer (Flasks). *Aspergillus nidulans* strains expressing Ma_OvA, Ma_OvaB, and Ma_OvaC were cultured in 25 ml of media in 125 ml flasks and the titer was measured on day 7.

3.2 Overexpression of Acetyl-CoA Carboxylase

To increase titer outside of optimization of culture media, we sought to increase malonyl coenzyme (malonyl-CoA) production in the *Aspergillus nidulans* fungal body. With regards to our platform, one unit of acetyl coenzyme A (acetyl-CoA) is used as a building block along with three units of malonyl-CoA to form hexanoyl-thioester, hexenyl-thioester, octanoyl-thioester, or octenyl-thioester, generated by the HRPKS (Ma_Ova) of *Metarhizium anisopliae*. Similarly, one unit of acetyl-CoA along with three units of malonyl-CoA are utilized by the HRPKS (Ti_OvaA) of *Talaromyces islandicus* to produce hexanoyl-thioester. Perusing through the literature, we

found that overexpression of the enzyme acetyl-CoA carboxylase was found to increase the malonyl-CoA production.[135] Acetyl-CoA carboxylase is responsible for converting one unit of acetyl-CoA to one unit of malonyl-CoA. The enzyme catalyzes the carboxylation of acetyl-CoA to malonyl-CoA. This reaction is ATP-dependent. Malonyl-CoA is a regulator of fatty acid oxidation and is the primary substrate for fatty acid synthase. In fact, in fungi, inhibition of acetyl-CoA carboxylase rapidly leads to cell death through membrane dysfunction due to fatty acid depletion caused by lack of the malonyl-CoA building block.[136] Therefore, we hypothesized that increase of the malonyl-CoA production through overexpression of acetyl-CoA carboxylase would lead to increased titers of olivetolic acid and its analogs. We mined for the acetyl-CoA carboxylase enzyme in *A. nidulans* and overexpressed the enzyme in combination with heterologous expression of Ti_OvaA, Ti_OvaB, and Ti_OvaC and measured the titers. (Figure 12) From the data, overexpression of acetyl-CoA carboxylase with Ti_OvA, Ti_OvAB, and Ti_OvaC in *A. nidulans* consistently led to improved olivetolic titers over the *A. nidulans* control strain expressing Ti_OvaA, Ti_OvaB, and Ti_OvaC with the acetyl-CoA carboxylase overexpression colonies producing more than 2.5-fold more olivetolic acid.

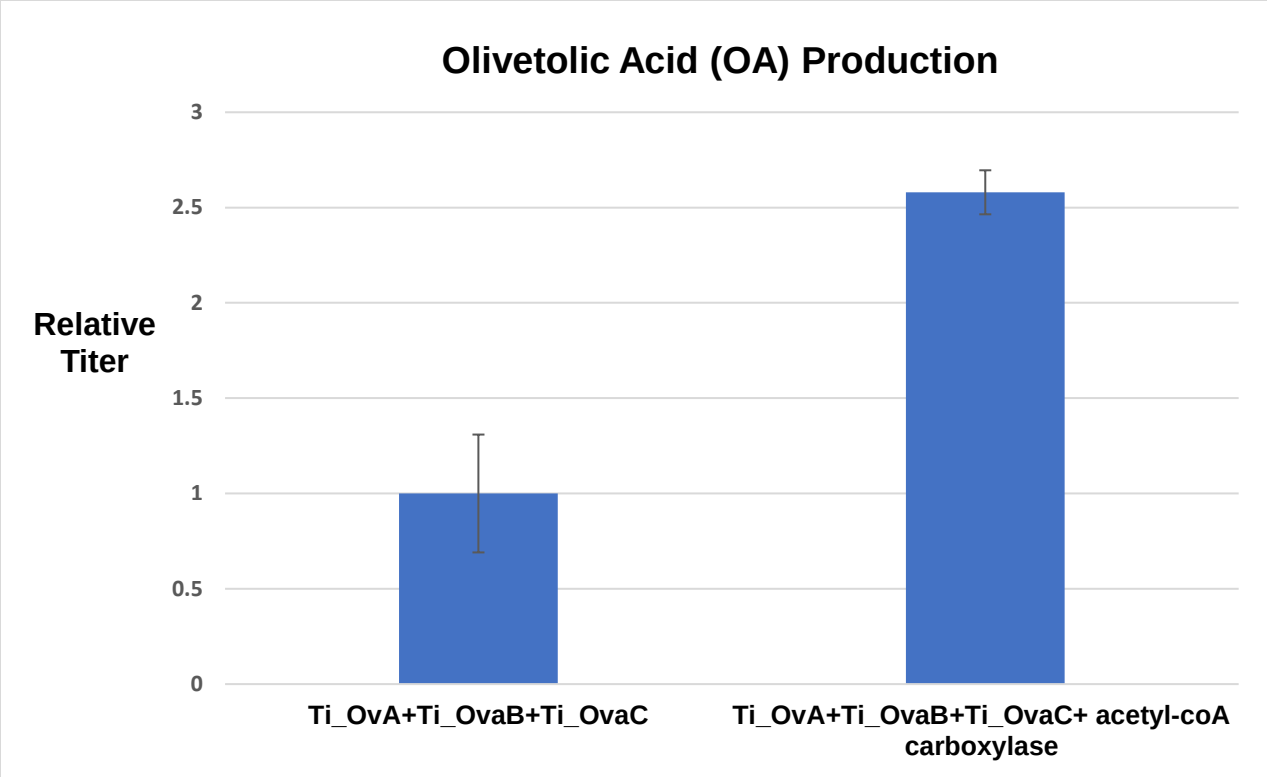

Figure 12. Relative Olivetolic Acid Titers of *Aspergillus nidulans* Colonies Expressing Ti_OvaABC by Itself and with Overexpression of the Endogenous Acetyl-coA Carboxylase Gene. Overexpression of acetyl-CoA carboxylase led to a 2 fold increase in titer olivetolic acid titer

3.3 Conclusion

Therefore, through optimization of production media utilizing DOE and increased malonyl-CoA production through overexpression of acetyl-CoA carboxylase, we were able to increase the titers of our platform's compounds. This is necessary as a step to generate an industrial relevant strain producing cannabinoids. Furthermore, high production of these intermediates in the cannabinoid biosynthetic pathway is important due to the high costs of these intermediates in the market due to their low availability. High production and isolation of these compounds can be used in combination with *in vitro* enzymatic methods to produce the final elaborated cannabinoids. These cannabinoids, especially the non-common ones which are not characterized, can be subjected to biological activity assays and thereby characterized, further

advancing the knowledge of the field and possibly providing therapeutic options. Even more so, as detailed in the next chapter, these intermediates can themselves have intriguing biological activities, making high production of these intermediates important.

4. Expansion of Diversity of Products Produced By Novel Platform

4.1 Microbial Properties of Olivetolic Acid and Variants

As previously described in Chapter 2, heterologous expression of the Ma_OvaA, Ma_OvaB, and Ma_OvaC genes from *Metarhizium anisopliae* in *Aspergillus nidulans* led to the production of four products: olivetolic acid, an unsaturated analog of olivetolic acid, sphaerophorolcarboxylic acid, and an unsaturated analog of sphaerophorolcarboxylic acid at high titers, thereby making this an attractive platform to further develop downstream in order to access rare or new to nature cannabinoids that have biological potential. Furthermore, even olivetolic acid and olivetolic acid analogs are proposed to have biological activity such as antibacterial, antifungal, cytotoxic, and photoprotective properties. One study published had demonstrated that olivetolic acid had shown an anticonvulsant effect in a mouse model of Dravet syndrome, similar in effectives to CBD.[137] Recently, a study chronicling the antibacterial effects of OA and a few of its analogs was published. Lee et al. chemically synthesized olivetolic acid as well as the propyl, heptyl, nonyl, undecyl, and tridecyl analogs of olivetolic acid. They tested these compounds for antibacterial activity against the bacteria *Bacillus subtilis* and *Staphylococcus aureus*. Although OA and the propyl variant showed very little antibacterial activity against both *Bacillus subtilis and Staphylococcus aureus*, the heptyl, nonyl, undecyl, and tridecyl variants did, with a partial trend of increasing activity based on length. Both the undecyl

and tridecyl analogs had a minimum inhibitory concentration (MIC) of 2.5 µM against Bacillus subtilis and 6.25 µM against Staphylococcus aureus[138] demonstrating that not only do cannabinoids have potent biological activity/therapeutic potential further to be explored but also the intermediates in the cannabinoid biosynthetic pathway also have biological activity and are worth further exploring.

Not only have the olivetolic acid variants shown promising activity, but also analogs of Δ^9-THC have also demonstrated potent biological activity. A report in 2019 was published in which the authors extracted the heptyl analog of Δ^9-THC, known as Δ^9-tetrahydrocannbiphorol (Δ^9-THCP) from the cannabis plant and performed assays to measure its biological activity. This rare cannabinoid displayed almost 30 times greater binding affinity to CB_1 than Δ^9-THC did and also six times greater binding affinity to CB_2 than Δ^9-THC. The pharmacological activity of Δ^9-THC is ascribed to its binding activity to the CB_1 receptor, with the length of the alkyl chain being directly correlated to the binding activity.[139] Therefore, a rare or new to nature cannabinoid that has greater binding affinity to the CB_1 receptor may potentially offer greater medicinal effects than what is currently known for Δ^9-THC. Therefore, although we already produced, through our platform, four compounds with potential activity, we sought to further diversity our product profile and ultimately access the final elaborated cannabinoids.

4.2 Mutation of Ketosynthase Domains Results and Discussion

To achieve this, the ketosynthase domain of the HRPKS (Ma_OvaA) was mutated. The ketosynthase domain is responsible for carbon chain length programming. The domain facilitates decarboxylative Claisen condensation, catalyzing the formation of a carbon-carbon bond, extending the growing acyl chain.[140] Therefore, modification of the KS domain can affect

polyketide elongation, generating olivetolic acid variants. Studying the *Saccharomyces cerevisiae* fatty acid synthase 2, Johannson et al. identified that amino acid M1251 was central to the KS channel.[141] Utilizing that information, Zhu et al. engineered variants with the mutations M1251W and G1250S and noted that they saw increased C6 as well as C8 production.[142] Additionally, Gajewski et al. performed mutations on the equivalent M1251 in the fatty acid synthase of *Corynebacterium ammoniagenes* as well as other mutations for directed polyketide production.[143] They ultimately determined that mutations of M1251 or its equivalent in other fatty acid synthases promoted chain length control by forming a kinetic barrier that steers the product from further KS elongation and onto release. With that knowledge, we sought to mutate the M1251 equivalent in our HRPKS gene as well as a wide host of other mutations (Figure 13). Utilizing the CastP program, we also identified the active site of the Ma_OvaA KS domain containing the canonical cysteine-histidine- histidine catalytic triad and sought to mutate amino acids residues surrounding the active site. (Figure 14)

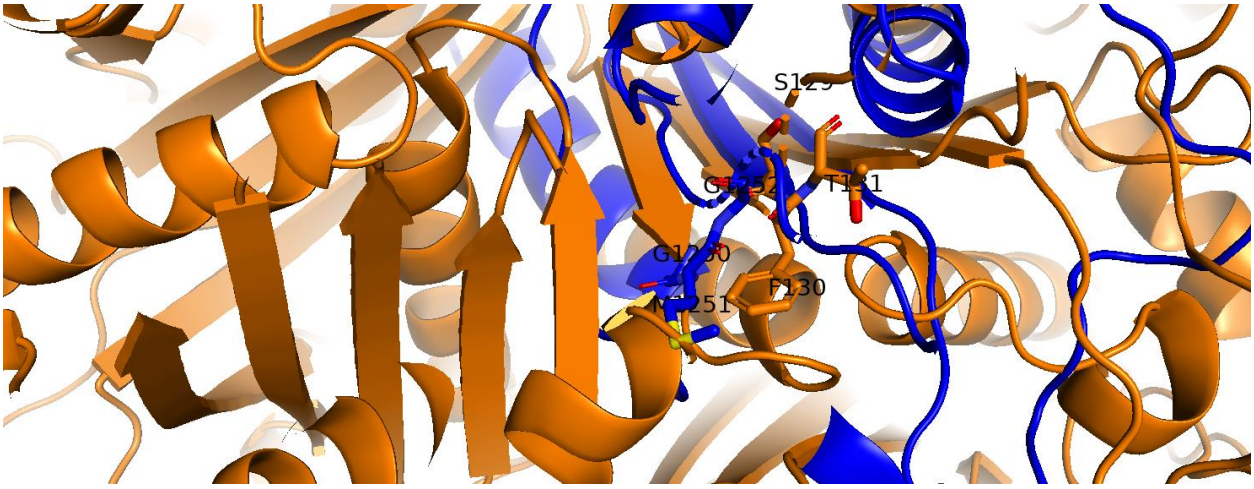

Figure 13. *Saccharomyces cerevisiae* FAS2 and Ma_OvaA KS Domain Alignment. G1250, M1251, G1252 of *Saccharomyces cerevisiae* FAS2 correlates to S129 F130 T131 of *Metarhizium anisopliae* OvaA.

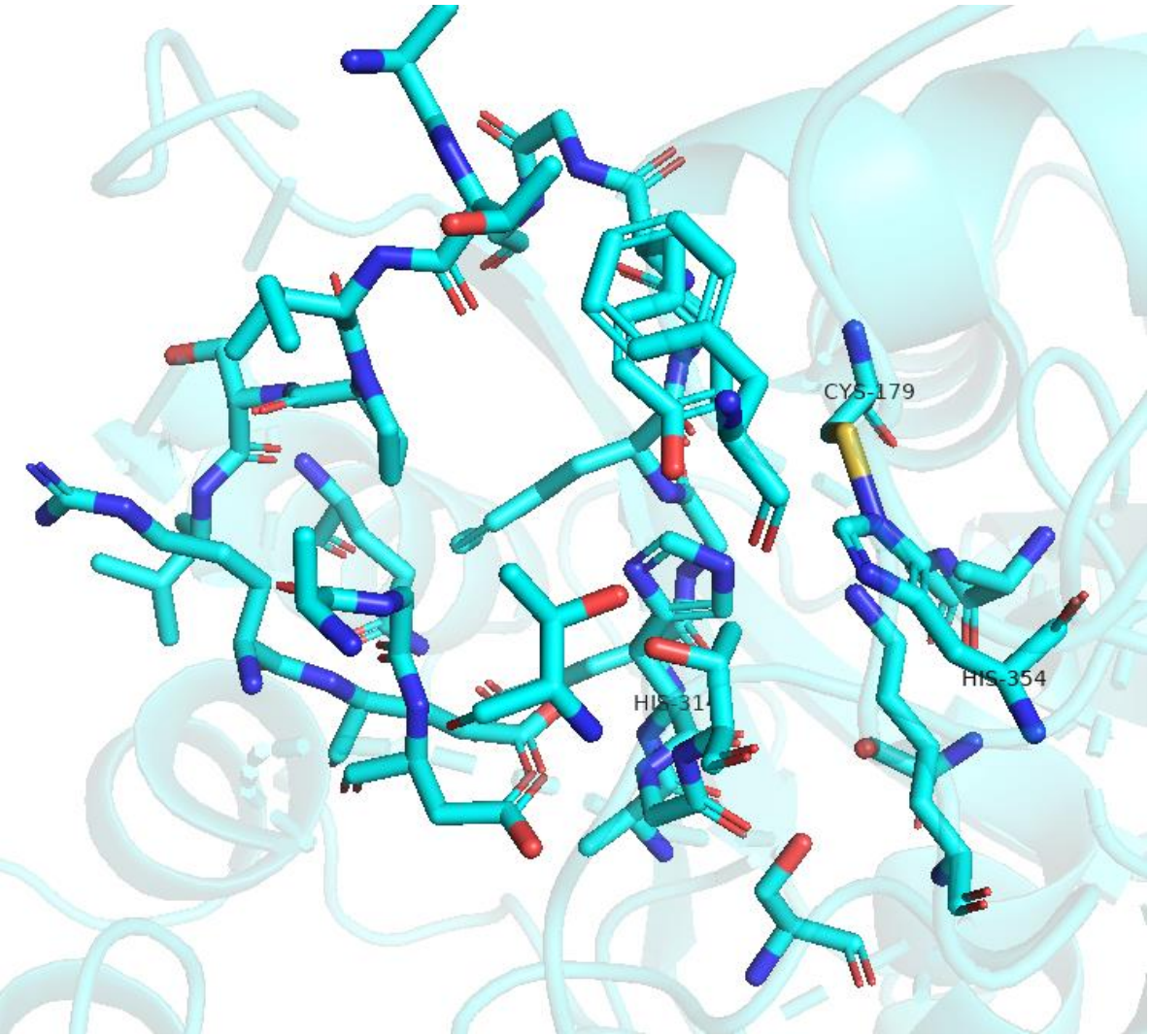

Figure 14. Predicted Active Site of Ma_OvaA Ketosynthase Domain. The KS domain contains the canonical type I PKS catalytic triad of Cys-His-His. Mutations around the active site were made to change the olivetolic acid alkyl chain length

To make these mutations in the active site of the KS region of Ma_OvaA, we utilized the Living Biofoundry located in the California NanoSystems Institute (CNSI) at UCLA. The Living Biofoundry is an automated, high throughput platform capable of performing tasks such as polymerase chain reaction, gene assembly, plasmid assembly, heterologous expression, transformation, amplification and metabolite analysist. The Living Biofoundry consists of a

ThermoFisher Laboratory Automation System (LAS),a Fluent Tecan liquid handling system, two Illumina sequencers, bioreactors, and a ThermoFisher TSQ Altis triple quadrupole liquid chromatography-mass spectrometer. (Figure 15) The LAS is the central technology in the Biofoundry "enabling execution of automated synthetic biology and workflows at >5000 samples per week".[143] The LAS is equipped with thermal cyclers, reagent dispensers, automated incubators, plate readers, racks/columns for plate storage, and a state-of-the-art Spinnaker™ robot. The LAS utilizes a Momentum application programming interfaces that seamlessly is compatible with a whole range of laboratory information systems (LIMS). With regards to the Spinnaker™ robot, it itself is a SCARA 4-axis microplate mover encompassed with not only a barcode reader and integrated vision system making it possible for inventory management at real time tracking but also a gripper that has plate detection and adjustable gripping force. That is helpful in order to minimize loss of supernatant as well as remove labware handling errors.

Figure 15. The Living Biofoundry. Tecan Liquid Handling systems (left) and ThermoFisher Laboratory Automation System (right). ThermoFisher TSQ Altis triple quadrupole liquid chromatography-mass spectrometer, bioreactors, and Illumina sequencers not shown.

The ThermoFisher Momentum API allows for relatively simple programming of the desired actions. The Momentum API gives the open to type out commands in the tpical fashion programmers are accustomed to or utilize its graphical interface to schedule actions (picture of

graphical interface). Therefore, the Momentum API is quite user friendly while offering optimal performance containing inventory controls and compatibility with over 325 automation friendly instruments.[144] Finally, the Living Biofoundry is a tool of the BioPolymers, Automated Cell Infrastructure, Flow, and Integration Chemistry Materials Innovation Platform (BioPacific MIP), "a platform dedicated to scalable production of bioderived building blocks and polymers from yeast, bacteria, and fungi."[145] BioPacific MIP is a collaboration of researchers from UCSB and UCLA, funded by the National Science Foundation (NSF).

We, therefore utilized the Living Biofoundry to construct the plasmids containing ketosynthase mutations for the purpose of diversifying our product profile. We programmed the system to be almost fully capable of automating the plasmid making process. The only steps that were not automated were the plating and the colony picking steps. (Figure 16). The process of implementing a process that is done on the benchtop to the automated system proved initially to be difficult due to the difference in what is possible to do on the LAS vs on the benchtop. For instance, typically after PCR, we perform gel electrophoresis, and purify the DNA band from the gel. However, that is not practical to do with the automated system; therefore, in order to purify the DNA from the PCR, we utilized a magnetic bead plate bound system. The magnetic bead plate was readily integrated into the Tecan Liquid Handling platform. As for another example on the difference between executing experiments on the benchtop vs on the LAS, we considered the ways we performed the *E.coli* transformation step. Typically, we electroporated the DNA into the *E.coli* competent cells using a cuvette and electroporator; however, we could not utilize electroporation on the LAS. There are 96 well plate electroporators, however, they are not equipped with the software to be integrable into the LAS. Therefore, instead of electroporation, we utilized chemically competent *E.coli* coli transformations and performed transformation

experiments with those chemically competent cells. These are just a couple of examples on how we had to conceptualize the plasmid making process differently on the LAS than how we typically do on the benchtop.

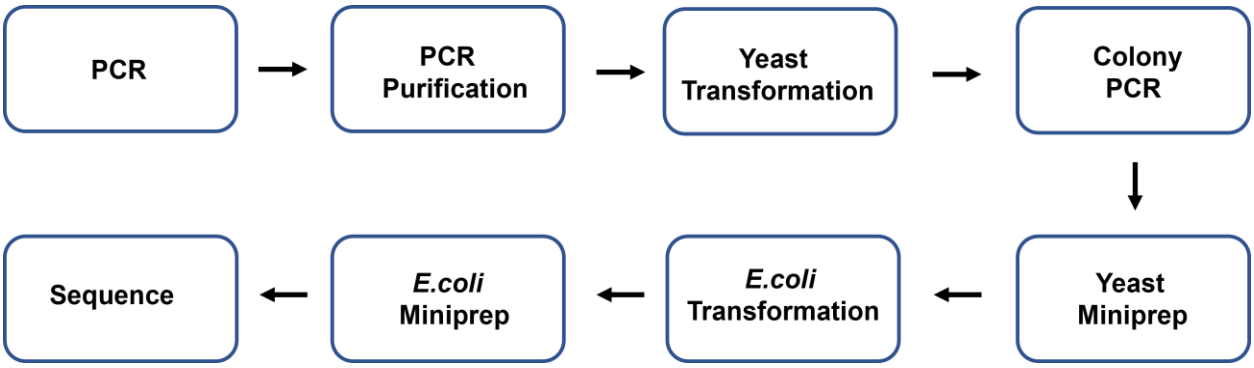

Figure 16. Tang Lab Plasmid Construction Process Flow Diagram. Plasmid construction begins with PCR and ends with sequencing to confirm that the plasmid is correctly constructed. We are able to do all these steps except colony pcr and sequencing utilizing the Tecan Liquid Handling System and the ThermoFisher Laboratory Automation System.

After the construction of mutation plasmids both manually and utilizing the Living Biofoundry, we heterologously expressed the mutated Ma_OvA plasmids with Ma_OvaB and Ma_OvaC in *Aspergillus nidulans*. Out of the many mutation plasmids we constructed, we identified two that produced olivetolic acid analogs. Heterologous expression of first plasmid, containing the F418A and Y420A mutations, with Ma_OvaB and Ma_OvaC produced the nonyl and undecyl variants of olivetolic acid, both previously mentioned as having antibacterial activity. (Figure 18) Heterologous expression of the second plasmid, containing the T318W and S347W mutations, with Ma_OvaB and Ma_OvaC produced orsellinic acid and divarinic acid which were confirmed by analytical standard and heterologous expression also produced what we propose to be ethyl variant based on mass and UV, although at low quantities so NMR was

not taken. (Figure 17) Orsellinic acid was also found to be in the original heterologous expression profile.

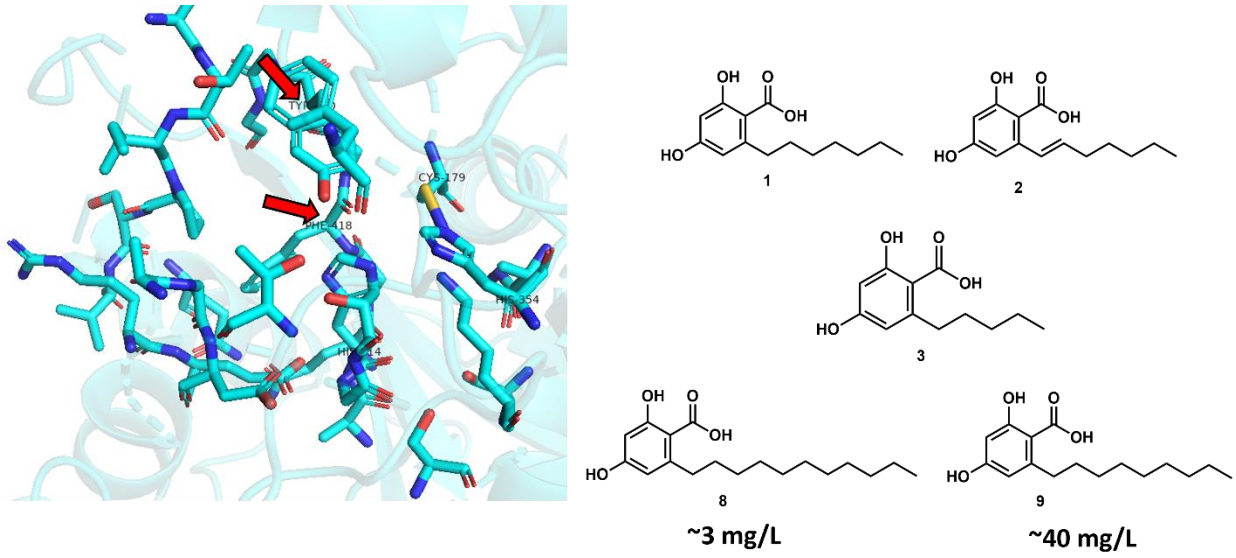

Figure 17. Heterologous Expression of Ma_OvaA (F418AY420)BC Results. The F418A+Y420A mutations of the KS domain of Ma_OvaA led to production of the nonyl and undecyl variant of olivetolic acid as well as the production of divarinic acid in addition to three of the original compounds produced by the platform.

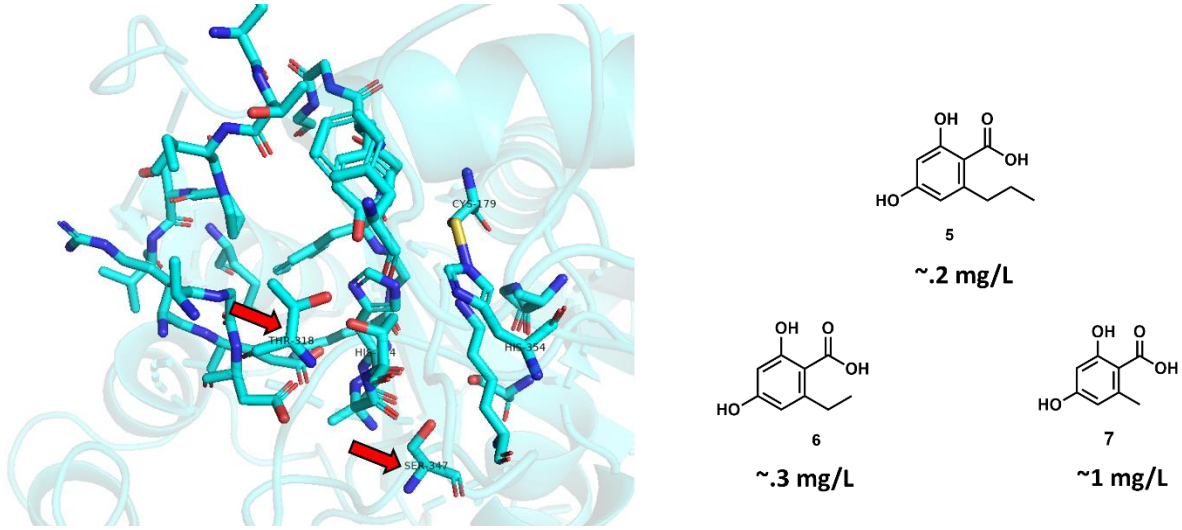

Figure 18. Heterologous Expression of Ma_OvaA(T318WS347W)BC Results. The T318W+S347W mutations of the KS domain of Ma_OvaA abolished most of the production of

SA as well as completely abolished unsaturated SA, OA, and unsaturated OA production. The mutations also led to production of divarinic acid, the ethyl variant of olivetolic acid, and more orsellinic acid.

4.3 Genome Mining for Homologous Clusters Results and Discussion

We also further utilized genome mining to elucidate new clusters producing olivetolic acid analogs. As previously detailed, we had identified three clusters homologous to the *Metarhizium anisopliae* cluster containing the Ma_OvaA, Ma_OvaB, and Ma_OvaC genes. As described, we identified the *Tolypocladium inflatum* and *Metarhizium rileyi* clusters in which heterologous expression produced the same product profile as *Metarhizium anisopliae* albeit at lower titers and the *Talaromyces islandicus* cluster which selectively produced olivetolic acid. From the percent identity comparisons between the enzymes, we determined that clusters harboring close to 50% or less homology to the *Metarhizium rileyi* cluster would produce the greatest variety in products different from the product profile of the *Metarhizium anisopliae* cluster. Equipped with this knowledge, we utilized the Targeted Genome Mining Information Finder (TGIF) program, a MATLAB based program develop by Dr. Nicholas Liu, an alumnus of the Tang lab. Employing MATLAB's Bioinformatics Toolbox which includes the ability to use Basic Local Alignment Search Tool (BLAST) to analyze FASTA formatted sequences, Dr. Liu developed a program to elucidate possible biosynthetic gene clusters (BGCs) based on a target queried for. Although this program was developed to query for target resistance gene clusters, it can be used for a variety of different purposes. We employed the program to query for tandem polyketide synthases and used the Tang lab's in-house fungal strain list as the database. We elucidated a cluster in *Penicillium thomii* containing 48%, 41%, and 36% homology to Ma_OvaA, Ma_OvaB, and Ma_OvaC, respectively. We heterologously expressed this cluster in

Aspergillus nidulans and produced the nonyl olivetolic acid variant with a diene at the C1 and C3 positions of the alkyl chain as well as the heptyl variant unsaturated at the C3 position of the alkyl chain and a hydroxy group at the C2 position, both of which are non-native to the *Cannabis sativa* plant and therefore can be further processed to new to nature cannabinoids.(Figure 19)

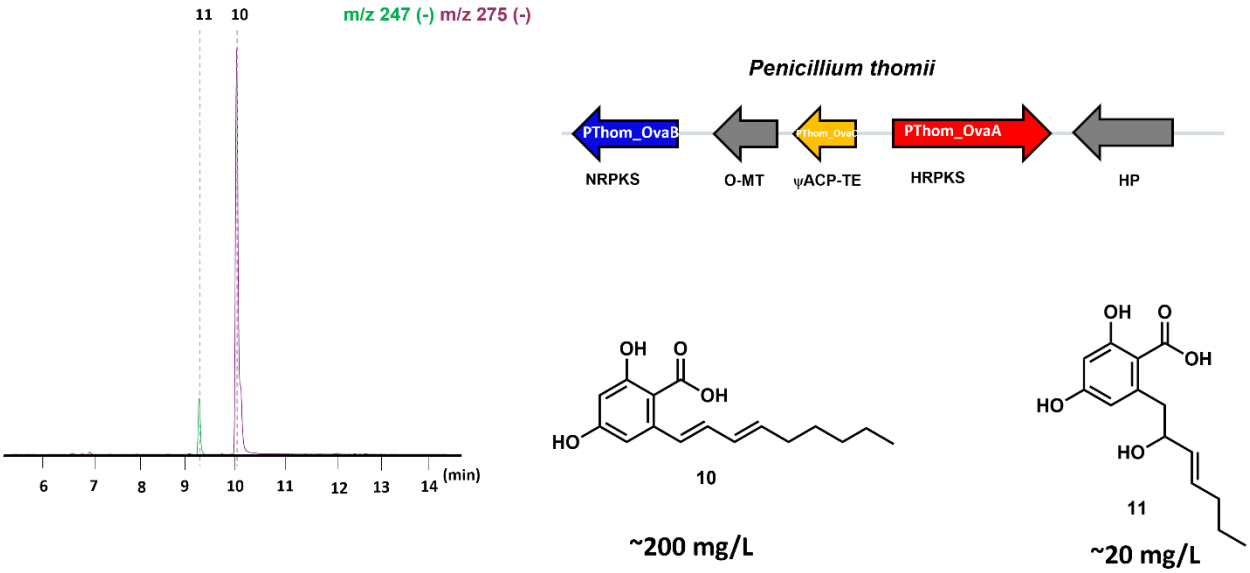

Figure 19. Heterologous Expression of Pthom_OvaABC Results. Heterologous expression in *A. nidulans* produced the diene nonyl olivetolic acid variant and a heptyl variant harboring a hydroxy group at the C2 position of the alkyl chain and unsaturation at the C3 position of the alkyl chain..

4.4 Conclusion

We have detailed ways in which we were able to be diversify our product profile to produce rare olivetolic acid analogs. There are still more mutations near the active site of the KS domain as well as the AT domain that can be made to produce even more olivetolic acid analogs with different alkyl chain lengths. With regards to homologous cluster expression, we only searched through the100+ sequenced fungal strains that we have. Therefore, there is a large number of fungal strains that can be queried to search for homologous clusters that can produce

rare olivetolic acid analogs. Testing of these variants and the ones produced utilizing the Living Biofoundry can lead to potentially promising results with regards to biological activities.

5. Attempts to Go Downstream of the Cannabinoid Biosynthetic Pathway

5.1 Introduction to Cannabigerolic Acid (CBGA)

As previously detailed, microbial production of naturally occurring and novel cannabinoids has potential to be a disruptive technology to the ~$10 billion global cannabis industry. From olivetolic acid, the next step in the cannabinoid biosynthetic pathway is the geranylation of olivetolic acid to produce cannabigerolic acid (CBGA), known as "the mother of all cannabinoids"[146] CBGA can be decarboxylated to form cannabigerol (CBG), a cannabinoid with intriguing therapeutic potential. In the *Cannabis sativa* plant, CBG is produced in larger quantities in the early stage of the plant but in minute quantities (1%) in the mature stage of the plant. Preliminary research has indicated that CBG is non-psychoactive but has anti-oxidant, antimicrobial, anti-inflammatory, anticancer, photoprotective, and appetite-enhancing properties.[147] Studies on the effect of CBG on the cannabinoid receptors have shown that CBG is a partial agonist for the CB_2 receptor but cannot bind to the CB_1 receptor, hence its non-psychoactive properties.[148] As previously described, the CB_2 receptors are primarily located in the nervous system and agonists of the receptors provide anti-inflammatory and anti-oxidant effects. CBG was first isolated in 1970 and was fully characterized shortly after.[149] We therefore sought to produce this cannabinoid microbially. To do so, we had to identify the prenyltransferase responsibly for geranylating the C_2 carbon position of olivetolic acid. This prenyltransferase activity was first demonstrated in the *Cannabis* plant and was proposed to be

attributed to cannabis sativa prenyltransferase 1 (CsPT1) and was soon patented. However, when Luo et al heterologously expressed CsPT1 in *Saccharomyces cerevisiae*, they observed no activity. Therefore, they mined for prenyltransferases with predicted activity similar to CsPT1 and heterologously expressed those candidate prenyltransferases. They demonstrated that the *Cannabis sativa* prenyltransferase 4 (CsPT4) was able to successfully prenylate olivetolic acid to produce CBGA. CsPT4 was found in the *Cannabis sativa* plant and is part of the UbiA-membrane bound family of prenyltransferases, predicted to contain eight transmembrane helices. When expressed in *Saccharomyces cerevisiae*, and with the plastid targeting amino acid sequence removed, the CsPT4 enzyme was found to be located in the microsomal fractions of the yeast strain. Luo et al performed *in vitro* assays with the microsomal fraction harboring CsPT4 and demonstrated that the enzyme displayed Michaelis Menten behavior when olivetolic acid concentration varied whilst GPP (geranyl pyrophosphate) concentration stayed constant but deviated from Michaelis Menten behavior when olivetolic acid concentration was held constant while GPP concentration varied.[38]

5.2 Aromatic Prenyltransferases

Aromatic prenyltransferases capable of geranylating olivetolic acid to produce CBGA outside of the *Cannabis sativa* plant have also been discovered. There are three classes of aromatic prenyltransferases: ABBA-type prenyltransferases, UbiA-type prenyltransferases, and dimethylallyl tryptophan synthase (DMATS)-type prenyltransferases. ABBA-type and DMATS-type prenyltransferases are found in bacteria and fungi and UbiA-type prenyltransferases are found in fungi, plants, and bacteria. These aromatic prenyltransferases catalyze formation of carbon nitrogen, carbon oxygen, and carbon-carbon bonds between the prenyl donor's carbon

and the aromatic substrate.[150] ABBA-type and DMATS-type have been elucidated as soluble aromatic prenyltransferases while UbiA prenyltransferases are membrane bound aromatic prenyltransferases.

5.2.1 UbiA-type prenyltransferases

UbiA-type prenyltransferases are membrane bound prenyltransferases found in a variety of organisms such as bacteria, fungi, plant, human, etc. These prenyltransferases have been observed to be involved in menaquinone and ubiquinone biosynthesis as well as fungal meroterpenoid biosynthesis, archaeal membrane lipid biosynthesis, and prenylated aromatic secondary metabolites biosynthesis in plants, among other biosynthesis reactions. These UbiA-type prenyltransferases typically contain eight to nine transmembrane helices. Regarding their structure, enzymes in the family contain two conserved aspartate rich motifs (NDXXDXXXD and DXXXD) with the first used for Mg^{2+} binding in order to catalyze the reaction; therefore, these prenyltransferases are metal dependent.[151,152]

5.2.2 DMATS-type Prenyltransferases

DMATS-type prenyltransferases have been elucidated in fungal and bacterial species. These aromatic prenyltransferases are metal independent although addition of metal ions like Ca^{2+} and Mg^{2+} have been reported to have enhanced the catalytic activities of several of these prenyltransferases.[153] DMATS-type prenyltransferases primarily act upon indole derivatives such as tryptophan, indole terpenoids, and cyclic dipeptides that contain tryptophan by prenylating these compounds. Reports have demonstrated that DMATS-type prenyltransferases have the ability to prenylate all positions of the indole ring and characterization of its structure have revealed that these prenyltransferase also have the α-β-β-α prenyltransferase folds that ABBA-

type prenyltransferases have.[154,155] Similarly to ABBA-type prenyltransferases, DMATS prenyltransferases show selectivity in prenyl donor, with most enzymes in the family utilizing dimethylallyl pyrophosphate (DMAPP) for prenylation, but have great flexibility with regards to prenyl acceptor, capable of prenylating not only those indole derivative previously mentioned but also xanthones, tricyclic and tetracyclic aromatic compounds, and tyrosine.[152]

5.2.3 ABBA-type Prenyltransferases

ABBA-type prenyltransferases are found in both fungi and bacteria. They primarily utilize DMAPP and geranyl pyrophosphate (GPP) as the prenyl donor. All the members of the ABBA-type family of prenyltransferases, except for NphB, do not need metal to assist in catalyzing the reaction. Although CloQ from S*treptomyces roseochromogenes* var. *oscitans* was the first member of the ABBA family of prenyltransferases to be discovered, NphB was the first in the family to have its crystal structure. The crystal structure revealed a structure containing an unique three dimensional α-β-β-α prenyltransferase fold, hence the name ABBA.[156]

NphB, a member of the ABBA family of prenyltransferases, from the bacteria *Streptomyces sp.* CL190 was discovered to have non-specific prenylation activity for the formation of CBGA.[157] These prenyltransferases are soluble and are capable of catalyzing the transfer of dimethylallyl (C5), geranyl (C10), or farnesyl (C15) prenyl groups onto a diverse set of electron-rich aromatic acceptors. Genome mining for analogs to CloQ, the first gene identified as part of the ABBA family of prenyltransferases, led to the discovery of NphB in *Streptomyces sp.* CL190.[153] Wildtype NphB is specific in prenyl donor, preferring the geranyl group but is promiscuous with regards to aromatic acceptor although the major substrate is 1,6-dihydroxynapthalene.[154] Wildtype NphB was shown capable of prenylating olivetolic acid to

CBGA although at low catalytic efficiencies (kcat = .0021+.00008 min^{-1}).[39] Wildtype Nphb was also non-specific in prenylation of OA, capable of producing not only CBGA when reacted with GPP but also 2-O-geranyl olivetolate.[154] Therefore Valliere et al. preformed mutations on NphB to increase specificity for the production of CBGA. They docked the olivetolic acid structure to the NphB crystal structure and then utilizing Rosetta, developed a 22-construct library, constructed the library, and screened for CBGA production. They identified two amino acid mutations that greatly increased specificity to CBGA. From the initial library, then they constructed a focused library and discovered that all but one of the mutations in the focused library had 100-fold higher activity than wildtype NphB with regards to kcat value. Ultimately, they determined that their two best mutations were Y288AG266S and Y288VA232S. Both mutations selectively produced CBGA and both had kcat values 1000-fold higher than the wildtype. Valliere et al. demonstrated that they were capable of producing 1.25g/L of CBGA in a cell free manner utilizing their mutated NphB enzyme.[39]

5.3 Attempts to Achieve CBGA Production Results and Discussion

Based on the Tang's lab collaboration with the Bowie lab, from where Valliere et al developed the mutated NphB enzyme, and the company that he helped found, Invizyne, we were given the mutated NphB enzyme which we used in order to test its ability to prenylate the olivetolic acid analogs *in vitro* as well as test for functional expression *in vivo.* We purified the enzyme and performed *in vitro* assays with our olivetolic acid analogs and GPP. Based on LC-MS/HPLC data, NphB was able to prenylate olivetolic acid analogs that we produced as well as other analogs bought commercially, although the final prenylated products were not confirmed by NMR. However, the CBGA product produced by the NphB reaction with olivetolic acid and

GPP was confirmed by an analytical standard. Additionally, based on the masses of the *in vitro* assays, we observed an interesting trend: the shorter alkyl chain variants reacted with NphB and GPP generated not only the C_3 geranylated product but also the C_3 geranylated product with an O-geranylation. As the alkyl chain length increased, the less appearance of this double geranylated product, with the C_3 geranylated product being the major product. (Supplementary) We then tested for the functional expression of NphB *in vivo* in *Aspergillus nidulans*.

We heterologously expressed NphB and the GPP synthase enzyme vrtD from *Penicillium aethiopicum*[158], along with Ma_OvaA, Ma_OvaB, and Ma_OvaC in *Aspergillus nidulans,* expecting to observe the CBGA and CBGA analog products. However, we did not observe any of the geranylated products. We also heterologously expressed Nphb and vrtD with Ti_OvaA, Ti_OvaB, and Ti_OvaC in *Aspergillus nidulans* and did observe production of CBGA but it was very minute. We additionally expressed CsPT4 as well as an aromatic prenyltransferase from *Aspergillus terreus* (ApAT) recorded to have prenylation activity *in vitro* [159] with our platform. However similar to NphB, we observed no production of CBGA. These results led us to postulate that the enzymes are not being properly expressed in *A. nidulans,* especially engineered NphB, after all a bacterial gene; therefore, we sought to look at its transcription. We performed mRNA extraction on the *Aspergillus nidulans* strain transformed with Ti_OvaA, Ti_OvaB, Ti_OvaC, vrtD, and NphB and obtained the cDNA and performed a PCR of the cDNA and observed bands for both vrtD and NphB, the two genes we were investigating. We then purified the bands and sent them out for sequencing in the case that the genes may be mutated but the sequenced results displayed no mutations.

With this information in mind, we decided to perform the NphB reaction with GPP and olivetolic acid using *A. nidulans* lysates expressing NphB. Zirpel et al. had demonstrated that

whole cell bioconversion in *Saccharomyces cerevisiae* expressing wildtype NphB, olivetolic acid, and GPP did not produce CBGA; however, employing lysates of that same *Saccharomyces cerevisiae* strain in assays with supplemented GPP and olivetolic acid did produce CBGA as well the O-geranylated analog.[154] Therefore we used *A. nidulans* lysates expressing NphB and supplemented olivetolic acid and GPP and we did observed CBGA production, much greater than what was observed *in vivo*. (Figure 20). We concluded therefore, that from the transcription and lysate data, that NphB was in fact correctly expressed in *A. nidulans* and that the issue could be low availability of GPP or that NphB is localized away from olivetolic acid and/or GPP.

Figure 20. *A. nidulans* Lysates Expressing NphB Reaction Results. A. nidulans lysates expressing NphB with supplementation of GPP converted olivetolic acid to cannabigerolic acid efficiently, much greater than *in vivo*. There was no observation of CBGA, however, when GPP was not supplemented

To further explore the issue of localization, we tagged the NphB enzyme C-terminal with green fluorescent protein (GFP) using a flexible 5 amino acid linker (GGSGG). Microscopic

images of the tagged NphB enzyme in *A. nidulans* displayed that the NphB was not localized in any punctuate organelles but rather was localized all throughout the fungal body indicating that the enzyme is located in the cytoplasm. (Figure 21) As previously described, most of olivetolic acid and its analogs produced from our platform are found in the media indicating that the compounds are being secreted from the fungal body and therefore, olivetolic acid and its analogs go through the secretory channel in *Aspergillus nidulans* into the media. Therefore, we sought to localize the NphB to where GPP and the compounds were. We had to then understand where GPP was localized.

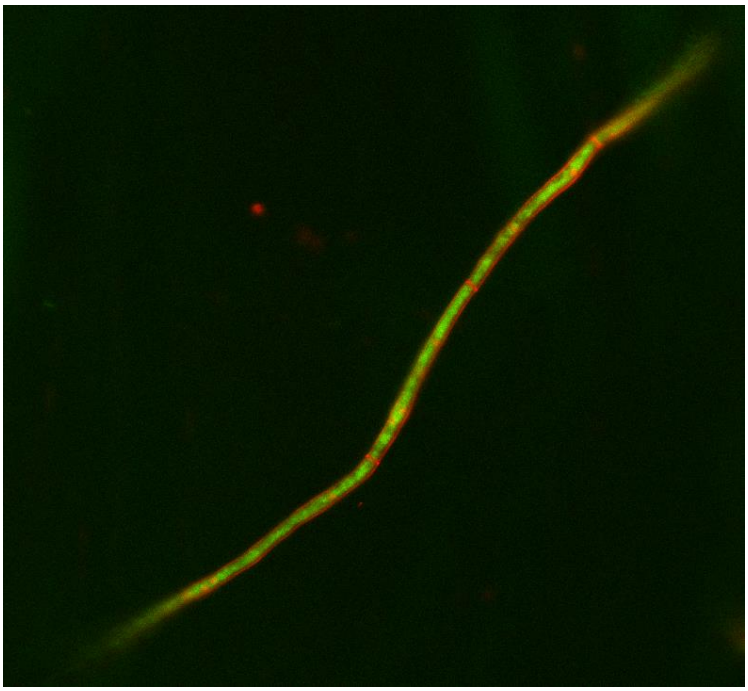

Figure 21. Microscopic Image of *Aspergillus nidulans* Expressing GFP Fused C-terminal to NphB. 147.6 x 147.6 micron. Nuclei staining Hoescht dye was added in order to locate the nuclei (red circles). The red rings are septa: internal cell well that separate the hyphae.

Further genome mining in our lab for prenyltransferases harboring activity to produce CBGA from olivetolic acid and GPP, revealed a prenyltransferase similar to the ascA prenyltransferase from *Acremonium egyptiacum*, found in *Colletotrichum higginsianum*. This

enzyme was discovered by Colin Johnson, a graduate student in the Tang Lab. The ascA prenyltransferase, a prenyltransferase belonging to the UbiA family, from *Acremonium egyptiacum* has been characterized to prenylate orsellinic acid with a farnesyl group.[160] However, we demonstrated that the prenyltransferase from *Colletotrichum higginsianum*, labeled colA, was able to prenylated orsellinic acid with a geranyl group instead of a farnesyl group which is ideal since CBGA contains a geranyl group as opposed to a farnesyl group. Colin had searched through databases of isolated fungal products for C3 geranylated β-resorcylic moieties. He was able to find a couple compounds known as Colletorin B and Colletotrichum B that fit the description. Through genome mining, he was able to identify the cluster producing these compounds which contained a NRPKS, an NRPKS-like enzyme, a halogenase, and UbiA-like prenyltransferase which he labeled colA. (Figure 22) Therefore, the colA gene was seen as a good candidate to test its ability to prenylate olivetolic acid and its analogs to CBGA and its analogs. Heterologous expression of colA with Ma_OvaA, Ma_OvaB, and Ma_OvaC as well as heterologous expression of colA with Ti_OvaA, Ti_OvaB, and Ti_OvaC unfortunately showed no production of prenylated olivetolic acid, unsaturated olivetolic acid, sphaerophorolcarboxylic acid, or prenylated unsaturated sphaerophorolcarboxylic acid; however, production of geranylated orsellinic acid was observed. Further probing through the literature indicated that *Aspergillus nidulans* harbors an endogenous biosynthetic pathway responsible for the production of orsellinic acid[161] explaining the geranylated orsellinic acid result. Furthermore, the production of geranylated orsellinic acid did indicate that the GPP pool in *Aspergillus nidulans* is sufficient answering our concerns and therefore further indicating that localization is the key reason why NphB has not been shown effective in *Aspergillus nidulans*.

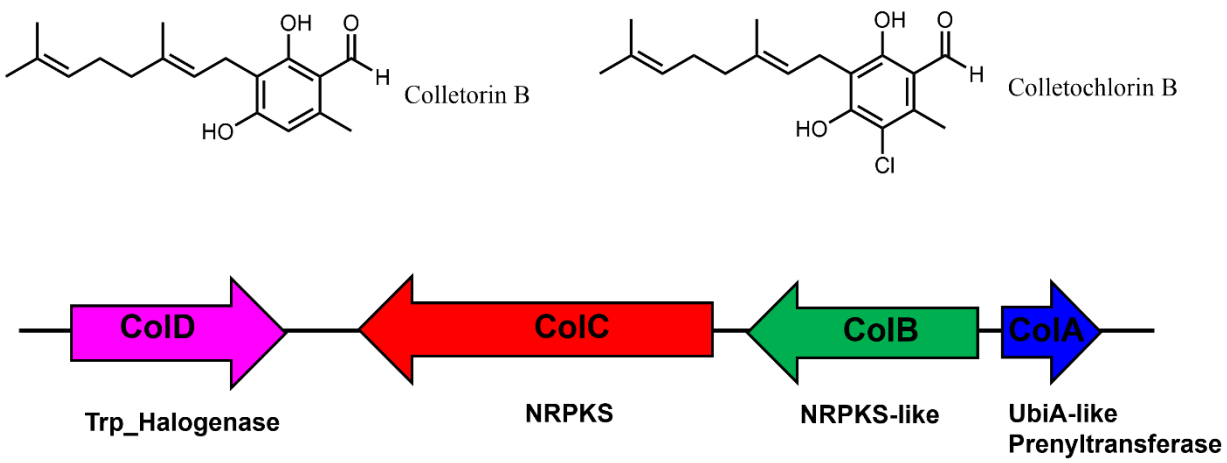

Figure 22. Elucidated Biosynthetic Gene Cluster for Colletorin B and Colletochlorin B. The BGC for Colletorin B and Colletochlorin B contains a halogenase, NRPKS, NRPKS-like enzyme, and a UbiA-like Prenyltransferase deemed colA. ColA is responsible for geranylating the aromatic ring at the C3 position.

ColA, a UbiA-prenyltransferase predicted to have seven transmembrane domains, could therefore not be purified and was subjected to feeding studies in both *Saccharomyces cerevisiae* and *Aspergillus nidulans*. *Saccharomyces cerevisiae* and *Aspergillus nidulans* strains expressing colA were supplemented individually with 200 µM orsellinic acid, 200 µM divarinic acid, 200 µM olivetolic acid and 200 µM sphaerophorolcarboxylic acid. The *Saccharomyces cerevisiae* feeding results demonstrated that colA was very efficiently able to prenylate orsellinic acid and to a lesser extent divarinic acid but although able to prenylate olivetolic acid and sphaerophorolcarboxylic acid, at very low efficiencies. *A. nidulans* feed results demonstrated that similar to *S. cerevisae*, colA was able to efficiently prenylate orsellinic acid: however, less so divarinic acid and prenylation of olivetolic acid and sphaerophorolcarboxylic acid was not observed. The differences between the feeding results of *S. cerevisiae* and *A. nidulans* were

attributed to the fact that the *S. cerevisiae* strain was much more heavily engineered with regards to optimization of pathways than the *A. nidulans* strain and therefore was more optimal for secondary metabolite production.

Prediction software (TMHMM 2.0)[162] indicated that the colA gene had its transmembrane domains localized in the endoplasmic reticulum (ER). Additionally, regarding the mevalonate pathway responsible for the production of the intermediate GPP, one key enzyme in the pathway, hydroxymethylglutaryl-coenzyme A reductase (HMG-CoA reductase), a rate determining enzyme responsible for the conversion of HMG-CoA to mevalonate[163] was also predicted by TMHMM 2.0 to be located in the ER, which we hypothesize explained why colA was able to geranylate orsellinic acid and divarinic acid and why NphB, located in the cytoplasm, was unable to geranylate any B-resorcylic acid *in vivo*. Faced with the difficulty that the engineered NphB which is able to efficiently geranylate olivetolic acid to CBGA is not able to do so *in vivo* based on localization issues and the issue that colA which is able to utilize GPP to prenylate orsellinic and divarinic acid *in vivo* but not longer alkyl chain variants, we decided therefore that fusion of the NphB enzyme C-terminal to colA would solve the localization problem, allowing NphB to utilize GPP to efficiently prenylate olivetolic acid and sphaerophorolcarboxylic acid. Once again, employing a flexible linker (GGSGG), we fused NphB C-terminal to colA and heterologously expressed the fusion product with both the Ma_OvaA, Ma_OvaB, Ma_OvaC and Ti_OvaA, Ti_OvaB, and Ti_OvaC set of genes in *Aspergillus nidulans* . LCMS traces of heterologous expression results did show that CBGA was in fact produced further indicating that localization was the key issue, but the CBGA production was at low levels which was perplexing. (Figure 23)

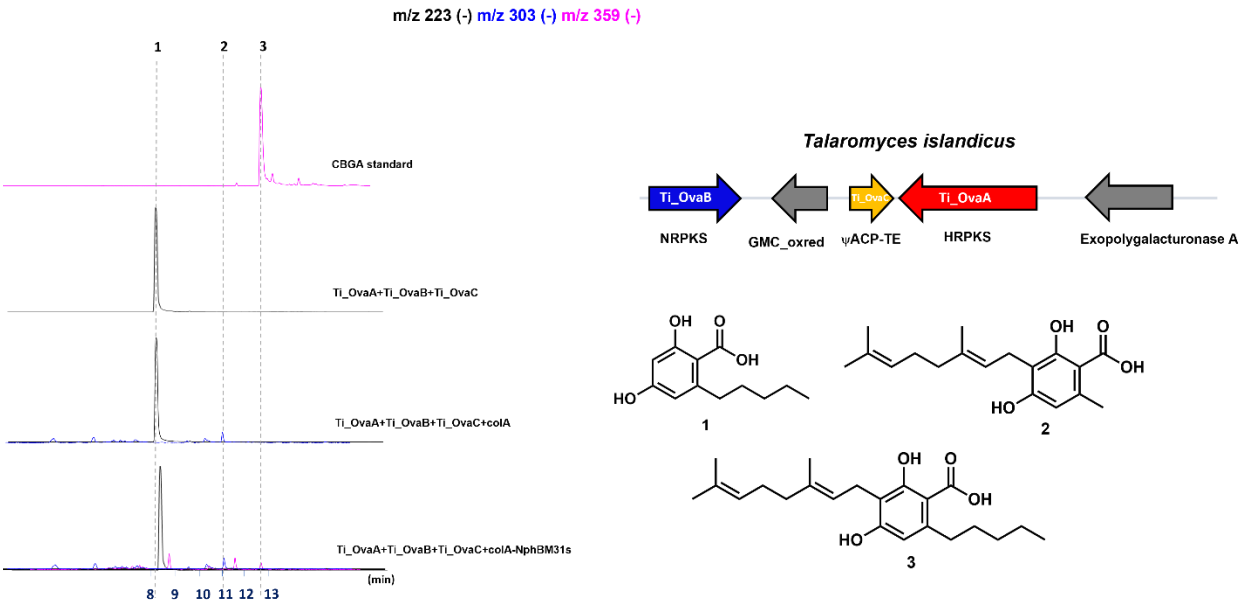

Figure 23. Heterologous Expression of Ti_OvaABC with ColA and ColA-NphB Fusion Results. Heterologous expression of Ti_OvaA+Ti_OvaB+Ti_OvaC with colA led to production of geranylated orsellinic acid and Heterologous expression of Ti_OvaA+Ti_OvaB+Ti_OvaC with the colA-NphB fusion construct produced the geranylated orsellinic acid as well as CBGA, although at low amounts

We purposed then to utilize this fusion approach with a wide variety of endogeneous *A. nidulans* enzymes localized in various membranes in the cell with the thought that there was possibly another region where the compounds and GPP were localized. We fused the NphB C-terminal to three other endoplasmic reticulum localized proteins: HMG-CoA reductase previously described, sec12p, the guanine nucleotide exchange factor (GEF), specific for the SAR1 gene which acts as a regulator of COPII vesicle budding from ER exit sites (ERES)[164], sec63p, encoding a protein essential for secretory protein translocation into the ER.[165] In addition to localizing NphB to the ER, we also localized the enzyme to the peroxisome employing the peroxisome targeting signal 1 (PTS1)[166] as well as to the nucleus using a nuclear localization signal (NLS)[167]. Not only did we localize NphB to the ER, peroxisome, and nucleus, we also fused the protein C-terminal to the mitochondria protein acetyl-CoA acyltransferase, responsible

for converting 2 units of acetyl-CoA to CoA and acetoacetyl-CoA molecules.[168] Lastly, we fused NphB to C-terminal to the plasma membrane protein tmpA, an oxidoreductase involved in the A. nidulans conidiation pathway.[169] (Figures 24 and 25) Similar to the colA-NphB construct, heterologous expression of all these tagged and fusion constructs were expressed in combination with Ti_OvaA, Ti_OvaB, and Ti_OvaC, the set of enzymes responsible for predominately producing olivetolic acid. LC-MS trace results showed that similar to the colA-NphB results, that in most of the fusion and localization tagged constructs, CBGA production was observed but at low levels. This could be due to the fact that NphB may not be folding as well in the fusion construct. Therefore, there is continued need to mine for other prenyltransferases.

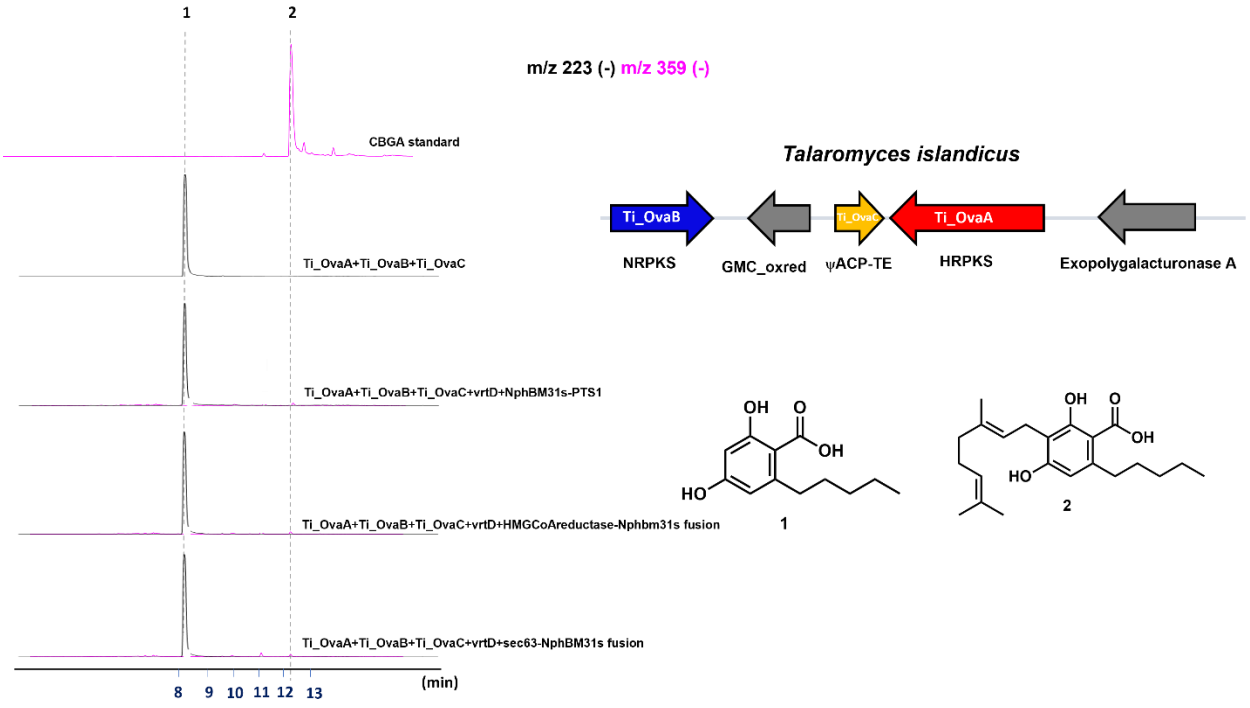

Figure 24. Heterologous Expression of NphB Fusion Constructs Results. Heterologous expression of Ti_OvaABC with NphB with the PTS1 peroxisome targeting signal, NphB fused with HMG CoA-reductase, and NphB fused with the sec63 protein produced low amounts of CBGA

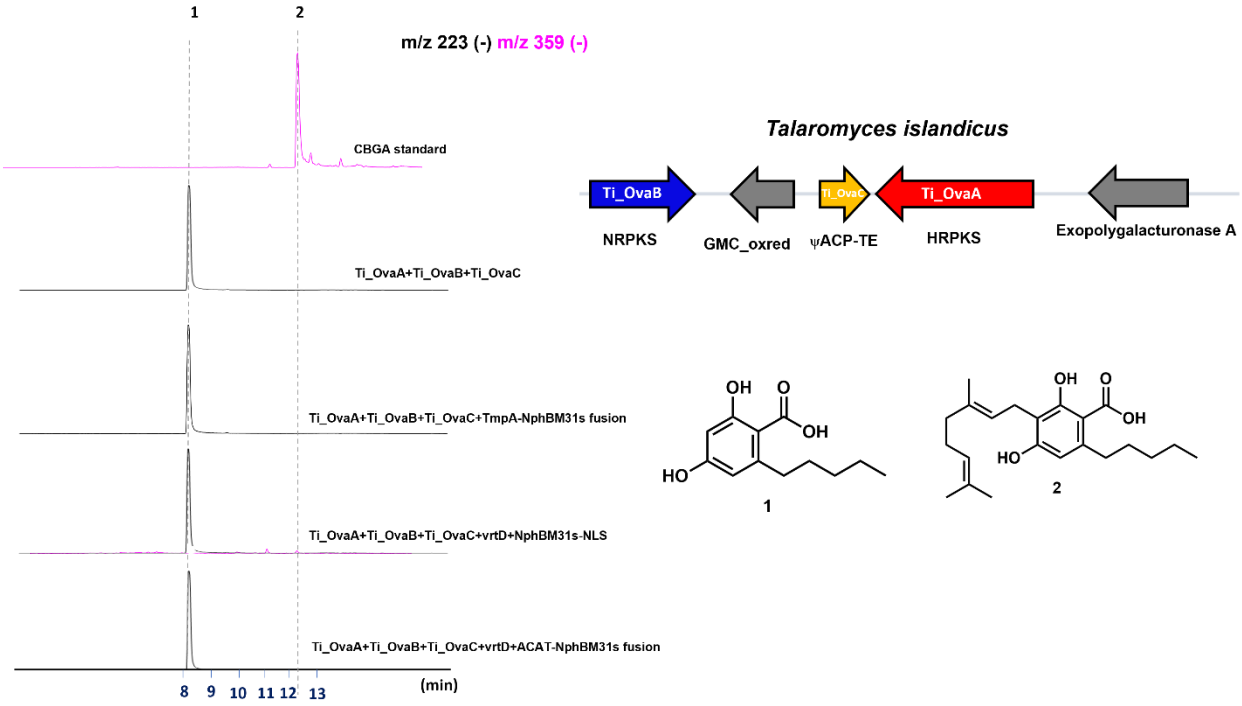

Figure 25. Heterologous Expression of NphB Fusion Constructs Results Part 2. Heterologous expression of Ti_OvaABC with NphB fused to tmpA and NphB fused with acetyl-coA acyltransferase protein produced no quantifiable amounts of CBGA while heterologous expression of Ti_OvA+Ti_OvaB+Ti_OvaC with NphB with the nuclear localization signal produced low amounts of CBGA

Blasting the colA enzyme across NCBI based genomes yielded a hit in the genome of *Talaromyces islandicus* having 55% identity to colA. Heterologous expression of this UbiA-type prenyltransferase from *Talaromyces islandicus*, labeled TislaUbiA, with the Ti_OvA, Ti_OvaB, and Ti_OvaC enzymes in *Aspergillus nidulans* showed the expected CBGA methyl variant result as well as prenylated olivetolic acid, albeit small, a result not observed with colA. (Figure 26) Therefore, with four fungal genes, we were able to access those two cannabinoids, a result not observed before without utilizing genes from the *Cannabis sativa* plant. To increase the CBGA production utilizing the TislaUbiA enzyme, we would need to perform mutations in the active site of the enzyme responsible for binding to the aromatic prenyl acceptor. To do this, we had to identify the active site. TislaUbiA, colA, and CsPT4 are all UbiA prenyltransferases, membrane

embedded prenyltransferases harboring two aspartate rich motifs associated for the divalent, cation-dependent prenylation.[148] A crystal structure of archaeal UbiA in both its substrate bound and apo form was elucidated by Cheng et al. Cheng et al were able to obtain a 3.3 (angstrom) crystal structure of the archaeal organism *Aeropyrum* pernix UbiA (ApUbiA) The group observed that the structure of the enzyme contained nine transmembrane helices arrange counterclockwise with a large central cavity. They also obtained a 360° crystal structure of ApUbiA in a substrate bound state, with the substrates p-hydroxybenzoic acid (PHB) and geranyl thiolpyrophosphate (GSPP) activated with magnesium ions. In the crystal structure, GSPP was bound in the central cavity and a small basic pocket near the GSPP binding site was determined to be binding pocket for PHB binding. With this in mind, Cheng et al performed mutations to determine which amino acids were critical for binding. For the PHB binding pocket site, they determined that Arg43 and Asn50 were both critical to PHB binding.[148] We therefore used this information to generate mutations for TislaUbiA with the purpose of opening the small basic pocket to accept large ß-resorcylic acid moieties. Using Alphafold, we generated a structural model for our TislaUbiA enzyme and comparted it to ApUbiA. The next steps, then would be to select for mutations that we postulate would open the binding pocket.

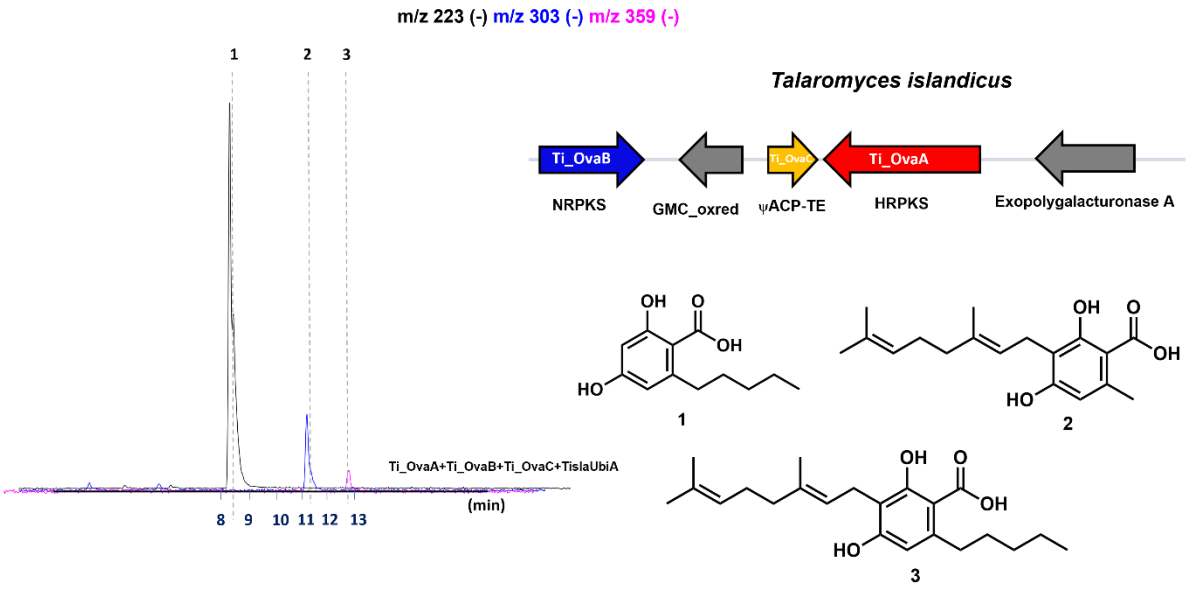

Figure 26. Heterelogous expression of Ti_OvaABC+TislaUbiA Results. Heterologous expression of Ti_OvaABC with TislaUbiA led to production of CBGA as well as the methyl variant of CBGA.

Going back to *Saccharomyces cerevisiae*, we tested to see if we were able to achieve functional expression of CsPT4, the prenyltransferase from *Cannabis sativa* that Luo et al. characterized. We had decided to continue production of the cannabinoid biosynthetic pathway in our model engineered *A. nidulans* host due to the high titers of olivetolic acid and its analogues that we were producing. We were unsure if changing the platform to *S. cerevisiae* would replicate the high titer production. Similar to Luo et al, we removed the N-terminal chloroplast targeting sequence of CsPT4. We heterologously expressed the enzyme in our *S. cerevisiae* super strain and subjected the transformed strain to feeding assays. We fed 200 µM of orsellinic acid and 200 µM of sphaerophorolcarboxylic acid and observed geranylation of both. We then heterologously expressed Ma_OvaA+Ma_OvaB+Ma_OvaC with CsPT4 and observed the results. We were able to produce the heptyl version of CBGA at moderate to high titer quantities, an exciting result since this is the direct precursor to THCP. (Figure 27) We also saw that although we did take a hit in titer when we moved our platform to *S. cerevisiae*, we were

still able to produce about 500 mg/L of SA. We then sought to achieve functional expression of THCAS.

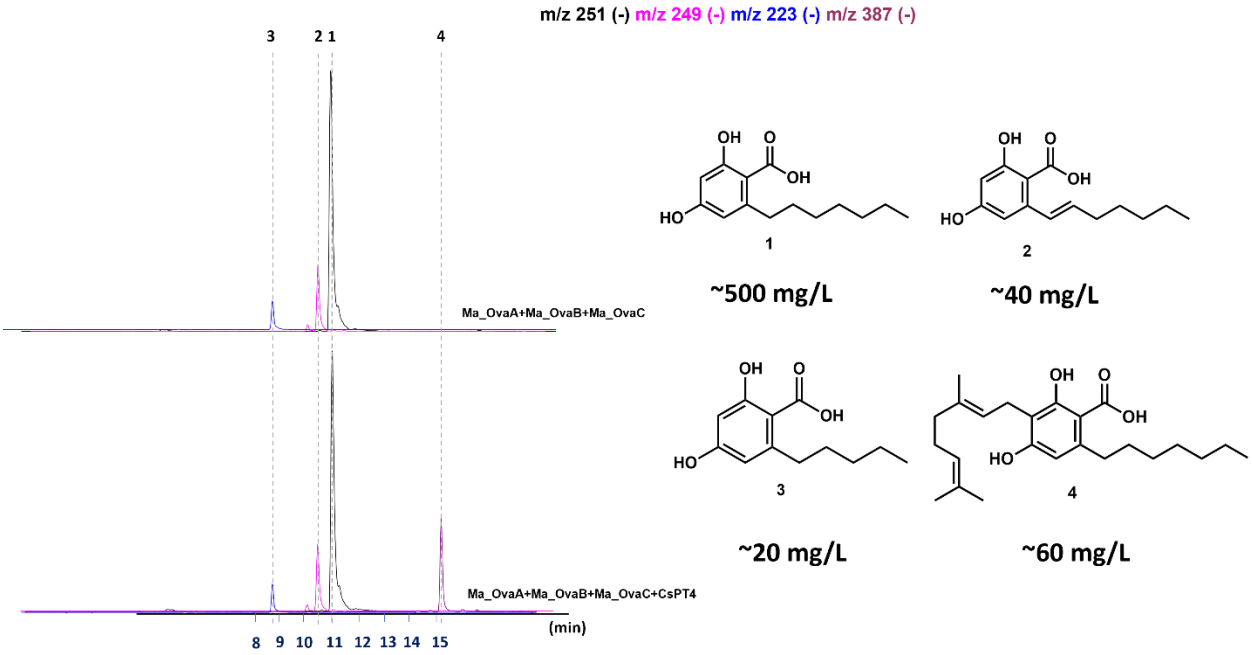

Figure 27. Heterologous Expression of Ma_OvaABC with CsPT4 in *S. cerevisiae* Results. Production of the heptyl variant of CBGA was observed at moderate to high titer quantities.

5.4 Introduction to Tetrahydrocannabinolic Acid (THCA) and Cannabidiolic Acid (CBD)

Production of the elaborated cannabinoids from CBGA involves the use of just one cyclase enzyme, with the final elaborated cannabinoid structure dependent on the cyclase enzyme employed. There are three elucidated dedicated cyclase enzymes from the *Cannabis* plant capable of cyclizing CBGA to the final cannabinoid: tetrahydrocannabinolic acid synthase (THCAS), which forms tetrahydrocannabinolic acid (THCA) from CBGA, cannabidiolic acid synthase (CBDA), which forms cannabidiolic acid (CBDA) from CBGA, and cannabichromenic acid synthase (CBCAS) which forms cannabichromenic (CBCA) acid from CBGA. All three of these oxidocyclase enzymes are part of the berberine-bridge enzyme (BBE)-like family of enzymes, harboring a flavin adenine dinucleotide (FAD)-binding domain, a substrate-binding

domain, an N-terminal signal peptide, and a BBE-like C-terminus part of the FAD-binding module.[170] THCAS and CBDAS have been more studied and characterized than CBCAS, although CBCAS's high sequence similarity (92%) with THCAS suggests it shares similar biological activities.[171] With regards to localization and expression in the *Cannabis sativa* plant, CBDAS and THCAS have been demonstrated to be catalytically active in the glandular trichome's extracellular cavity and need FAD as well as oxygen in order to functionally express.[172,173] In contrast, the CBCAS enzyme is not oxygen dependent and can also be inhibited by hydrogen peroxide.[174]

As mentioned, THCAS and CBCAS share a 92% sequence similarity with each other, whereas THCAS and CBDAS are 84% identical to each other and CBCAS and CBDAS are 83% identical to each other; therefore, all three cyclase enzymes have high sequence similarity with each other. Sequence analysis of variants of the cyclase enzymes indicated that CBDA is likely the ancestral enzyme from which THCAS evolved from. Further sequence analysis of THCAS showed a flavinylation consensus sequence (Arg^{110}-Ser-Gly-Gly-His^{114}) with His^{114} being the likely FAD-binding site, exhibiting similarity to CBDAS in this regard.[167] Since both CBDAS and THCAS are flavinated enzymes, it is postulated that they have the same reaction mechanism. With regards to CBCAS, although much is unknown, it has been reported that based on its kinetic data , CBCAS has higher affinity for CBGA than both THCAS and CBDAS.[175] These oxidocyclase enzymes are only capable of enzymatically acting up CBGA, not the decarboxylated CBG product.

5.5 Achieving Functional Expression of THCAS`

Due to the reported potent biological activity of THCP, the heptyl analog of THC, we determined to focus on achieving function expression of THCAS in our platform since our novel

platform produces the heptyl variant of olivetolic acid. As previously described, THCP was isolated from the Cannabis plant in small quantities in 2019 with pharmacological data showing that THCP has a K_i to CB_1 of 1.2 mM, and a K_i to CB_2 of 6.2 mM, ~ 30 and 6 times more effective in binding than THC, respectively.[102] Even the THCA molecule, although unlike its decarboxylated form THC, is not psychoactive, has been investigated for its neuroprotective, anti-neoplastic, immunomodulator, and anti-inflammatory effects[176] further making the pursuit and optimization of *in vivo* functional expression of THCAS a priority.

Different groups have reported of engineering strains from *Saccharomyces cerevisiae* and *Komagataella phaffi* capable of functional expression of THCAS. Zirpel et al. demonstrated through the engineering of THCAS, optimization of culturing conditions, and overexpression of helper proteins, 83% conversion of CBGA to THCA in *Komagataella phaffi*. Zirpel et al were first able to obtain functional expression of THCAS in both *S. cerevisiae* and *K. phaffi* by utilizing a signal peptide from the vacuolar proteinase, proteinase A. The group cleaved the 28 amino acid N-terminal plastid signal peptide from the THCAS and inserted the proteinase A signal peptide. Additionally, they knocked out the proteinase A gene in both strains, responsible for degrading genes targeted to the vacuole. With functional expression in both yeast strains achieved through this process, they sought to optimize culturing conditions.[176] The group assayed the strains at different temperatures and times and observed that the highest intracellular activity of THCAS was achieved at 15°C for 192 hours. The temperature of the expression was the key change from other groups which had expressed THCAS at 30°C and 37°C. The expression of THCAS at 15 °C increased volumetric THCAS by 6350%. Additionally concerning culturing conditions, Zirpel et al observed that addition of casamino acids, biotin, riboflavin, and yeast nitrogen base further increased THCAS functional expression. Lastly, the

overexpression of ER chaperones, Kar2p, CNE1p, the Pd1p foldase, the unfolded protein activator (HAC1s), as well as the FAD synthetase (FAD1) increased functional expression of THACS in *K. phaffi*, with the expression of HAC1p, having the greatest impact, increasing functional expression 4-fold.[177]

Through implementation of these concepts, we achieved functional expression of THCAS in our *Saccharomyces cerevisiae* strain. We already had obtained a *S. cerevisiae* strain with the pep4 knockout, so with transformation of the THCAS gene with the proA signal and with feeding CBGA, we observed production of THCA in YPD (yeast extract peptone dextrose) media at 30°C. To increase functional expression, we added 13.8g/L yeast nitrogen base and 5 g/L casamino acids into the YPD media and observed a slight increase in production. To further increase expression, we overexpressed the HAC1p with the THCAS in our S. cerevisiae strain and observed a notable increase in production. We also then tested the temperature similar to Zirpel et al. The initial THCAS functional expression assays were done in media cultured at 30°C. We therefore tested the temperature in a few different ways: 1) Culturing the seed culture and growth culture at 15°C and feeding CBGA at day 2 2) Culturing the seed culture and growth culture at 30°C and feeding CBGA at day 2 3) Culturing the seed culture and growth culture at 30°C for 5 days and feeding CBGA at day 6. 4) Culturing the seed culture and growth culture at 15°C for 5 days. At the 6th day, feed CBGA and culture at 30°C 5) Culturing the seed culture and growth culture at 15°C for 5 days and feeding CBGA at day 6. (Figures 28 and 29) As the data indicates, option 4 had the greatest increase in functional THCAS expression, achieving greater than 50% conversion of CBGA to THCA based on UV area under the curve, a significant increase over the 3% estimated conversion rate when we initially expressed THCAS in *S.*

cerevisiae.

In conclusion, we have greatly increased functional expression of THCAS in *S. cerevisiae* by culturing at lower temperatures and by optimizing the media. The next steps would therefore be to achieve *in vivo* production of THCP, by integrating the HAC1s and THCAS into the *S. cerevisiae* strain and heterologously express Ma_OvaABC with CsPT4 in that strain

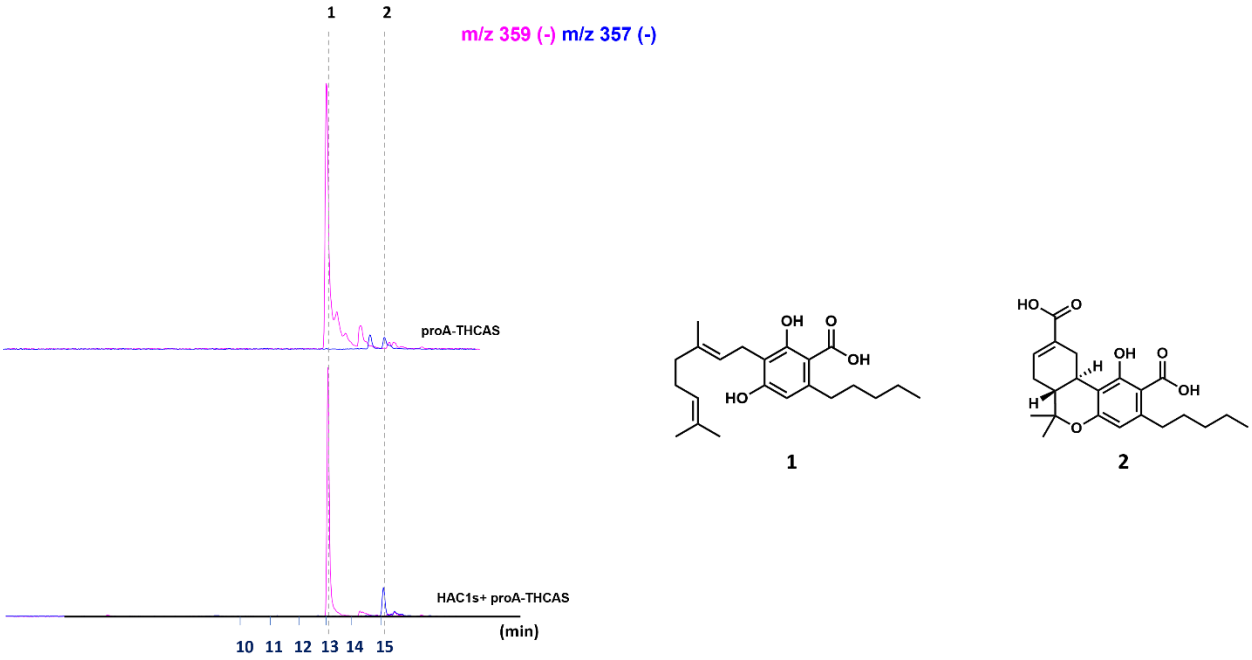

Figure 28. Optimizing Functional THCAS Expression. THCAS with the plastid targeting sequence removed and with a vacuolar signal (proteinase A) sequence added N-terminal was transformed in S. cerevisiae. Expression of the spliced unfolded protein activator (HAC1s) with THCAS increased functional expression. Cultures were grown in YPD media and cultured at 30°C. After 24 hours, 5 µM CBGA was fed to the cultures.

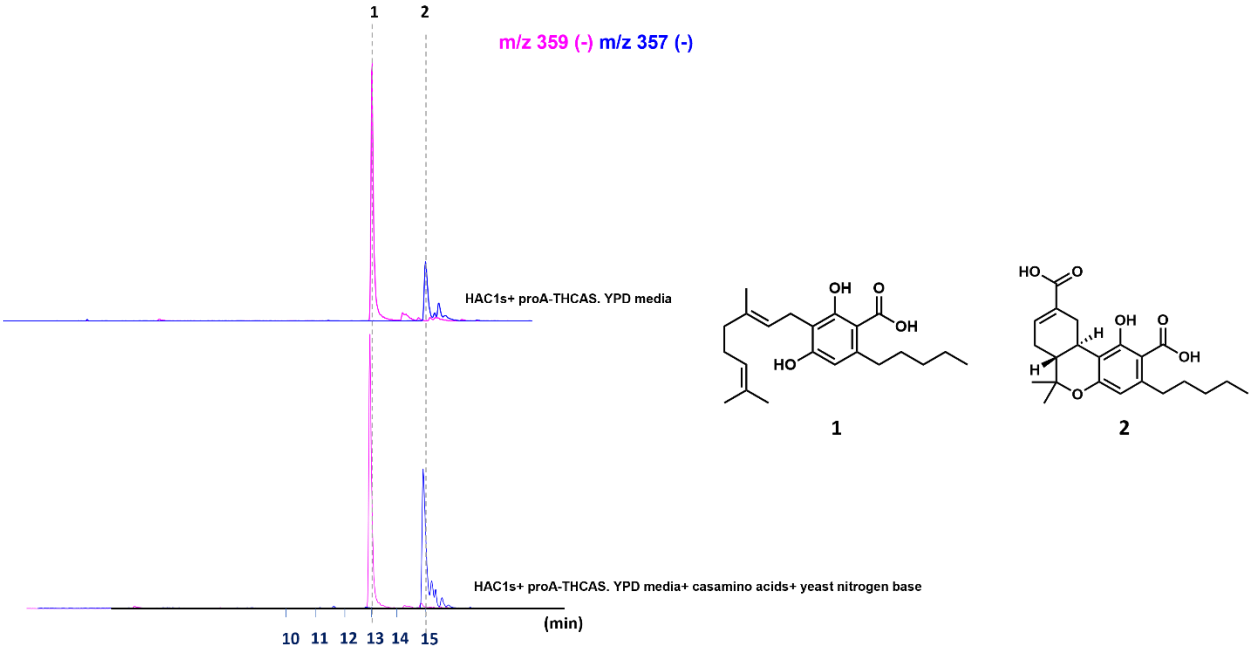

Figure 29. Optimizing Functional THCAS expression Part 2. Cultures were cultured at 15 C for 5 days. After 5th day 5 µM CBGA was fed and cultures were cultured at 30°C. Addition of casamino acids and yeast nitrogen base to the YPD media along with culturing at 15°C for 5 days greatly increased functional expression of THCAS.

6. Final Conclusion

In conclusion, we have demonstrated that through genome mining of fungal biosynthetic gene clusters, we were able to identify a cluster in *Metarhizium anisopliae* that produces olivetolic acid, the first key intermediate in the cannabinoid biosynthetic pathway as well as unsaturated olivetolic acid, sphaerophorolcarboxylic acid, and unsaturated sphaerophorolcarboxylic acid at moderate to high titers. We also identified homologous clusters that produced these same compounds as well as a homologous cluster found in *Talaromyces islandicus* that selectively produces olivetolic acid. These clusters represent a non-plant platform to access olivetolic acid and its analogs. From there, we desired to engineer our platform in three different aspects: i) by increasing the titer ii) by increasing the diversity our product profile iii) by going downstream to achieve the final elaborated cannabinoids.

To increase the titer, we utilized two different approaches. In one, we utilized JMP software to develop a design of experiments (DOE) approach to increase titer by optimizing the culture media. We initially screened for nine different components in the media, testing to determine which components had statistically significant effects on the titer production. We identified three components which we then optimized for using a response surface methodology (RSM) approach. Using this approach, we were able to identify a culturing media that assists us in reaching titers almost 2-fold more than our original CD-ST culturing media. In our second approach to increasing the titer of our platform, we increased the malonyl-CoA pool in our model *Aspergillus nidulans* host by overexpressing the acetyl-CoA carboxylase gene, the enzyme responsible for converting acetyl-CoA to malonyl-CoA. Overexpressing of acetyl-CoA carboxylase helped us achieve greater than 2.5-fold increase in titer.

We also desired to increase the diversity of our product profile. To do so, we also employed two different approaches. In one, we made mutations to the ketosynthase (KS) domain of our HRPKS, Ma_OvaA. The KS domain is responsible for decarboxylative Claisen condensation, extending the carbon-carbon chain length. We made mutations in the KS domain both manually and through the use of the automated Tecan liquid handling system integrated with a ThermoFisher Momentum Laboratory Automation System. We were able to identify a couple of mutations that produced different products from our original platform including divarinic acid as well as the olivetolic acid nonyl variant, undecyl variant, and ethyl variant. We also further genome mining to identify more homologous clusters to our original platform. Utilizing our in-house strain database, we were able to identify a cluster in *Penicillium thomii* r89 that when heterologously expressed in *Aspergillus nidulans*, produced a nonyl variant of olivetolic acid with two degrees of unsaturation and a heptyl variant containing one degree of

unsaturation as well as a hydroxy group. Therefore, both methods were effective in producing more olivetolic acid variants and there is still much potential in discovering more variants with regards to these methods since especially with regards to the genome mining aspect, there is still much unexplored space.

Lastly, we attempted to go downstream of the pathway to achieve the final elaborated cannabinoids. To do so, we mined for different prenyltransferase enzymes capable of geranylating olivetolic acid to form cannabigerolic acid. We were able to identify one in *Talaromyces islandicus* capable of geranylating olivetolic acid to form cannabigerolic acid in *Aspergillus nidulans*, giving us a platform where through the heterologous expression of four fungal genes, we were able to produce the first cannabinoid, CBGA. Utilizing CsPT4, we were also able to achieve de novo production of the heptyl variant of CBGA, when we expressed the Ma_OvA genes with CsPT4 in *Saccharomyces cerevisiae*. We also were able to achieve functional expression of THCAS in *S. cerevisiae* and were able to greatly increase expression by optimization of media, overexpression of helper proteins, and culturing at lower temperatures. Therefore, we have developed a different method for microbial production of cannabinoids, one that does not rely heavily on the cannabis plant genes and has potential to produce rare and new-to-nature cannabinoids.

7. Materials and Methods

Strain and Culture Conditions

Metarhizium anisopliae ARSEF23, *Tolypocladium inflatum*, *Metarhizium rileyi*, and *Talaromyces islandicus* were all separately grown on PDA (potato dextrose agar) for 3 days and then transferred to liquid PDB (PDA medium without agar) for the isolation of genomic DNA. *Aspergillus nidulans* 1145 was used as the model host for heterologous expression. *Aspergillus nidulans* 1145 was first grown on CD plates (10 g/L glucose, 20 g/L agar, 50 mL/L 20× nitrate salts, 1 mL/L trace elements) at 28 °C and then cultured in 25 mL of CD-ST medium (20 g/L starch, 20 g/L casamino acids, 50 mL/L 20× nitrate salts, and 1 mL/L trace elements) in a 125 mL flask at 28 °C and 250 rpm. 120 g of $NaNO_3$, 10.4 g of KCl, 10.4 g of $MgSO_4 \cdot 7H_2O$, and 30.4 g of KH_2PO_4 were dissolved in 1 L of distilled water to make 20× nitrate salts. 2.20 g of $ZnSO_4 \cdot 7H_2O$, 1.10 g of H_3BO_3, 0.50 g of $MnCl_2 \cdot 4H_2O$, 0.16 g of $FeSO_4 \cdot 7H_2O$, 0.16 g of $CoCl_2 \cdot 5H_2O$, 0.16 g of $CuSO_4 \cdot 5H_2O$, and 0.11 g of $(NH_4)_6Mo_7O_{24} \cdot 4H_2O$ were dissolved in 100 mL of distilled water, with the pH being adjusted to 6.5 to make the trace element solution.

Plasmid Construction and Expression

Plasmids pYTU, pYTP, and pYTR containing auxotrophic markers for uracil (*pyrG*), pyridoxine (*pyroA*), and riboflavin (*riboB*), respectively, were digested and used as backbones to insert genes. The genes expressed (OvaA, OvaB, and OvaC) were amplified through polymerase chain

reaction (PCR) using the genomic DNA of *Metarhizium anisopliae* ARSEF23, *Tolypocladium inflatum*, *Metarhizium rileyi*, and *Talaromyces islandicus* as templates. *StcJ/K* genes were amplified through PCR using the genomic DNA of *Aspergillus nidulans*. A *glaA* promoter and *trpC* terminator were amplified through PCR using pYTR as a template. The PCR fragments were transformed in yeast, and through homologous recombination, the plasmids pYTU-*glaA*-OvaB-*trpC*, pYTP-*glaA*-OvaC, and pYTR-*glaA*-OvaA-*trpC* were generated. Yeast transformation was performed using the Frozen-EZ Yeast Transformation II kit (Zymo Research). The plasmids were extracted from yeast and transformed into *E. coli* TOP10 by electroporation to isolate single plasmids. After extraction from *E. coli*, plasmid sequences were confirmed by sequencing. All three plasmids (pYTU-*glaA*-OvaB-*trpC*, pYTP-*glaA*-OvaC, pYTR-*glaA*-OvaA-*trpC*) were transformed into *A. nidulans* using standard protocols to form the OA-producing strain.[102] The strain was then cultured in 10 mL of CD-ST medium in a 50 mL Falcon tube and kept in a shaker at 28 °C and 250 rpm overnight. The next day, 25 μL of the culture was inoculated into 25 mL of CD-ST medium in a 125 mL flask and kept in a shaker at 28 °C and 250 rpm.

C. Sativa acyl-activating enzyme (CsAAE1) was ordered as a gene block from Integrated DNA Technologies (IDT). CsAAE1 was amplified through PCR and cloned onto the pYTR backbone containing the *gpdA* promoter. After following the previously outlined protocol to construct and confirm the sequence of plasmids, we transformed the pYTR-*gpda*-CsAAE1, pYTU-*glaA*-OvaB-*trpC*, and pYTP-*glaA*-OvaC plasmids into *A. nidulans*. After 5 days of growth at 37 °C on CD sorbitol plates, the strain was cultured in 25 mL of CD-ST medium in 125 mL flasks at 28 °C and 250 rpm. On day 2, 1 mM hexanoic acid was added to the culture, and analysis of the sample was done on days 3, 4, and 5.

Aspergillus nidulans Heterologous Expression

To produce protoplasts, *Aspergillus nidulans* 1145 was grown on CD agar plates with 10 mM uridine, 5 mM uracil, 0.5 μg/mL of pyridoxine HCl, and 2.5 μg/mL of riboflavin at 37 °C for 4 days. *Aspergillus nidulans* 1145 spores were then inoculated in 25 mL of CD liquid medium containing 10 mM uridine, 5 mM uracil, 0.5 μg/mL of pyridoxine HCl and 2.5 μg/mL of riboflavin in a 250 mL flask and grown at 28 °C and 250 rpm for 16 h. The mycelia were harvested by centrifugation at 4300*g* for 20 min and washed with osmotic buffer (1.2 M $MgSO_4$, 10 mM sodium phosphate, pH 5.8). After harvesting by centrifugation once more, mycelia were then transferred to a 250 mL flask containing 10 mL of osmotic buffer with 30 mg of lysing enzymes from *Trichoderma* and 20 mg of yatalase. The mycelia were digested for 5 h at 28 °C and 80 rpm. The cells were then transferred to a 50 mL centrifuge tube, overlaid gently by 10 mL of trapping buffer (0.6 M sorbitol, 0.1 M Tris-HCI, pH 7.0), and centrifuged at 5300 rpm for 20 min at 4 °C. Two layers appeared with the protoplasts at the interface of the two layers. The protoplasts were collected and placed in a sterile 15 mL Falcon tube, washed with 10 mL of STC buffer (1.2 M sorbitol, 10 mM $CaCl_2$, 10 mM Tris-HCI, pH 7.5), and centrifuged for 10 min at 4300*g* and 4 °C. The protoplasts were then suspended in 1 mL of STC buffer, aliquoted in 60 μL increments in 1.5 mL microcentrifuge tubes, and stored at −80 °C.

For the transformation, 2 μL of each plasmid needed for the heterologous expression was added to the 60 μL aliquots of *Aspergillus nidulans* 1145 protoplasts and then kept on ice for 60 min. The aliquots were then mixed with 600 μL of PEG solution (60% PEG, 50 mM calcium chloride, and 50 mM Tris-HCl, pH 7.5), incubated at room temperature for 20 min, and plated on CD

sorbitol agar plates (CD solid medium with 1.2 M sorbitol and the appropriate supplements, according to the markers on the plasmids). Plates were then incubated at 37 °C for 3–5 days. For hexanoyl-SNAC feeding, the *A. nidulans* strain containing pYTU-*glaA*-OvaB-*trpC* and pYTP-*glaA*-OvaC plasmids was cultured in 25 mL of CD-ST in a 125 mL flask at 28 °C and 250 rpm for 5 days. On day 2, 1 mM hexanoyl-SNAC was fed into the cultures, and analysis of the sample was done on days 3, 4, and 5.

Sample Preparation, Detection, Isolation, and Quantification

Individual colonies from transformation plates were cultured in 25 mL of liquid CD-ST medium in 125 mL flasks and grown for 5 days. On the sixth day, 500 μL of cells and medium was extracted with 800 μL of an ethyl acetate acid mix (1:9 methanol to ethyl acetate with 0.1% formic acid). The extracted sample was then dried and placed in 50 μL of methanol and then loaded onto the LC-MS.

LC-MS analyses were performed using a Shimadzu 2020 LC-MS (Phenomenex Kinetex, 1.7 μm, 2.0 × 100 mm, C-18 column) using positive- and negative-mode electrospray ionization. The elution method was a linear gradient of 5–95% (v/v) acetonitrile/water in 13.25 min followed by 95% (v/v) acetonitrile/water for 4.75 min with a flow rate of 0.3 mL/min. The LC mobile phases were supplemented with 0.1% formic acid (v/v).

The large-scale production of compounds for the purpose of isolation and structural determination was carried out by cultivating transformants in 1 L of CD-ST. After 5 days of growth at 28 °C, the media were extensively extracted with acidified ethyl acetate. The extract was concentrated under reduced pressure. Purification was carried out as previously reported with slight modifications. (23) In brief, the residue was loaded to a RediSep Rf Gold reversed-

phase C18 column on a Teledyne Combi-Flash system. Subsequently, high-performance liquid chromatography (HPLC) purifications were performed with a Phenomenex Kinetex column (5 μ, 10.0 × 250 mm, C18) using a Shimadzu ultrafast liquid chromatography (UFLC) system. For the HPLC purification, a flow rate of 4 mL/min with solvents A (0.1% formic acid in water) and B (0.1% formic acid in acetonitrile) was used. NMR spectra of **1**–**3** were acquired on a Bruker AV500 spectrometer with a 5 mm dual cryoprobe (^{1}H 500 MHz, ^{13}C 125 MHz). Quantification of the compounds was done by first making a standard curve on the HPLC. Known concentrations of isolated compound were analyzed on the HPLC, and a standard curve was constructed correlating the area under the UV peak corresponding to the compound to the concentration of the compound. Cultured samples were then extracted and analyzed on the HPLC, where the area under the UV peak was used to calculate the concentration of the sample.

8. Appendices

1. Supplementary Tables

2. Supplementary Figures.

1. Supplementary Tables

Table S1. Plasmids used in this study

Plasmid	Vector	Genes
pYTR01	pYTR	n/a
pYTU01	pYTU	n/a
pYTP01	pYTP	n/a
pMetarR03	pYTR	glaAp-Ma_OvaA-trpC
pMetarU03	pYTU	glaAp-Ma_OvaB-trpC
pMetarP03	pYTP	glaAp-Ma_OvaC
pTolyR01	pYTR	gpdAp-To_OvaA
pTolyU01	pYTU	gpdAp-To_OvaB
pTolyP01	pYTP	glaAp-To_OvaC
pRileyiR01	pYTR	gpdAp-Mr_OvaA
pRileyiU01	pYTU	gpdAp-Mr_OvaB
pRileyiP01	pYTP	glaAp-Mr_OvaC
pTislaR01	pYTR	gpdAp-Ti_OvaA
pTislaU01	pYTU	gpdAp-Ti_OvaB
pTislaP01	pYTP	glaAp-Ti_OvaC
pAnidR01	pYTR	gpdAp-StcK; POgpdAp-StcJ
pMetarU05	pYTU	gpdAp-OvaB; POgpdAp-OvaC

Table S2. Primers used in this study.

Primers	**Sequence (5'-3')**
gpda-stcK-F	ATTACCCCGCCACATAGACACATCTAAACAATGACTCCATCACC GTTTCTCGATG
pogpda-stcJ-F	GCATACAGAACACTTCAAACAATCGCAAAAAATGACCCAAAAG ACTATACAGCAGGTC
stcJ-riboB-R	CTAAAGGGTATCATCGAAAGGGAGTCATCCATTGCACAGCGGCT TCTATCATTAAATTCG
stcJ-shortF	GCCAGAACGGTACGGGATTCC
stcJ-shortR	CTCCTGCAGTGCGTCGGATTG
stcK-pogpda-R	CAGTAAGCTCACATGTATTCCTGGAGCAAACCTTCCATTTCATCC ATTTAGCGGC
stcK-shortF	CGCGAGTATGCGATGAGCCAG
stcK-shortR	CGACAAGATAATACCGGCACAGCG
pToly-ACPTE-F1	CTTCATCCCCAGCATCATTACACCTCAGCAATGGCTGTCACTGTG TGGCAAG
pToly-ACPTE-R1	TGATGAGACCCAACAACCATGATACCAGGGGTGGCGACTGCGA GGCATTAGTTAAAT
pToly_HRPKS_F1	CATTACCCCGCCACATAGACACATCTAAACAACAATGCAAGCTC CACCACCAAGAGACG
pToly_HRPKS_R1	CTAAAGGGTATCATCGAAAGGGAGTCATCCAGCATGATGGTGTT GTGTTGGCGAC
pToly_HRPKS_shortF	CAGCGCAGTATGCCATTAGGGTATC
pToly_HRPKS_shortR	GCCGTGCCCAAGTAGAGCTC
pToly_NRPKS_F1	ATTACCCCGCCACATAGACACATCTAAACAATGAAACTTCATGC TACGAACTTCCTC
pToly_NRPKS_R1	CAACACAGTGGAGGACATACCCGTAATTTTCTGCAAACGTACGG AGTAGTACCGGTA
glaA-R	TGCTGAGGTGTAATGATGCTGGGG
PYTP-glaA-F	TCGCGGGTGTTCTTGACGATGGCATCCTGCCCTGATCTTCCGAAC TGGTCGTAC
pRileyi-ACPTE-R1	GATGAGACCCAACAACCATGATACCAGGGGGCAAGGGTTGATA GAATCGGGAGAGG
pRileyi-HRPKS-F1	ATTACCCCGCCACATAGACACATCTAAACAATGGAGGCTTCGTC ACAATCAAGAGACG
pRileyi-HRPKS-R1	TAAAGGGTATCATCGAAAGGGAGTCATCCATCGCCCGTTTTCAG CAAGCAG

pRileyi-HRPKS-shortF	GCTGAGCTTAGACGCGGTGCCGTAC
pRileyi-HRPKS-shortR	GCCACGATGATCTTGCCTCCG
pRileyi-NRPKS-F1	ATTACCCCGCCACATAGACACATCTAAACAATGAAAATCCGGGCTACAAACTTCCTC
pRileyi-NRPKS-R	CACAGTGGAGGACATACCCGTAATTTTCTGGGCAACACCAAGACAGACATTGAG
pToly-ACPTE-F1	CTTCATCCCCAGCATCATTACACCTCAGCAATGGCTGTCACTGTGTGGCAAG
pTisla-ACPTE-F	CTTCATCCCCAGCATCATTACACCTCAGCAATGTCTGCGAGCGTAGAAACAGC
pTisla-ACPTE-R	GATGAGACCCAACAACCATGATACCAGGGGTTCCTTAAAAAGACCCCGAATGCCG
pTisla-HRPKS-F	ATTACCCCGCCACATAGACACATCTAAACAATGGCGACAACGAATGAAGTCCG
pTisla-HRPKS-R	TAAAGGGTATCATCGAAAGGGAGTCATCCAAATCACCAGCAGTTGATGACCTCTAAC
pTisla-HRPKS-shortF	GCACAGGCCATGGATGAGAACGTC
pTisla-HRPKS-shortR	GGGATGATTTTGCTTCGCAGAGAAGTAC
pTisla-NRPKS-F	ATTACCCCGCCACATAGACACATCTAAACAATGCATCAAGAGATCCAGGATCAGAC
pTisla-NRPKS-F2	ATTACCCCGCCACATAGACACATCTAAACAAACAATGCATCAAGAGATCCAGGATCAGAC
pTisla-NRPKS-R	GTGGAGGACATACCCGTAATTTTCTGAATCAATGGCTCGTTTTTGACAAAAACTCTTT
pTisla-NRPKS-R2	GTGGAGGACATACCCGTAATTTTCTGGAATCAATGGCTCGTTTTTGACAAAAACTCTTT
Metar_HRPKS_1	GAGTGGAAGCCGGCAATCGACTTGCTGAC
Metar_HRPKS2	CGTTGCGCAAAACGACCTCTAGCTTTGCGTG
pMetarR01_1	TTACCCCGCCACATAGACACATCTAAACAATGCAAGCGCCAGCACCATCAAGAGACGA
pMetarR02_0	CTGTTTGATGATTTCAGTAACGTTAAGTGGCTAGTTCAATTTCACCAAAGTAGACATGGA
pMetarR02_1	TCCATGTCTACTTTGGTGAAATTGAACTAGCCACTTAACGTTACTGAAATCATCAAACAG
pMetarR03_0	CTAAAGGGTATCATCGAAAGGGAGTCATCCAAAGAAGGATTACCTCTAAACAAGTGTAC
Metar_NRPKS_2	CCTCTTCGAACTGGCCCAAGATGGGATCAAG
Metar_NRPKS1	GGACCTATTAACCACCGCTTTCCTGATCTAG

pMetarO03_3	TTGGCCGGCTGGTTCACGATGCTCGGTAACCACTTAACGTTACTGAAATCATCAAACA
pMetarU01_1	CTTCATCCCCAGCATCATTACACCTCAGCAATGAAACTGCGTGTCGCAAACTTCCTCCTC
pMetarU03_0	TCATTTATAGCTCGTTCGGCACCTTTAATCTCTAAAAGCAATTCTTGCTGTTCACCAGAT
pMetarU03_4	CAGTGGAGGACATACCCGTAATTTTCTGGAAGAAGGATTACCTCTAAACAAGTGTACC
pMetarP02_2	GTGATGAGACCCAACAACCATGATACCAGGGCGAAGCACTGAATAGCAAAATTCCTATC
pMetarR01_5	TCATCCCCAGCATCATTACACCTCAGCAATGGCCGTCACCGTGTGGCAAGATGCGC
pMetarU05-ACPTE-F-pogpda	GCATACAGAACACTTCAAACAATCGCAAAAATGGCCGTCACCGTGTGGCAAG
pMetarU05-ACPTE-R-pyrG	CACAGTGGAGGACATACCCGTAATTTTCTGCAGCTGAGAAGACACGGCGC
pMetarU05-NRPKS-R-pogpda	GTAAGCTCACATGTATTCCTGGAGCAAATCTAAAAGCAATTCTTGCTGTTCACCAGATAG
POgpda-F	TTTGCTCCAGGAATACATGTGAGC
POgpda-R	TTTTGCGATTGTTTGAAGTGTTCTGTATG
HR-A311W-F	GCTACGTCGAGTGGCACGGAACGG
HR-A311W-R	CCGTTCCGTGCCACTCGACGTAGC
HR-A357W-F	CTCGAAGCCTGCTGGGGACTGGCCTCG
HR-A320W-F	GGCACCCAGTGGGGCGACACGCGTG
HR-A320W-R	CTCACGCGTGTCGCCCCACTGGGTGCCCGTTC
HR-I284W-R	CGCCTCGACGCTGGGCCAGGTGAAGCCCTTTG
HR-V287W-F	CCATCCCCAGCTGGGAGGCGCAAGC
HR-V287W-R	GCTTGCGCCTCCCAGCTGGGGATGG
HR-A350T-F	GATCAGTCAAGACAAATATCGGACATCTCG
HR-A350T-R	CGAGATGTCCGATATTTGTCTTGACTGATC
HR-A350W-F	GATCAGTCAAGTGGAATATCGGACATCTCG
HR-A350W-R	CGAGATGTCCGATATTCCACTTGACTGATC
HR-F126WS129N-F	GGACGGGCGTCTGGATGGCCAACTTCACGAGCGACTACC
HR-F126WS129N-R	CGGTAGTCGCTCGTGAAGTTGGCCATCCAGACGCCCGTCC
HR-L183MC186T-F	GTCCAGTATGGTCGCCACCCATCTCGCCTGC
HR-L183MC186T-R	GCAGGCGAGATGGGTGGCGACCATACTGGACGAG
HR-F222A-F	CCAGCAGGCTCTGGCCCCCGAC

HR-F222A-R	GCCGTCGGGGGCCAGAGCCTGCTGGTTG
HR-F222W-F	CCAGCAGTGGCTGGCCCCCGAC
HR-F222W-R	GCCGTCGGGGGCCAGCCACTGCTGGTTG
HR-F416A-F	CACCCAGGGTGCTGGATATGGCGG
HR-F416A-R	GTACCGCCATATCCAGCACCCTGGGTGCTGATC
HR-F416AY418A-F	CAGCACCCAGGGTGCCGGAGCCGGCGGTACAAACG
HR-F416AY418A-R	CGTTTGTACCGCCGGCTCCGGCACCCTGGGTGCTG
HR-F416W-F	GCACCCAGGGTTGGGGATATGGCGG
HR-F416W-R	CCGCCATATCCCCAACCCTGGGTGC
HR-I284W-F	CAAAGGGCTTCACCTGGCCCAGCGTCGAGGCG
HR-L364M-F	GGACTGGCCTCGATGATAAAGTGCGTCTAC
HR-L364M-R	GACGCACTTTATCATCGAGGCCAGTCCCG
HR-L364W-F	GACTGGCCTCGTGGATAAAGTGCGTCTAC
HR-L364W-R	GACGCACTTTATCCACGAGGCCAGTCCCG
HR-M214L-F	GAACCCCGACCTGTTCCTGTACCTTTCCAACCAG
HR-M214L-R	CTGGTTGGAAAGGTACAGGAACAGGTCGGGGTTC
HR-F130W-F	CATGGCCAGCTGGACGAGCGACTACCGCGAGATGCTGTAC
HR-F130W-R	GTAGTCGCTCGTCCAGCTGGCCATGAAGACGCCCGTCCGC
HR-Q221H-Freal	GTACCTTTCCAACCAGCATTTTCTGGCCCCCG
HR-Q221H-Rreal	CGGGGGCCAGAAAATGCTGGTTGGAAAGGTAC
HR-Y217F-F	GACATGTTCCTGTTCCTTTCCAACCAGCAG
HR-Y217F-R	CTGCTGGTTGGAAAGGAACAGGAACATGTC
Metar-HRPKS1new	GAGTGGAAGCCAGCAATCGACTTGTTGAC
Metar-HRPKS2new	GTTGCGCAAAACGACCTCTAGCTTG
pMetarR01_1	ttaccccgccacatagacacatctaaacaATGCAAGCGCCAGCACCATCAAGAGACGa
pMetarR03_0	CTAAAGGGTATCATCGAAAGGGAGTCATCCAaagaaggattacctctaaacaagtgtac
HR-S129N-F	TCTTCATGGCCAACTTCACGAGCGACTACC
HR-S129N-R	GGTAGTCGCTCGTGAAGTTGGCCATGAAGA
HR-S129V-F	CGTCTTCATGGCCGTCTTCACGAGCGACTACC
HR-S129V-R	GTCGCTCGTGAAGACGGCCATGAAGACGCC
HR-C230S-F	CCCCCGACGGCCAGTCTAAGAGCTTTGAC
HR-C230S-R	GTCAAAGCTCTTAGACTGGCCGTCGGGGG
HR-Q229K-F	CCCCCGACGGCAAGTGCAAGAGCTTTGAC
HR-Q229K-R	GTCAAAGCTCTTGCACTTGCCGTCGGGGG

HR-S345W-F	CTGCTAGTGGGATGGGTCAAGGCAAATATC
HR-S345W-R	GATATTTGCCTTGACCCATCCCACTAGCAG
HR-T316A-F	GAGGCTCACGGAGCGGGCACCCAGGCC
HR-T316A-R	GGCCTGGGTGCCCGCTCCGTGAGCCTC
HR-T316W-F	GAGGCTCACGGATGGGGCACCCAGGCC
HR-T316W-R	GGCCTGGGTGCCCCATCCGTGAGCCTC
HR-T323K-F	CCGGCGACAAACGTGAGATGGAAGGC
HR-T323K-R	GCCTTCCATCTCACGTTTGTCGCCGGCC
HR-T323KR324C-F	GGCCGGCGACAAATGTGAGATGGAAGGC
HR-T323KR324C-R	GCCTTCCATCTCACATTTGTCGCCGGCC
HR-V175W-F	GCCCAGCTTCACCTGGAACACGGCCTG
HR-V175W-R	GCAGGCCGTGTTCCAGGTGAAGCTGGGC
HR-V287A-F	CCATCCCCAGCGCCGAGGCGCAAGC
HR-V287A-R	GCTTGCGCCTCGGCGCTGGGGATGG
HR-V287F-F	CCATCCCCAGCTTTGAGGCGCAAGC
HR-V287F-R	GCTTGCGCCTCAAAGCTGGGGATGG
HR-V287M-F	CCATCCCCAGCATGGAGGCGCAAGC
HR-V287M-R	GCTTGCGCCTCCATGCTGGGGATGG
HR-V287Y-F	CCATCCCCAGCTACGAGGCGCAAGCC
HR-V287Y-R	GGCTTGCGCCTCGTAGCTGGGGATGG
HR-M214LY217F-F	GAACCCCGACCTGTTCCTGTTCCTTTCCAACCAGCAG
HR-M214LY217F-R	CTGCTGGTTGGAAAGGAACAGGAACAGGTCGGGGTTC
HR-M214LY217FQ221H-F	TGAACCCCGACCTGTTCCTGTTCCTTTCCAACCAGCACTTTC
HR-M214LY217FQ221H-R	GAAAGTGCTGGTTGGAAAGGAACAGGAACAGGTCGGGGTTC
HR-Y418A-F	CCCAGGGTTTTGGAGCTGGCGGTACAAAC
HR-Y418A-R	GTTTGTACCGCCAGCTCCAAAACCCTGGG
HR-Y418W-F	CCAGGGTTTTGGATGGGGCGGTACAAACG
HR-Y418W-R	CGTTTGTACCGCCCCATCCAAAACCCTGG
P.thombiHR-F-gpdA	ATTACCCCGCCACATAGACACATCTAAACAATGACAGAAAACATGGCGACACC
PThombiHR-F-2	GAGCACGCCAGAGGAGGTCG
PThombiHR-R-1	CGCCTGAAGCTCTTGAGACAACC

pThombiHR-R-riboB	AAAGGGTATCATCGAAAGGGAGTCATCCAAGTGGAAGATGCTAAATTCTCCGGGAG
pThombiACPTE-F-POGpdA	CATACAGAACACTTCAAACAATCGCAAAAATGGATTTTGAGAAATACCTGAGCATCATTG
pThombiACPTE-R-pyrG	CAGTGGAGGACATACCCGTAATTTTCTGGTTAAGTATTCGAGGACTCAATTTCTGGTTCG
pThombiNR-F-2	GGTCTACTCTCCTCCCCGTGC
PthombiNR-F-gpdA	ATTACCCCGCCACATAGACACATCTAAACAATGGCACAGCTGGAGACCCAC
pThombiNR-R-1	CCACCCGCGATATCCTTGAAC
pThombiNR-R-PogpdA	agtaagctcacatgtattcctggagcaaaCTACAGTCTAACATTTGAGGTCTTCTTGCTG
M31sopt-F-Pck1p	CAACTAATTATTCCATAATAAAATAACAACATGAGCGAGGCCGCTGACG
ADH2P-F-ori	CAGGGGGGCGGAGCCTATGGAAAAACGCCGgcaaaacgtaggggcaaacaaacg
ADH2t-R-CEN	CATTAAAAGATACGAGGCGCGTGTAAGTTACgggagcaaaaagtagaatattatc
CNE-F-ADH2P	CAACTATcaactattaactatatcgtaatATGAAATTTTCTGCGTATTTATGGTGGCTG
CNE1-R-Spg5t	GTAATAGCGCGATGAAACAACGTCTTTGCCTATGTAAATACTACACAACAAAGAACCGAC
FAD1-F-Pck1p	CAACTAATTATTCCATAATAAAATAACAACATGCAGTTGAGCAAGGCTGC
FAD1-R-ADH2T	catacttgataatgaaaactataaatcgTTAATTCTTGATCCTGCCTGCTCTCTCTAAAG
BPT1-F-ADH2p	ctatcaactattaactatatcgtaataccatATGTCTTCACTAGAAGTGGTAGATGGGTG
BPT1-R-ADH2t	gataatgaaaactataaatcgtgaaggcatTTATTTCAAATACCCACCTTTCTCACAAAG
Pck1p-R-proA	gtagccctatcgcaatggacatcgtggtcccatcgaaaatcatGTTGTTATTTTATTATG
proAtrunTHCAS-F	attgcgatagggctactttcaacgctgggcataggcgcagaagcgAATCCTCGAGAAAAC
colA-R-spg5t	GGTAATAGCGCGATGAAACAACGTCTTTGCTCAAGCGGAGCCTTTGAGAACG
colA-XW55-F	actatcaactattaactatatcgtaataccatATGGCACCTCCATCATCCAAAGTCACTG
trunTHCAS-F-Pck1p	CAACTAATTATTCCATAATAAAATAACAACATGAATCCTCGAGAAAACTTCCTTAAGTGC
HAC1s-F-ADH2p	tatcaactattaactatatcgtaataccatATGGAAATGACTGATTTTGAACTAACTAG
HAC1s-R-spg5t	GGTAATAGCGCGATGAAACAACGTCTTTGCTCATGAAGTGATGAAGAAATCATTCAATTC

colA-F-Pck1p	CAACTAATTATTCCATAATAAAATAACAACATGGCACCTCCATCATCCAAAGTC
colA-R-ADH2T	gataatgaaaactataaatcgtgaaggcatTCAAGCGGAGCCTTTGAGAACGTATTG
mFPS-F-ADH2p	tatcaactattaactatatcgtaataccatATGCATAAATTTACTGGTGTCAATGCCAAG
mFPS-R-spg5t	GGTAATAGCGCGATGAAACAACGTCTTTGCTCATTTCTGGCGTTTGTAGATCTTCTGTG
TislaUbiA-R-ADH2t	gataatgaaaactataaatcgtgaaggcatTCAAACGGCATCGTATCTGCCG
NphBM31sopt-F-ADH2P	aactatcaactattaactatatcgtaatacATGAGCGAGGCCGCTGACGTG
NphBM31sopt-R-ADH2T	gataatgaaaactataaatcgtgaaggcatTTAGTCCTCCAGAGAATCGAATGCCTTG
ADH2p-F-upstreamyprcty2	TCCACCTGGGCCACAATCACAGTTTCCGCAgcaaaacgtaggggcaaacaaacgg
ADH2t-R-downstreamyprcty2	TGGTTACCATATGAAGCATCGCTTATTGCGgggagcaaaaagtagaatattat
yprctydownstream2-F	CGCAATAAGCGATGCTTCATATGGTAAC
yprctyupstream2-R	TGCGGAAACTGTGATTGTGGCC
trunTHCAS-F-ADH2P	aactatcaactattaactatatcgtaatacATGAATCCTCGAGAAAACTTCCTTAAGTG
trunTHCAS-R-ADH2T	gataatgaaaactataaatcgtgaaggcatGTGATGATGAGGGGGCAAAGGC
HRPKS-F-ADH2P	CAACTATcaactattaactatatcgtaatATGCAAGCGCCAGCACCATCAAGAGACg
HRPKS-R-ADH2T	catacttgataatgaaaactataaatcgCTAGTTCAATTTCACCAAAGTAGACATGGATG
2u ori F pmd29	aacgaagcatctgtgcttcattttgtag
ADH2P-F-oripmd29	AGGGGGGCGGAGCCTATGGAAAAACGCCCAgcaaaacgtaggggcaaacaaacg
ADH2T-R-2uoripmd29	CAAAATGAAGCACAGATGCTTCGTTgggagcaaaaagtagaatattatcttttattcgtg
oripmd29-R	TGGGCGTTTTTCCATAGGCTCC
CsPT447t1-checkR	ggcactcgtggttgcagagtaag
CsPT477t1-F-ADH2P	aactatcaactattaactatatcgtaatacatgtctgctggctctgaccaaattg
CsPT477t1-R-ADH2T	gataatgaaaactataaatcgtgaaggcatttaaataaatacgtagacgaaat

Table S3. Spectroscopic data of OA (**3**) in CD_3CN.

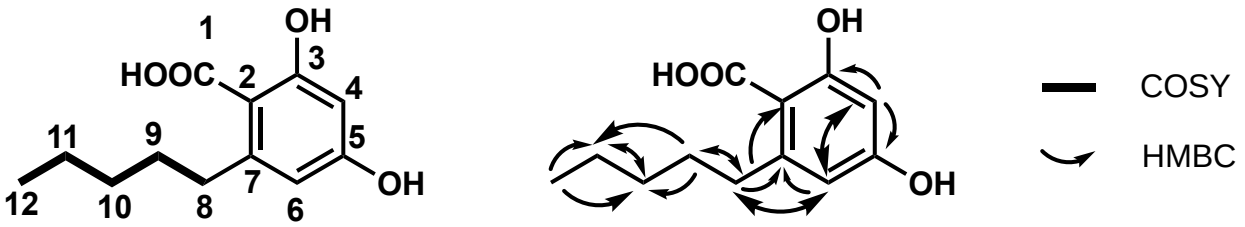

Position	δ_C	δ_H (mult., $J_{H\text{-}H}$ in Hz)
1	173.1	
2	149.8	
3	166.3	
4	101.0	6.18 (d, 1H, J = 2.5 Hz)
5	162.5	
6	110.9	6.23 (d, 1H, J = 2.5 Hz)
7	103.8	
8	36.4	2.85 (m, 2H)
9	31.7	1.53 (m, 2H)
10	32.1	1.31 (m, 2H)
11	22.5	1.31 (m, 2H)
12	13.7	0.88 (m, 3H)

Table S4. Spectroscopic data of **2** in CD_3CN.

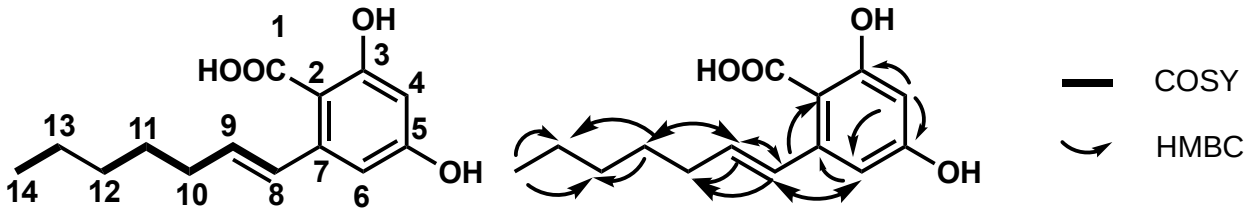

Position	δ_C	δ_H (mult., J_{H-H} in Hz)
1	172.9	
2	144.9	
3	165.7	
4	101.8	6.23 (d, 1H, J = 2.5 Hz)
5	162.5	
6	108.1	6.41 (d, 1H, J = 2.5 Hz)
7	103.0	
8	130.9	7.00 (m, 1H)
9	133.7	5.97 (m, 1H)
10	32.9	2.17 (m, 2H)
11	28.9	1.46 (m, 2H)
12	31.4	1.33 (m, 2H)
13	22.6	1.34 (m, 2H)
14	13.7	0.90 (m, 3H)

Table S5. Spectroscopic data of SA (**1**) in CD_3CN.

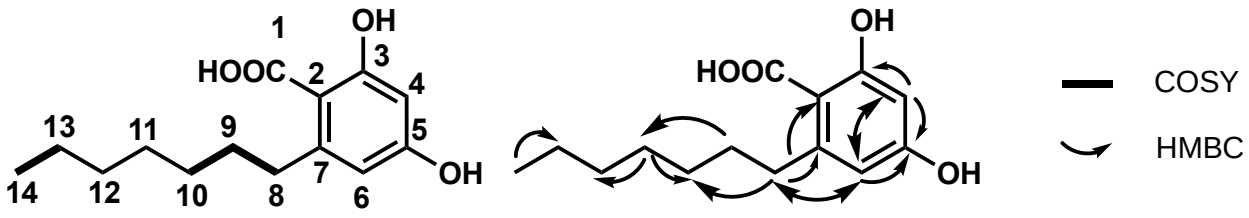

Position	δ_C	δ_H (mult., J_{H-H} in Hz)
1	173.8	
2	150.3	
3	166.9	
4	101.6	6.21 (d, 1H, J = 2.5 Hz)
5	163.0	
6	111.6	6.26 (d, 1H, J = 2.5 Hz)
7	104.4	
8	37.0	2.87 (m, 2H)
9	32.6	1.55 (m, 2H)
10	32.5	1.29 (m, 2H)
11	30.4	1.33 (m, 2H)
12	29.7	1.34 (m, 2H)
13	23.3	1.30 (m, 2H)
14	14.3	0.90 (m, 3H)

HRMS (ESI, $M+H^+$) calculated for $C_{14}H_{20}O_4$: 252.14; found 252.1495

2. Supplementary Figures

a)

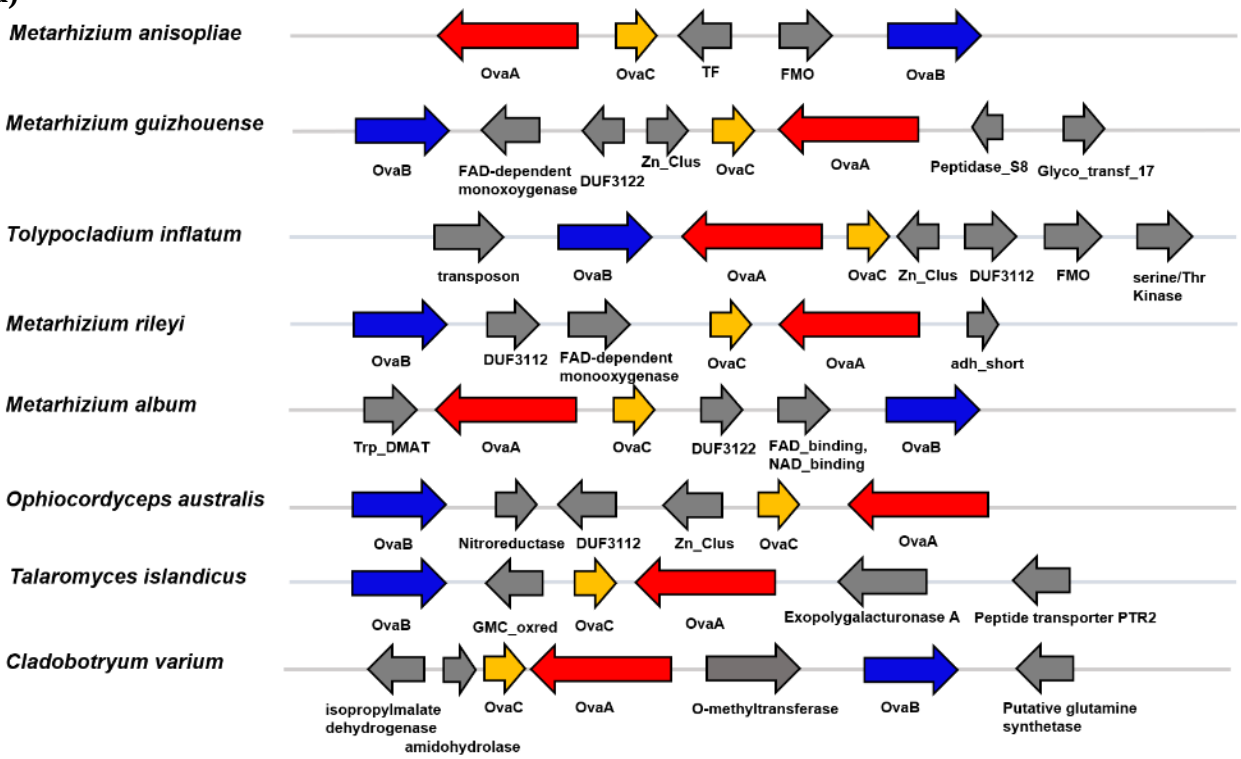

b)

	OvaA HRPKS (% identity)	**OvaB NRPKS (% identity)**	**OvaC ψACPTE (% identity)**
Metarhizium guizhouense	97.85	97.04	96.83
Tolypocladium inflatum	88.48	87.28	83.51
Metarhizium rileyi	85.98	84.68	83.82
Metarhizium album	70.02	76.65	76.68
Ophiocordyceps australis	70.4	65.44	63.98
Talaromyces islandicus	52.37	51.43	45.58

Cladobotryum varium	48.83	38.04	40.06

Figure S1. a) Homologous clusters all containing the HRPKS, NRPKS, and ψACP-TE. b) Comparison of protein sequences from the homologous clusters to the *M. anisopliae* enzymes.

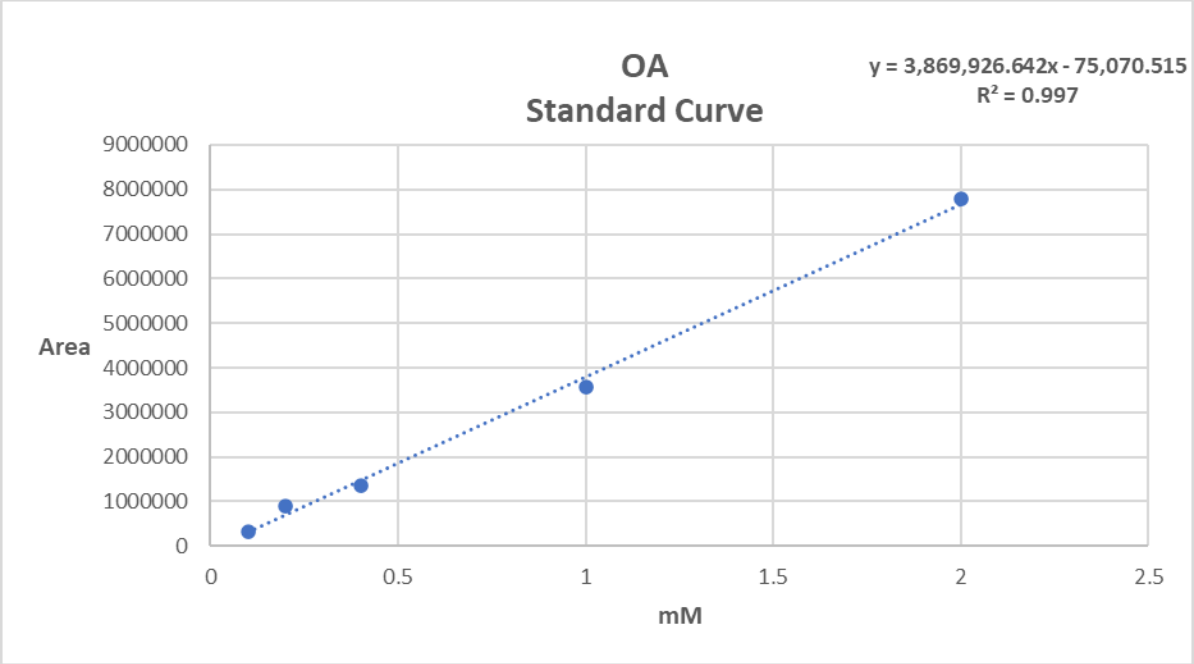

Figure S2. Standard curve of OA (**3**) used for quantification. Different concentrations of purified olivetolic acid were measured on the HPLC where the area under the peak was recorded and plotted with the olivetolic acid concentration.

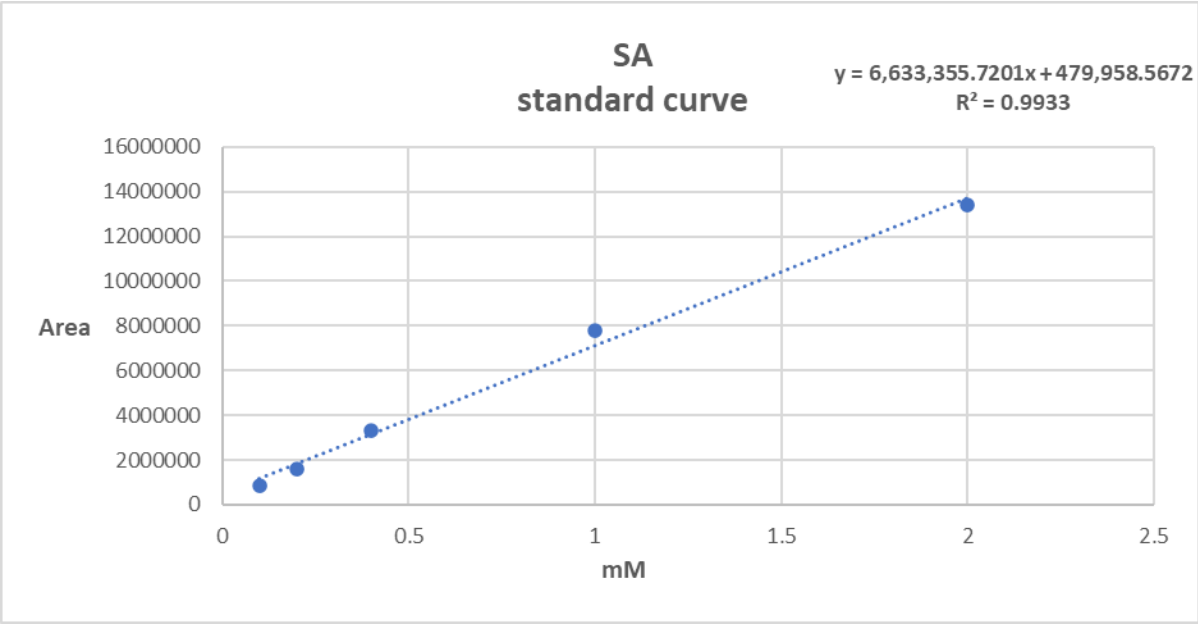

Figure S3. Standard curve of SA (**1**) used for quantification. Different concentrations of purified **1** were measured on the HPLC where the area under the peak was recorded and plotted with the **1** concentration.

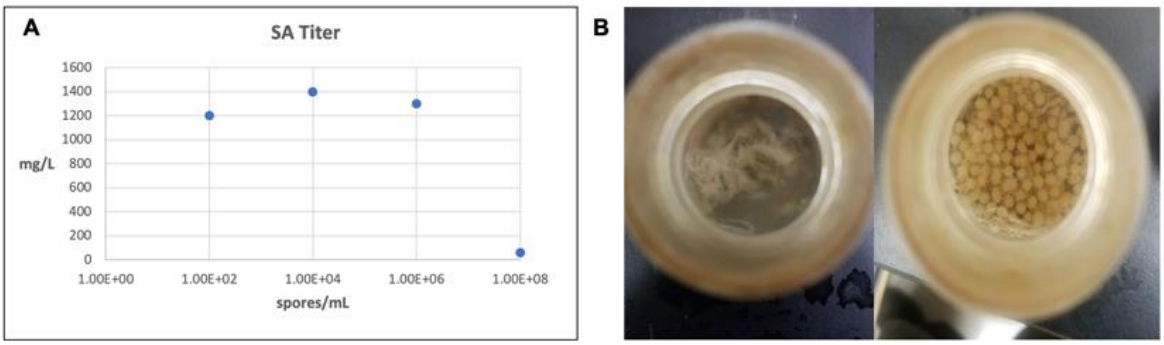

Figure S4. Varying spore inoculum size led to differentiated production of SA and analogues. A) Plot of SA titers from the *Metarhizium anisopliae ova* cluster vs spore inoculum measured in 125 mL flasks containing 25 mL of culture. 10^4 spores/mL led to highest production of SA at 1.4 g/L. 10^8 spores/mL inoculum size led to dispersed hyphae and abrogation of high titer production. B) Appearance of dispersed hyphae (left) and pellets (right). A dispersed hyphae morphology was observed when cultures were started from high inoculum spore counts (10^8 spores/mL). A pelleted hyphae morphology was observed at cultures that were started from spore counts of 10^6 spores/mL and lower.

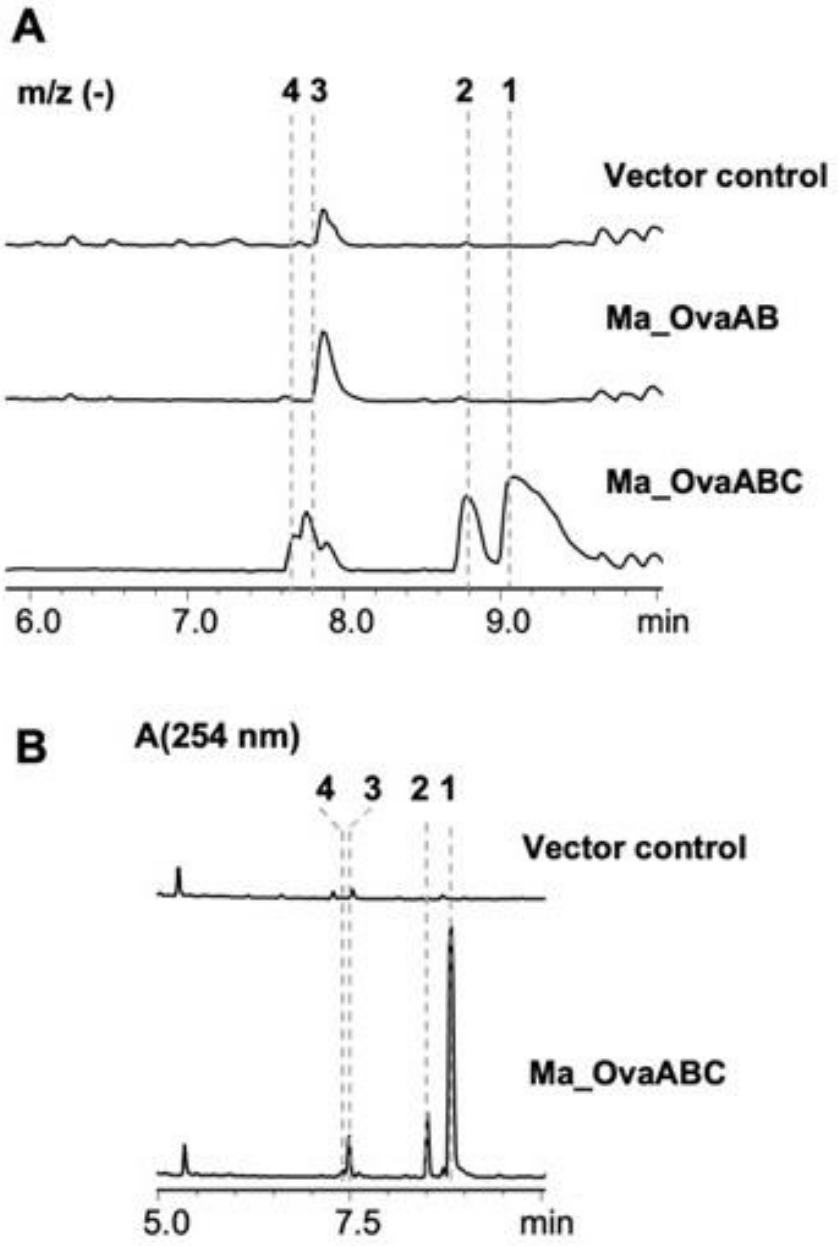

Figure S5. The production of SA, OA, and their analogues requires the co-expression of Ma_OvaABC. A) m/z (-) trace of *A. nidulans* harboring Ma_OvaABC compared with those of vector control and *A. nidulans* harboring Ma_OvaAB revealed that all three genes are required for the production of compounds of interest. B) UV profiles of *A. nidulans* strain harboring control vectors and that expressing Ma_OvaABC.

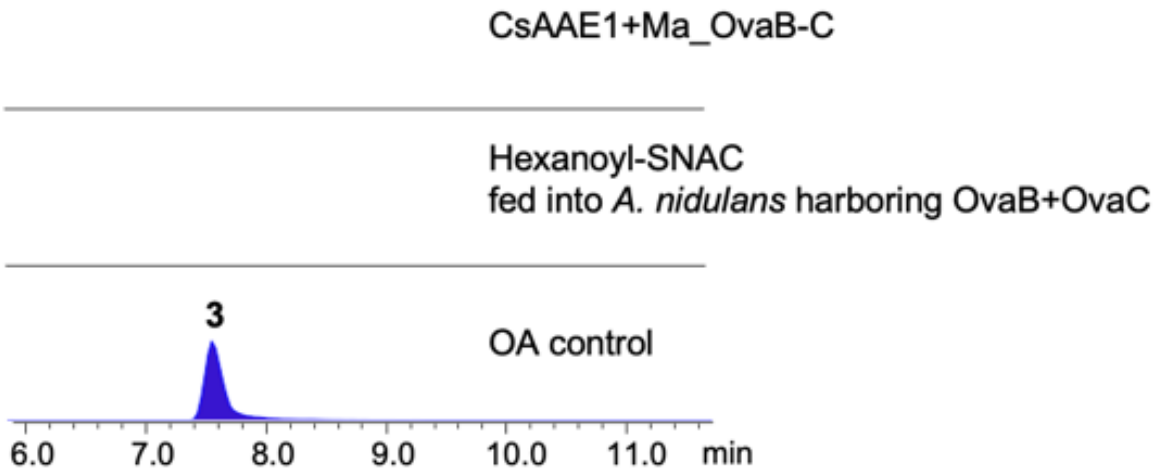

Figure S6. Feeding hexanoyl-SNAC into *A. nidulans* expressing Ma_OvaBC did not yield OA, nor did coexpression of CsAAE1 with Ma_OvaBC.

[M+H]$^+$=223

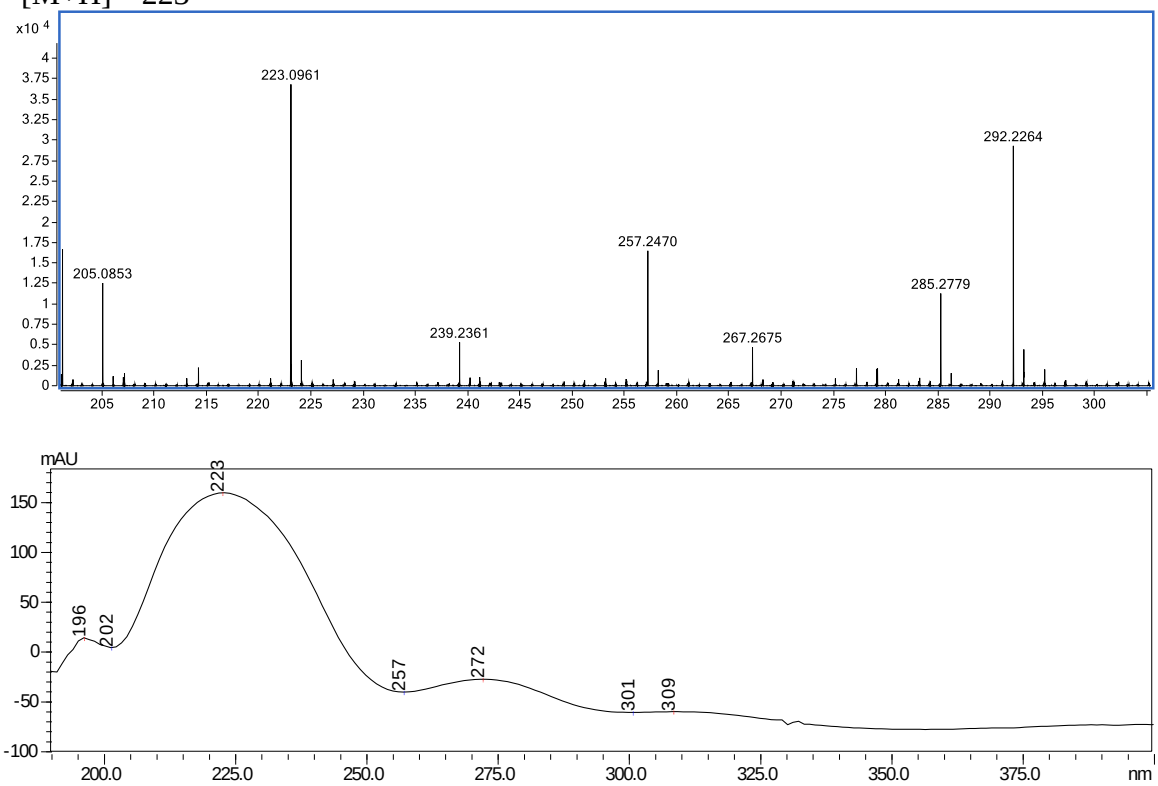

Figure S7. MS and UV spectra of **4.**

HRMS (ESI, M+H$^+$) calculated for $C_{12}H_{14}O_4$ 222.0892; found 222.0961

[M+H]$^+$=225

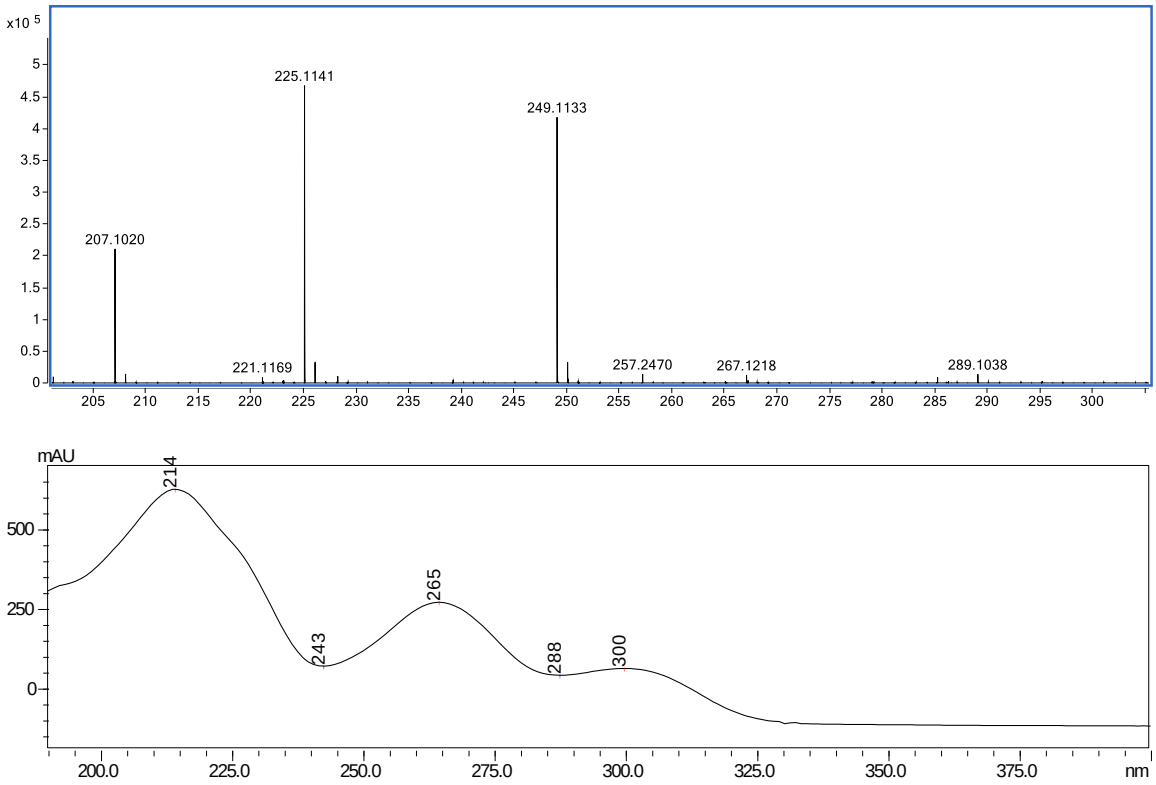

Figure S8. MS and UV spectra of OA (**3).**

HRMS (ESI, $M+H^+$) calculated for $C_{12}H_{16}O_4$ 224.1049; found 224.1141

$[M+H]^+$=251

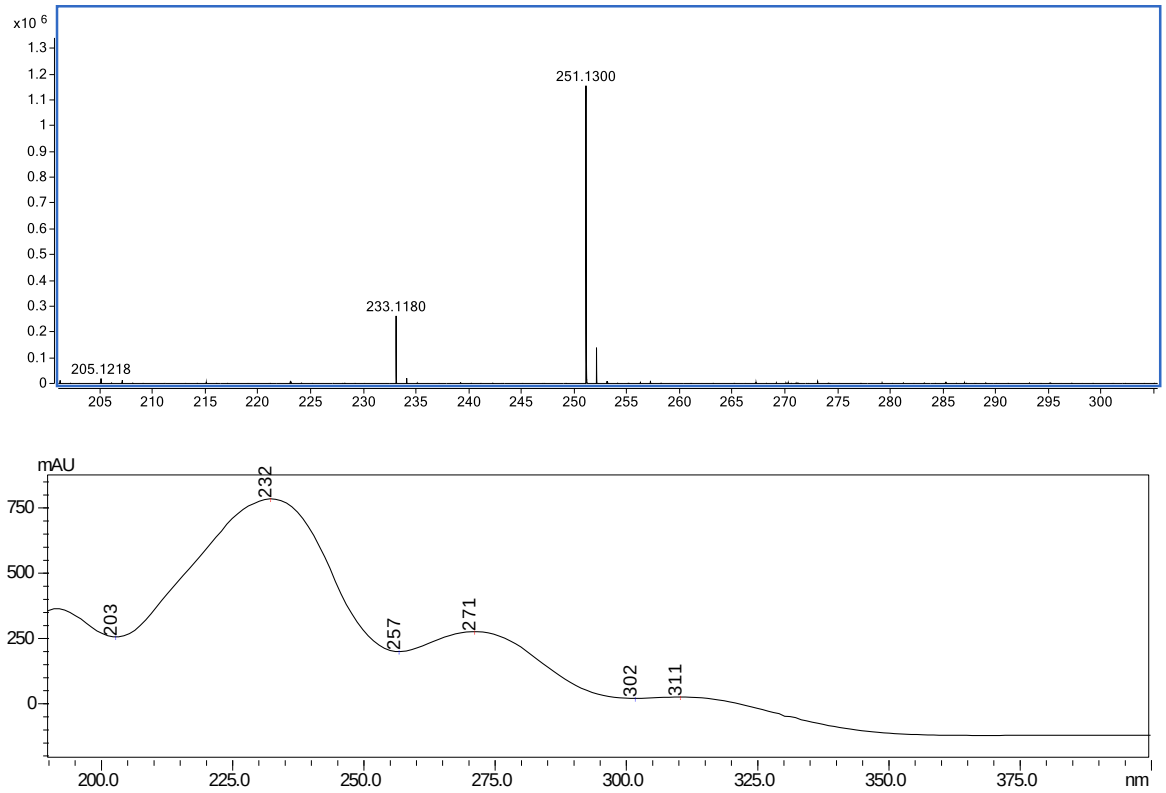

Figure S9. MS and UV spectra of **2.**

HRMS (ESI, $M+H^+$) calculated for $C_{14}H_{18}O_4$ 250.1205; found 250.1300

$[M+H]^+$=253

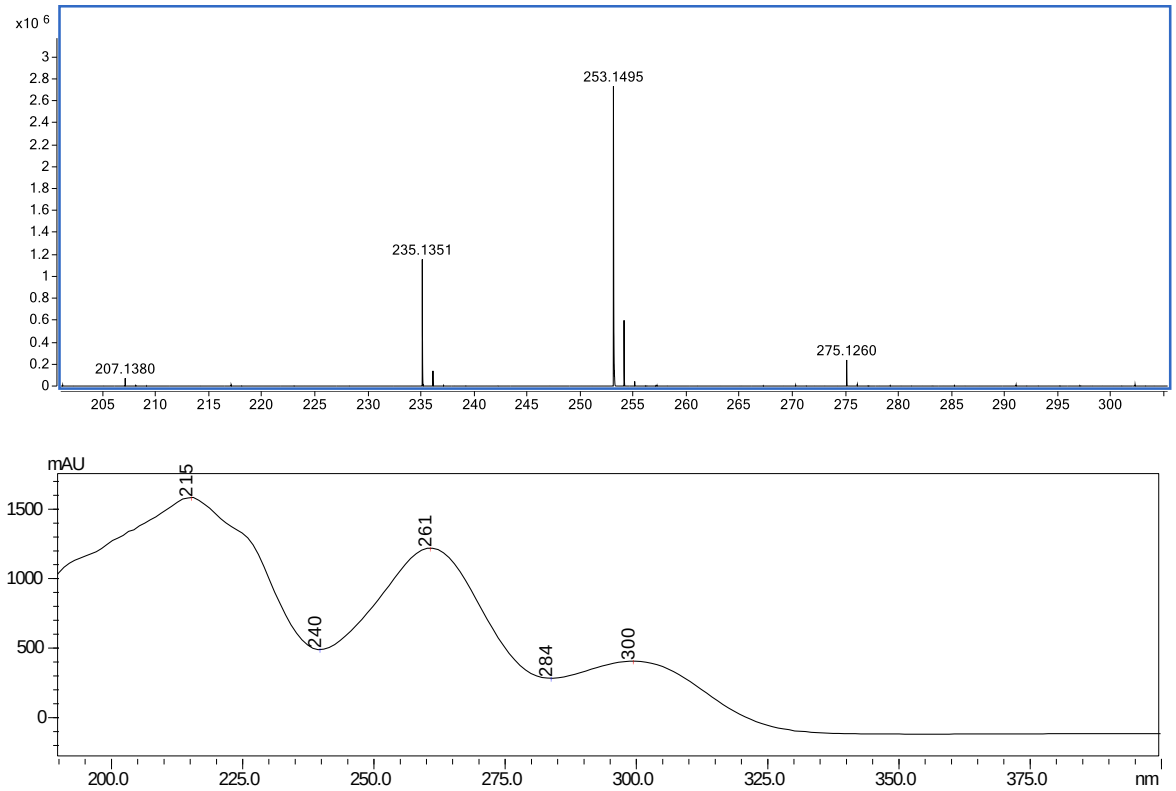

Figure S10. MS and UV spectra of SA (**1**).
HRMS (ESI, $M+H^+$) calculated for $C_{14}H_{20}O_4$ 252.1362; found 252.1495

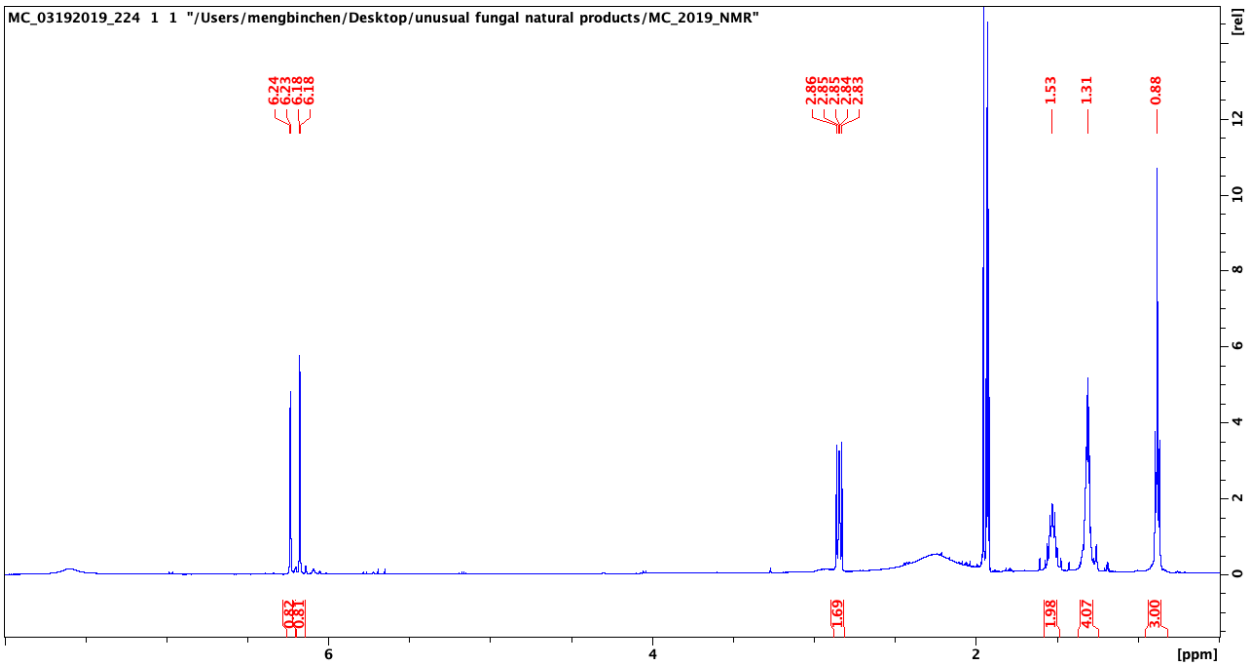

Figure S11. ^{1}H spectrum of **OA** in CD_3CN, 500 MHz.

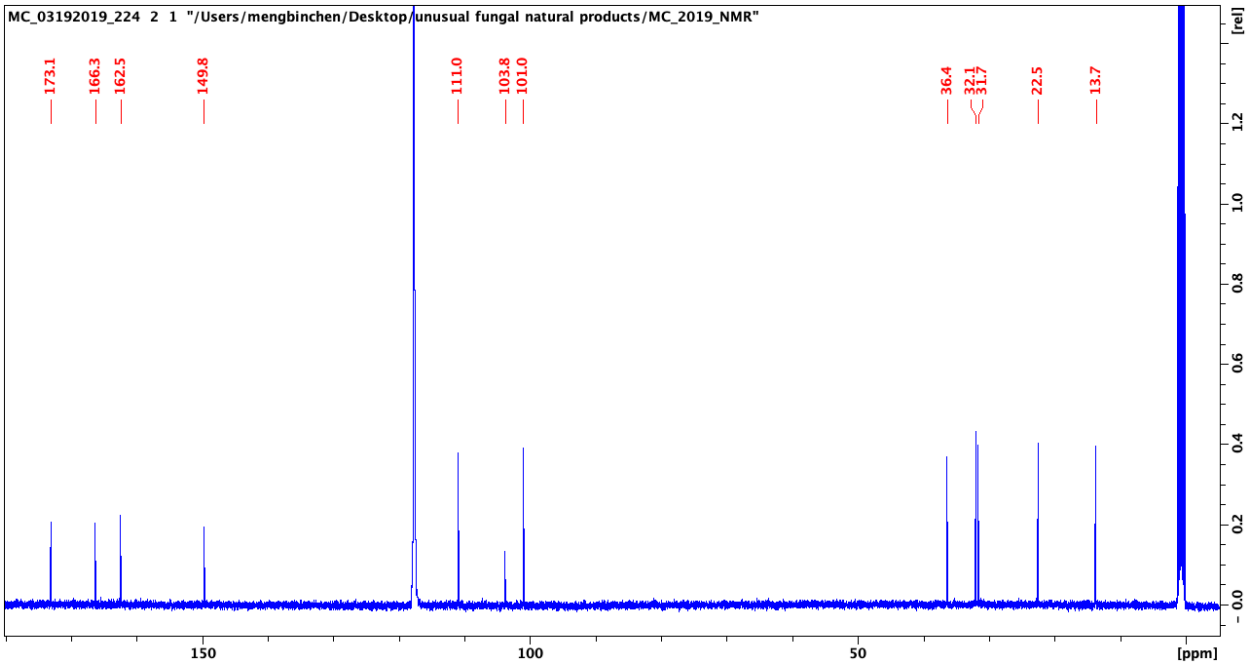

Figure S12. ^{13}C spectrum of OA in CD_3CN, 125 MHz.

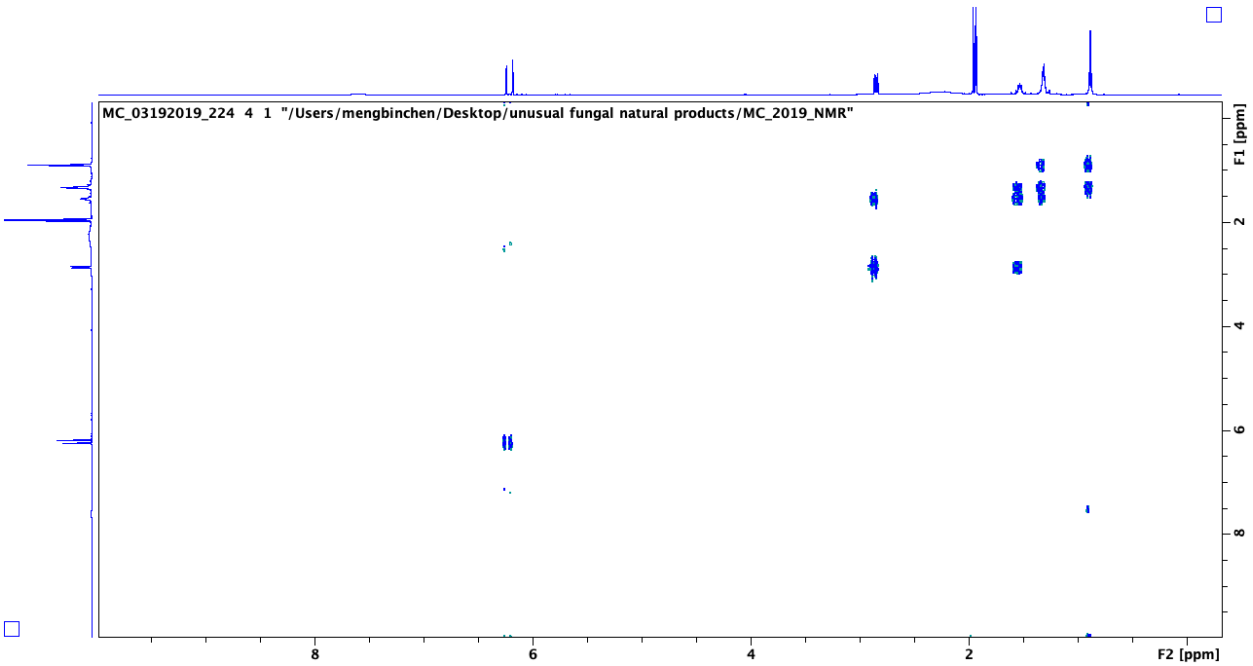

Figure S13. COSY spectrum of compound OA in CD_3CN.

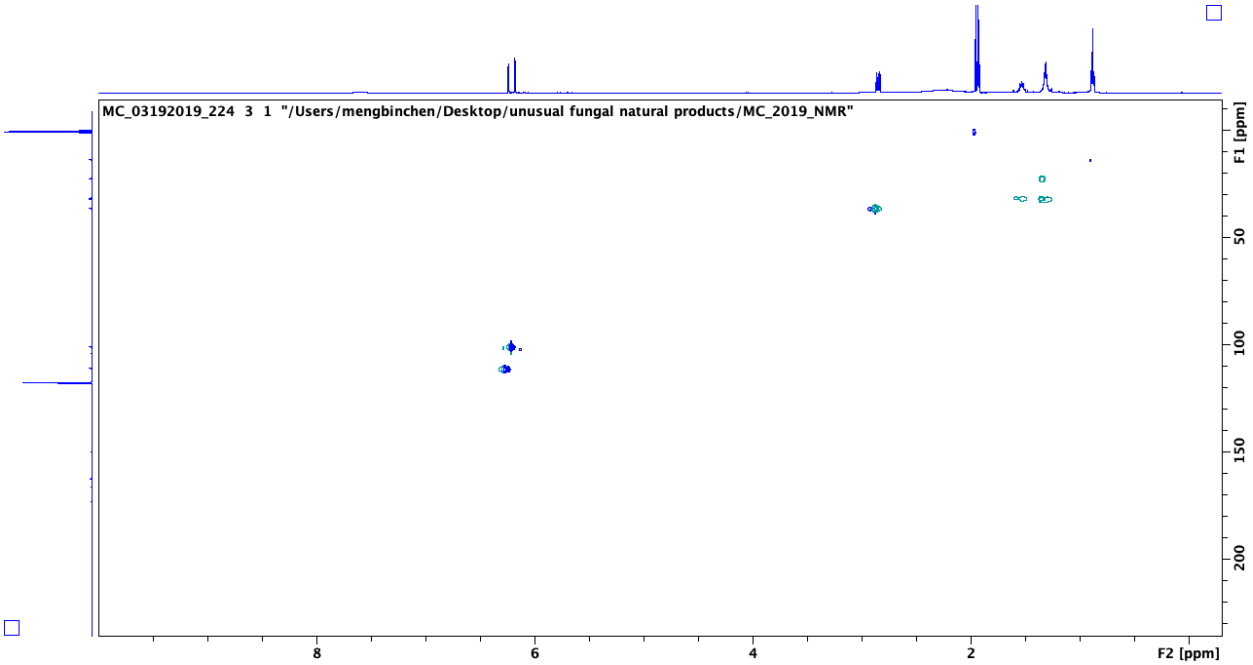

Figure S14. HSQC spectrum of compound OA in CD_3CN.

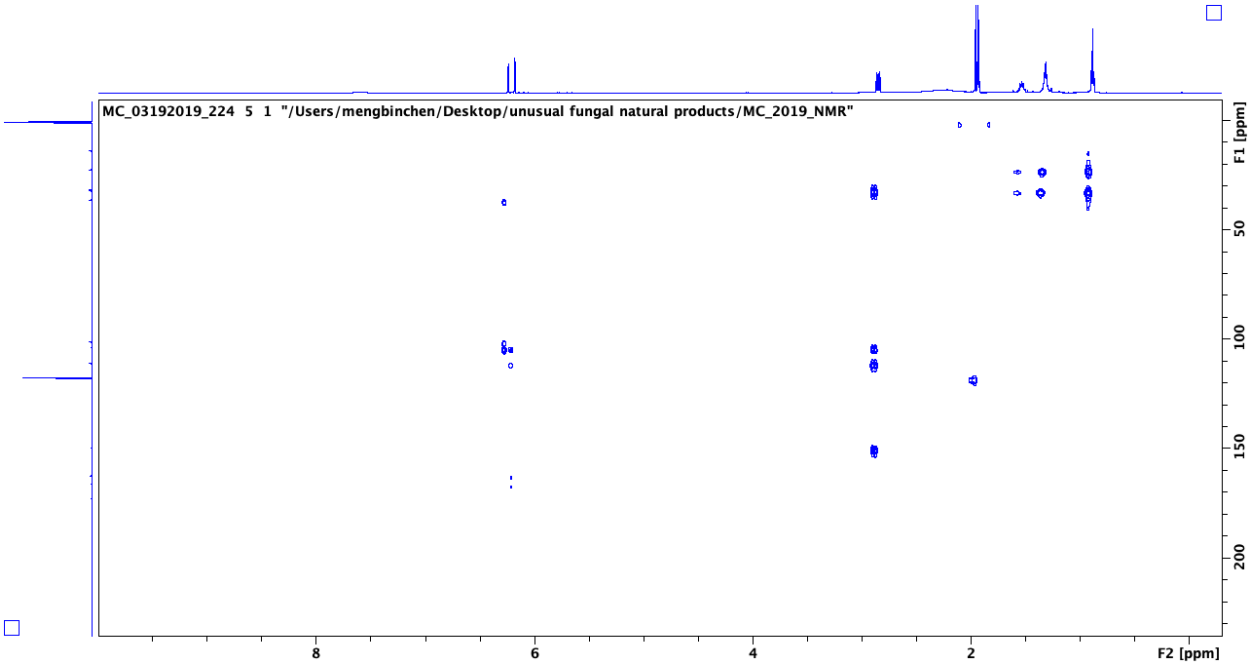

Figure S15. HMBC spectrum of compound OA in CD_3CN.

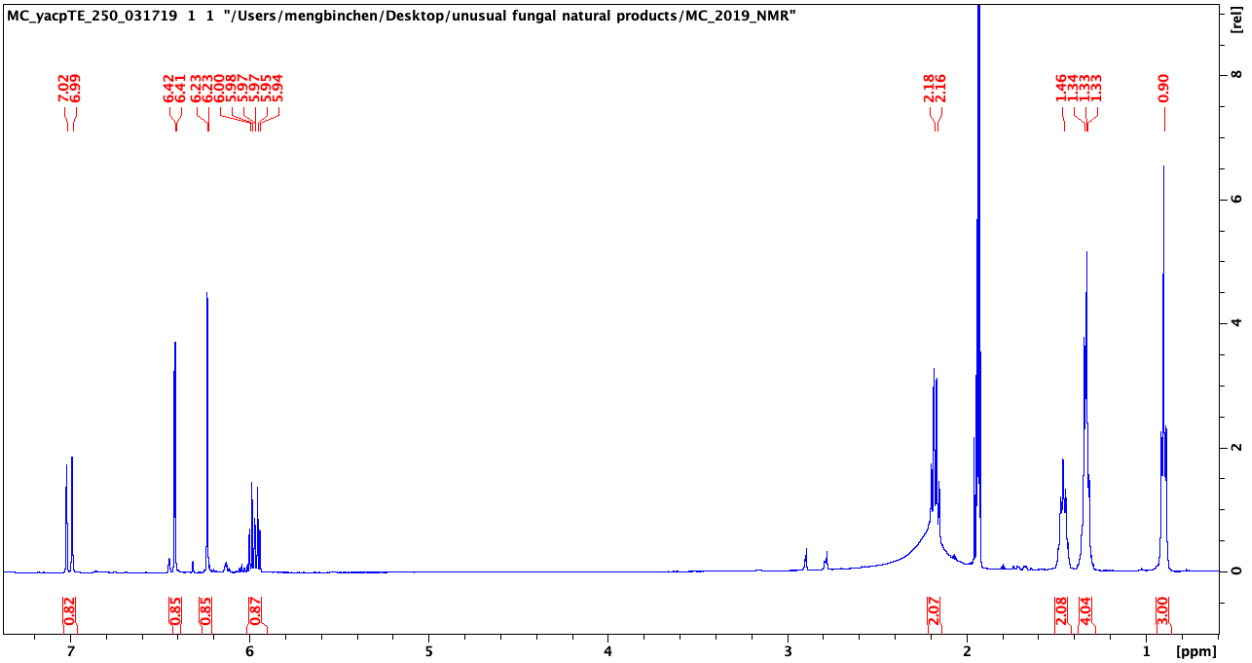

Figure S16. ^{1}H spectrum of **2** in CD_3CN, 500 MHz

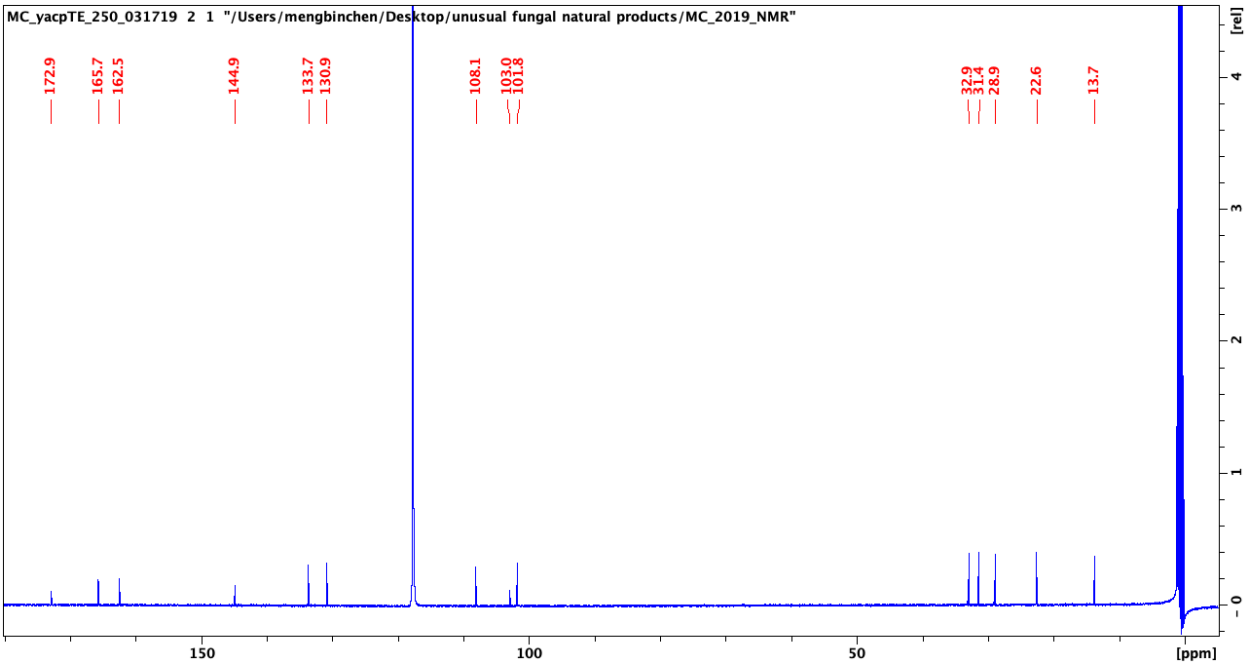

Figure S17. ^{13}C spectrum of **2** in CD_3CN, 125 MHz

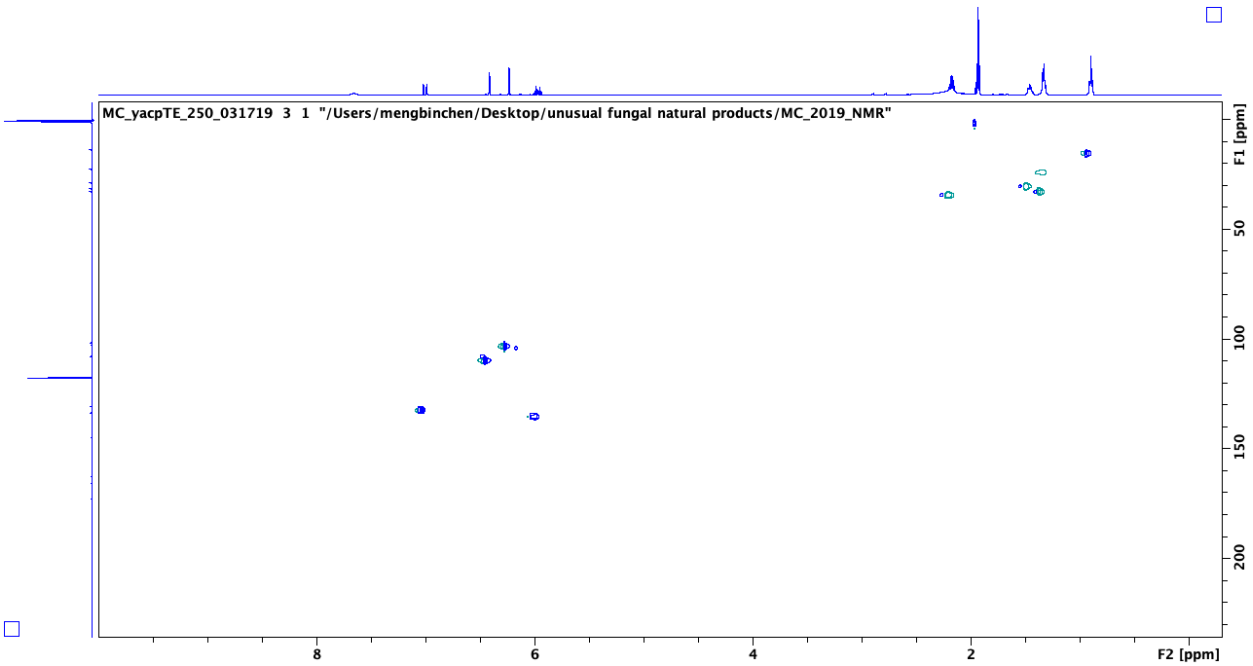

Figure S18. HSQC spectrum of compound **2** in CD_3CN

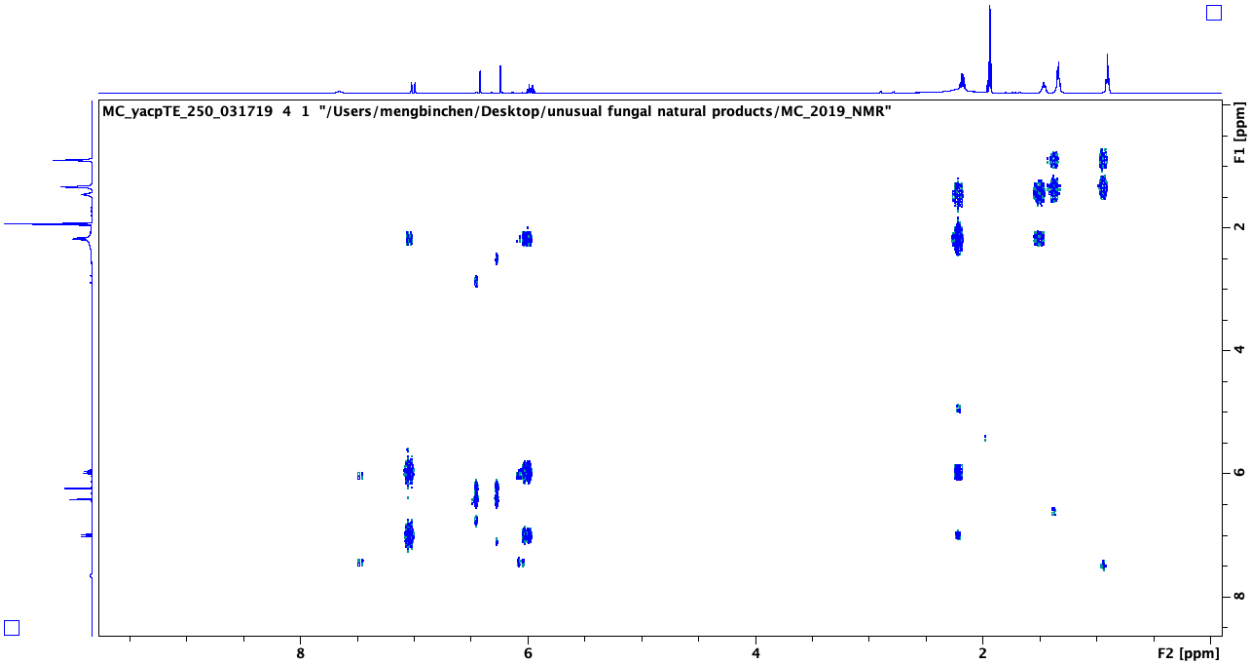

Figure S19. COSY spectrum of compound **2** in CD_3CN

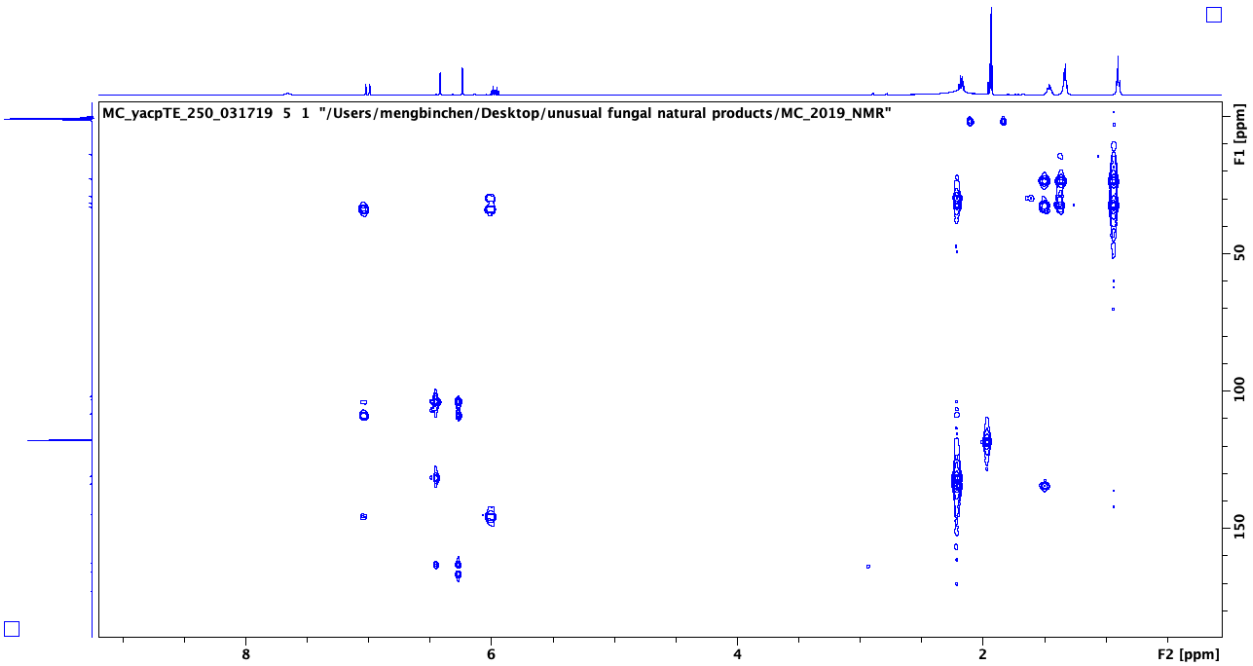

Figure S20. HMBC spectrum of compound **2** in CD_3CN.

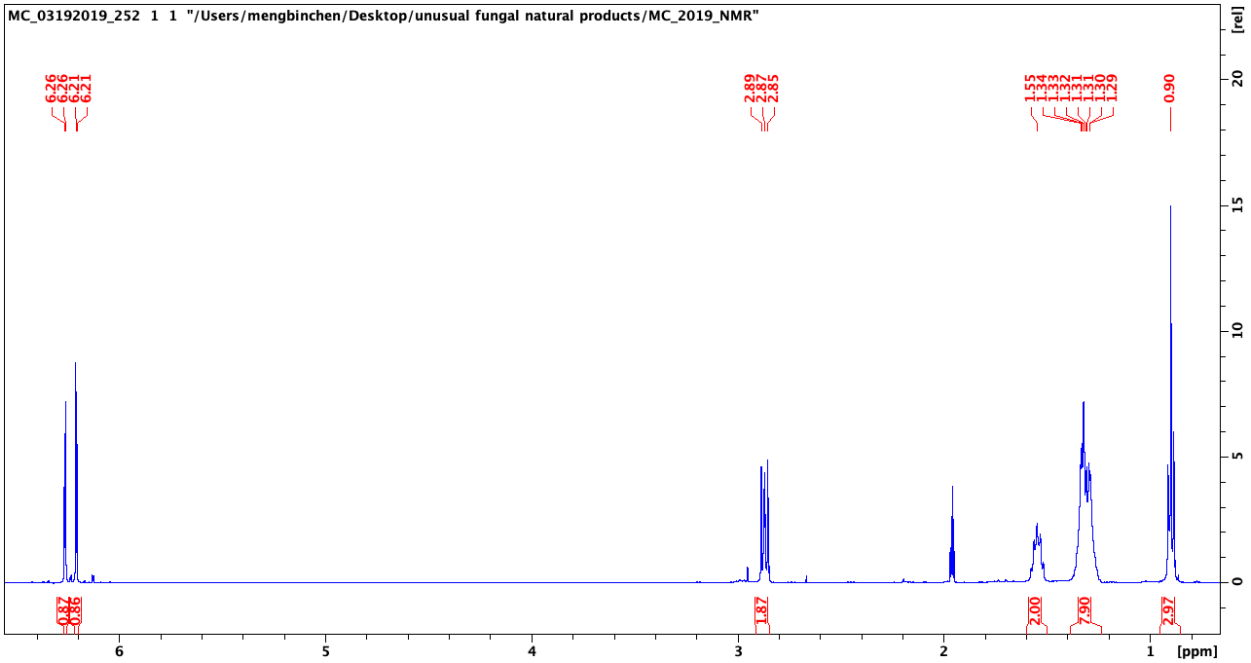

Figure S21. ^{1}H spectrum of SA in CD_3CN, 500 MHz

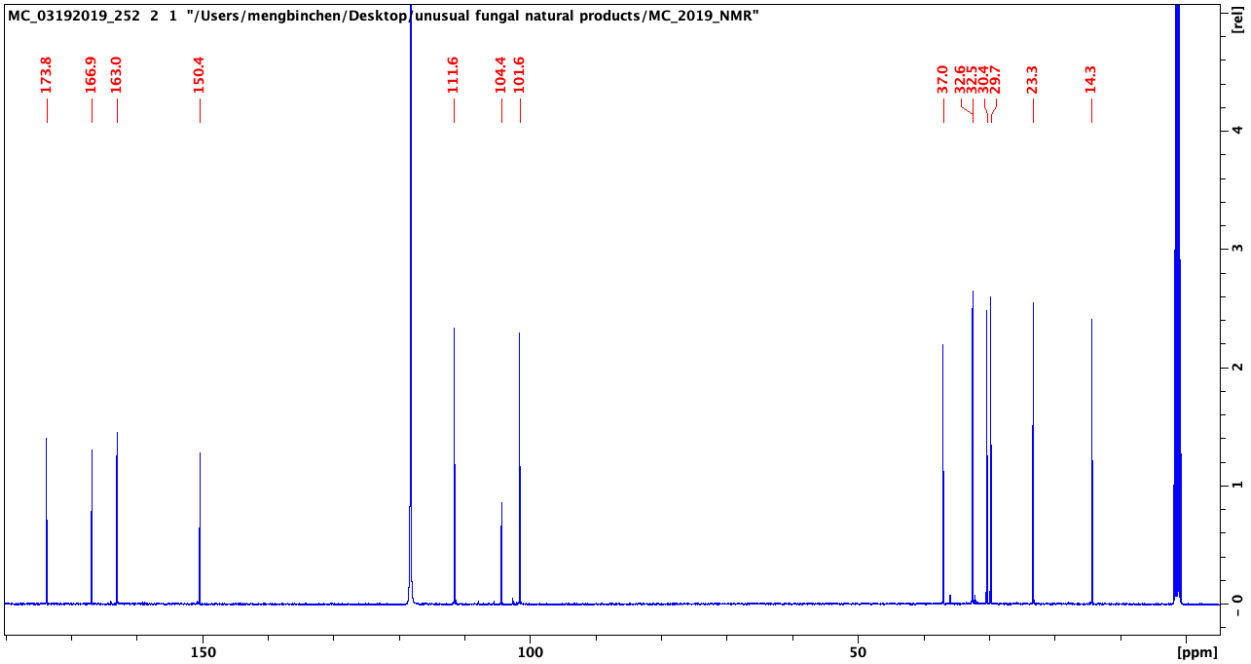

Figure S22. ^{13}C spectrum of SA in CD_3CN, 125 MHz

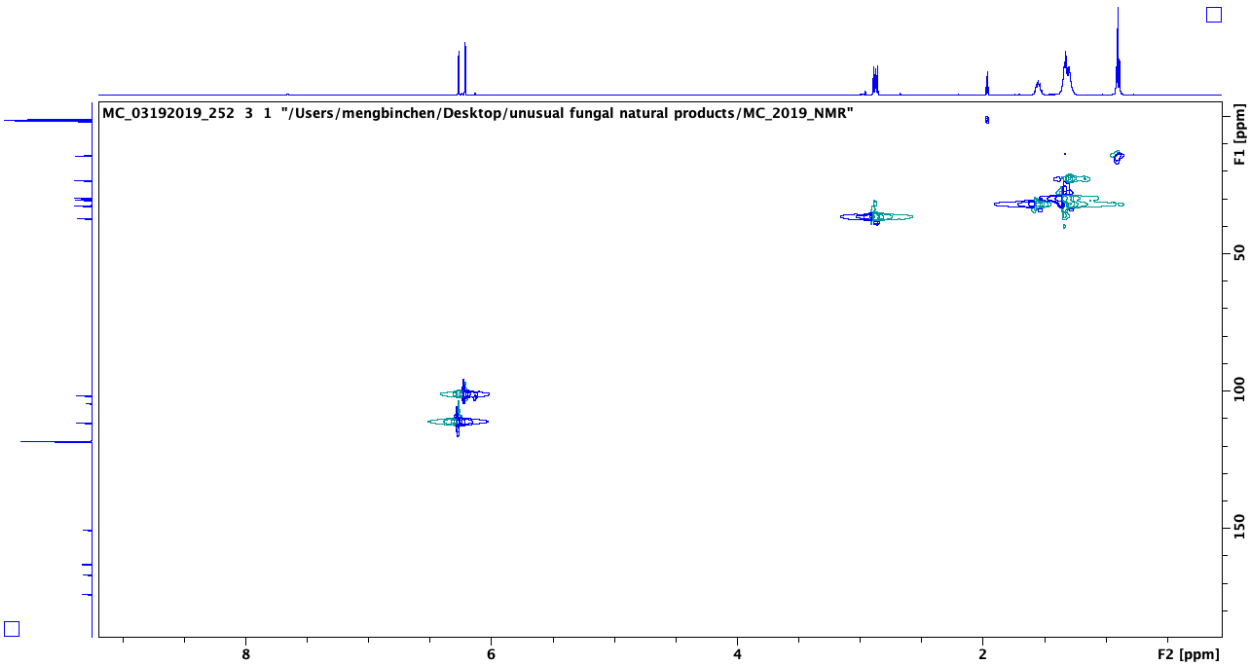

Figure S23. HSQC spectrum of SA in CD_3CN

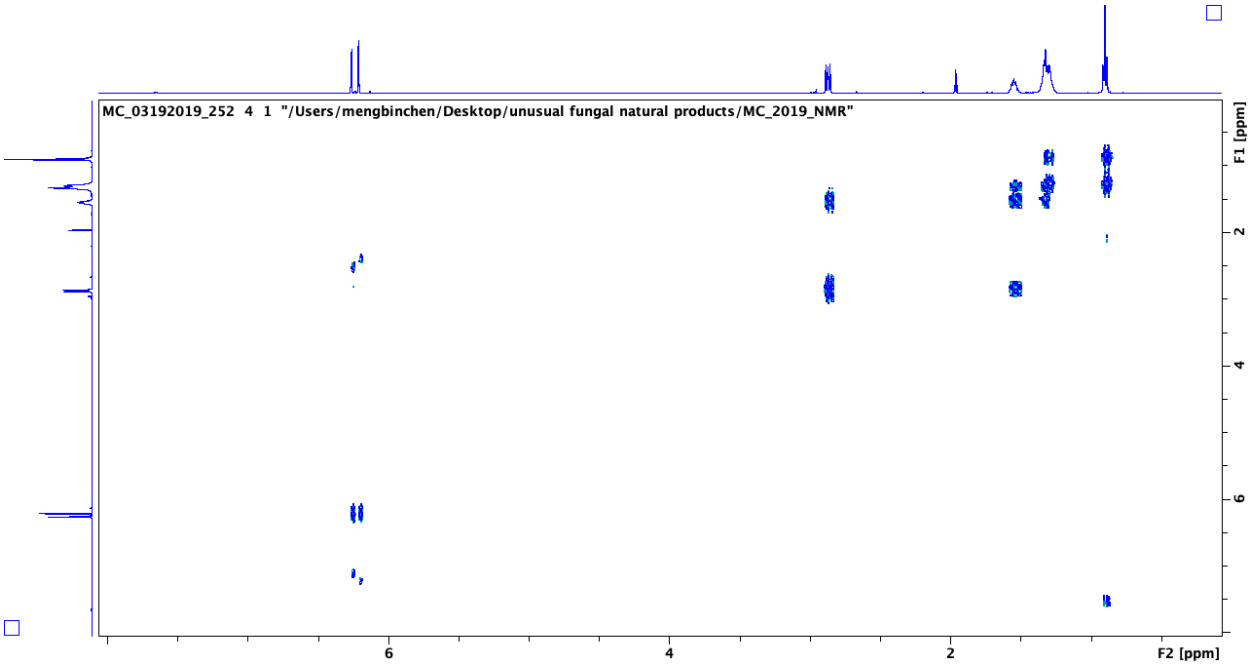

Figure S24. COSY spectrum of SA in CD_3CN

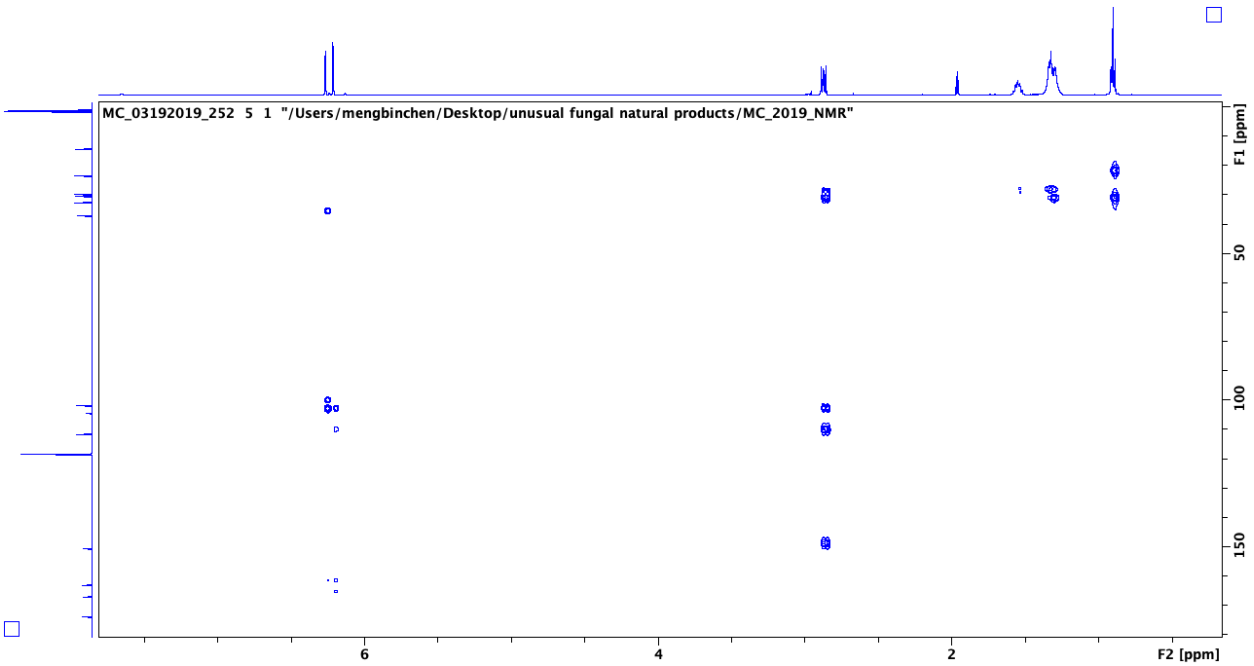

Figure S25. HMBC spectrum of SA in CD_3CN

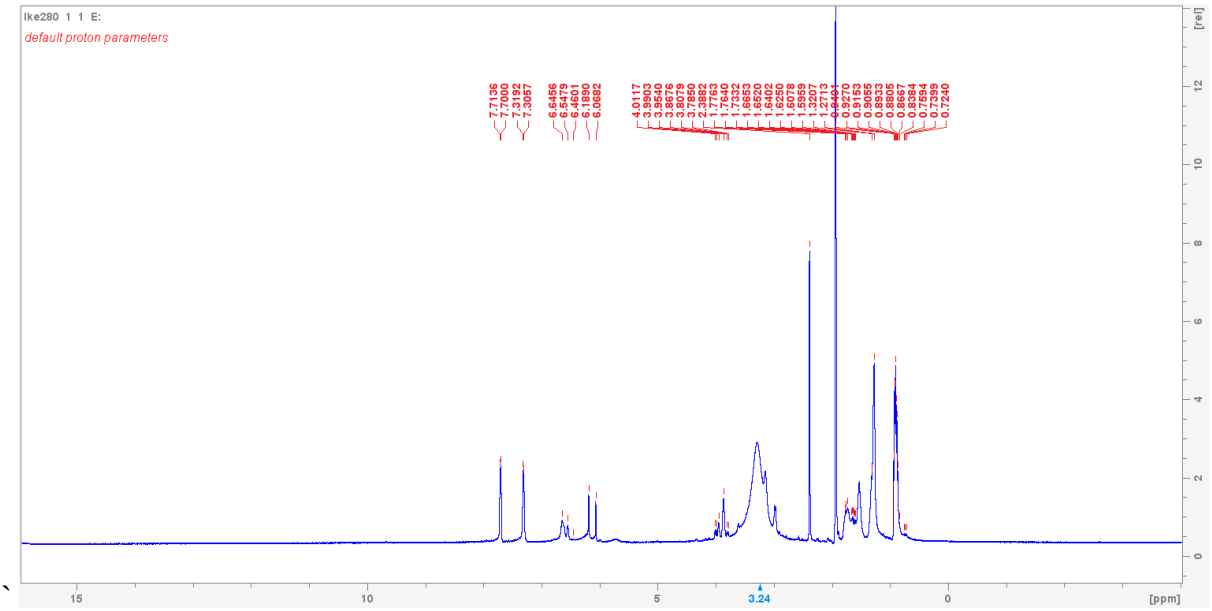

Figure S26. ^1H spectrum of compound **9** in CD_3CN (500 MHz)

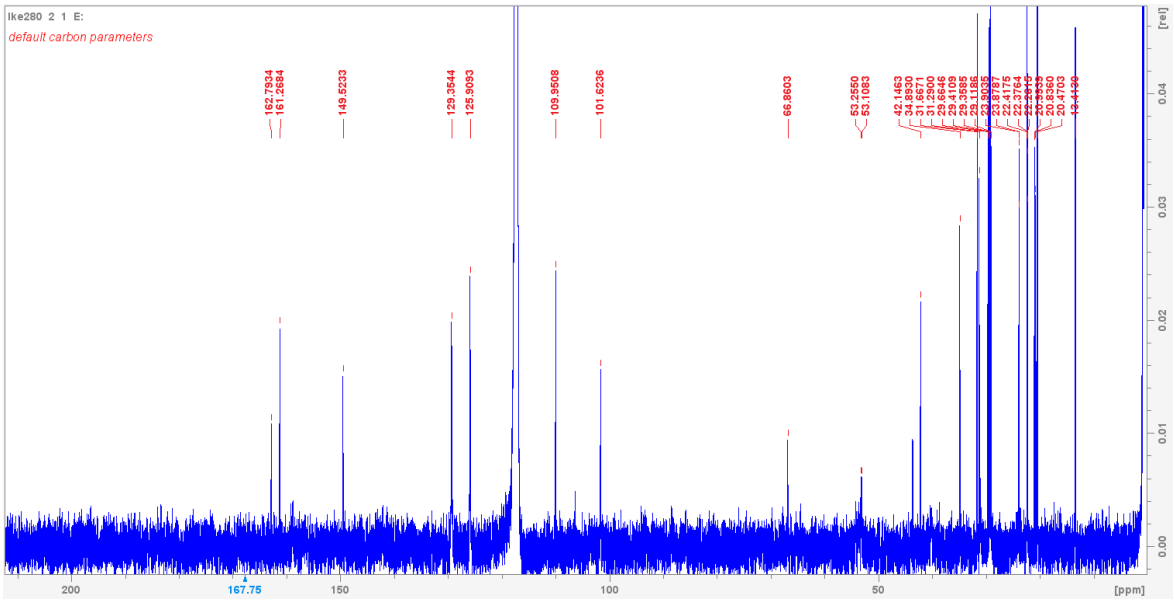

Figure S27. ^{13}C spectrum of compound **9** in CD_3CN (500 MHz)

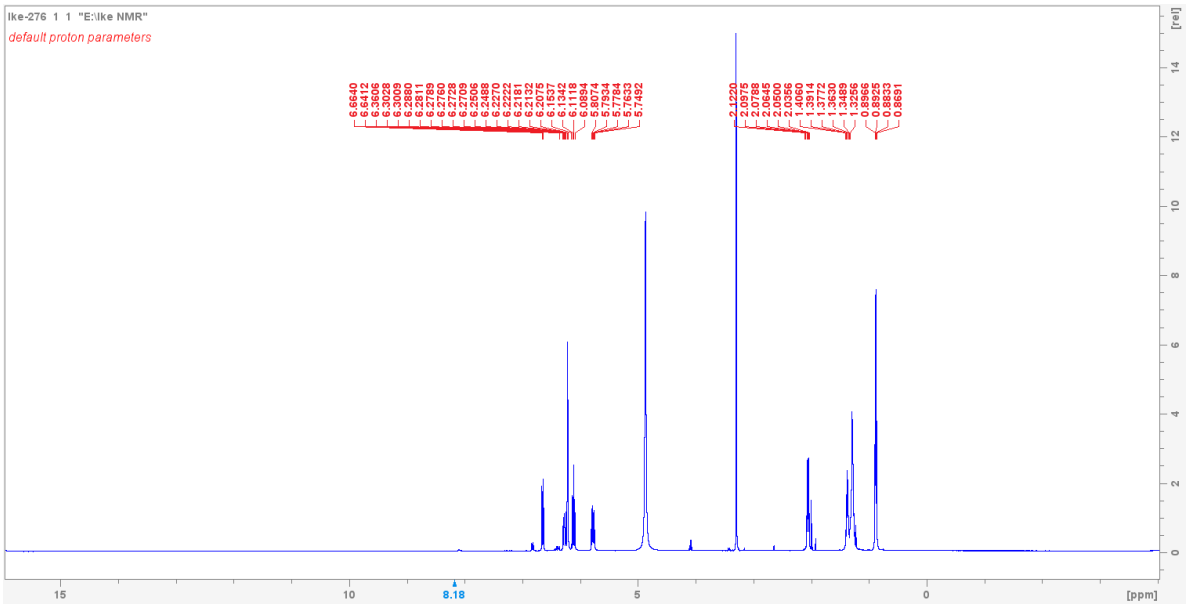

Figure S28. ^{1}H spectrum of compound **10** in CD_3OD (500 MHz)

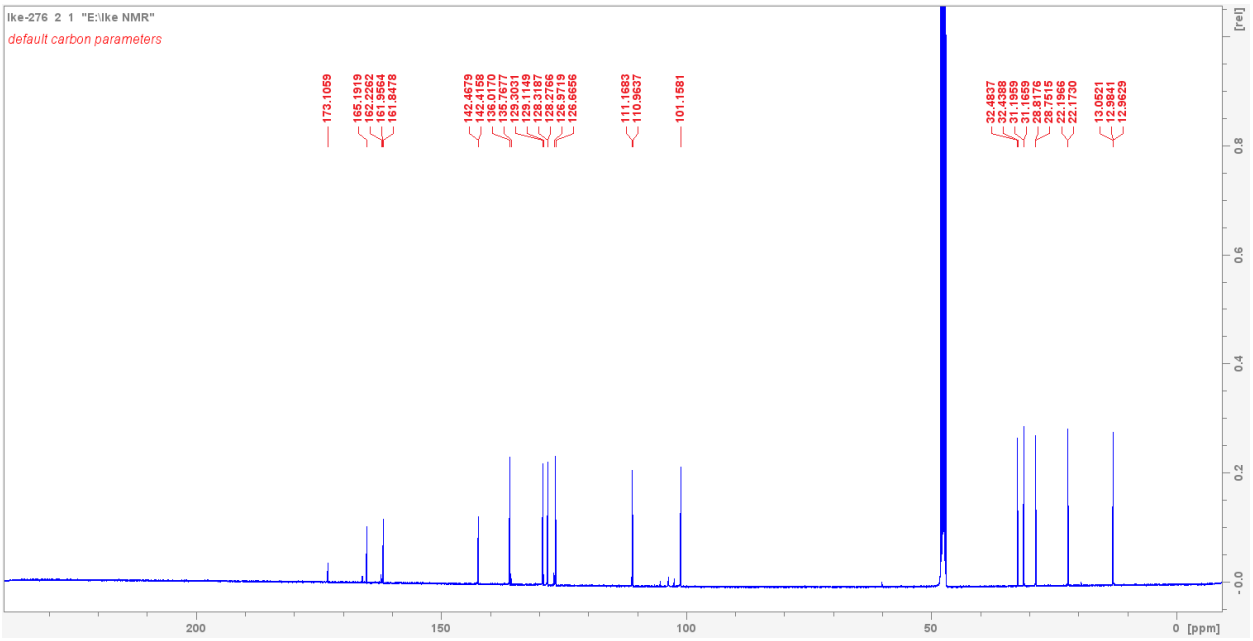

Figure S29. ^{13}C spectrum of compound 10 in CD_3OD (500 MHz)

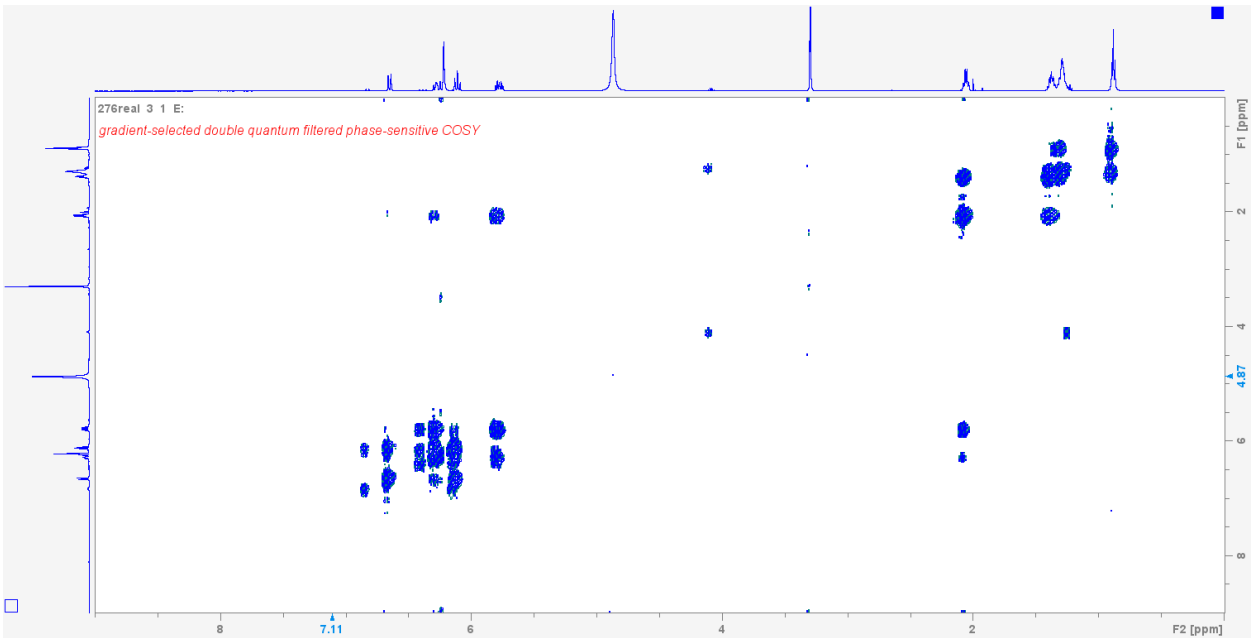

Figure S30. HSQC spectrum of compound **10** in CD_3OD

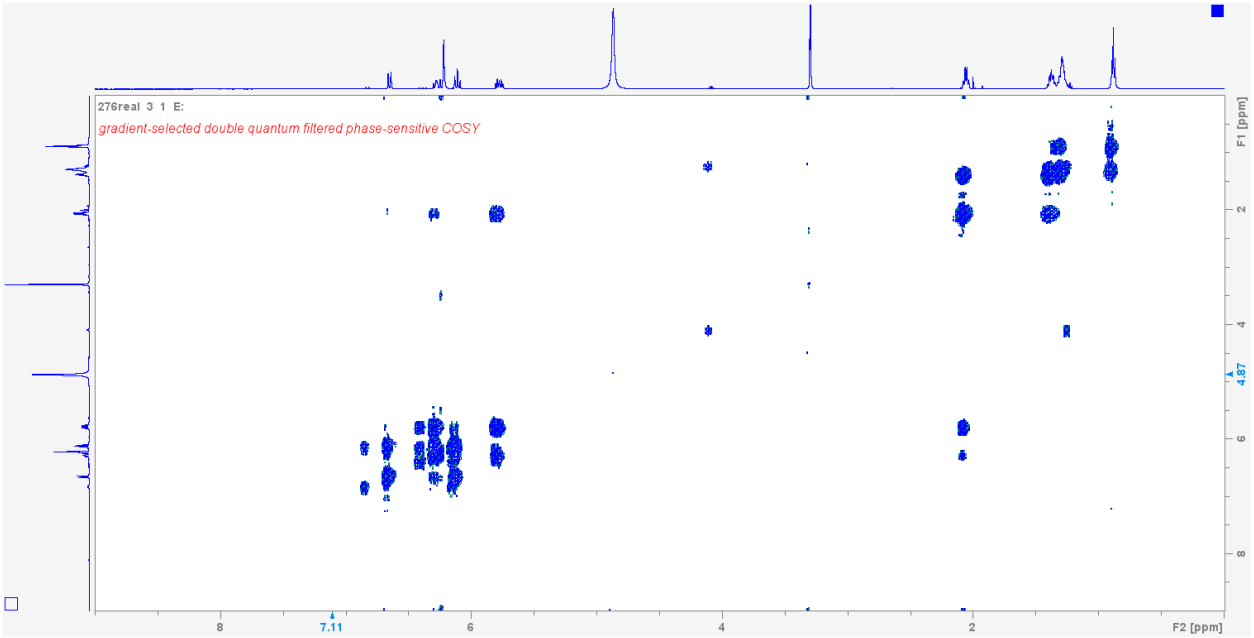

Figure S31. COSY spectrum of compound **10** in CD_3OD

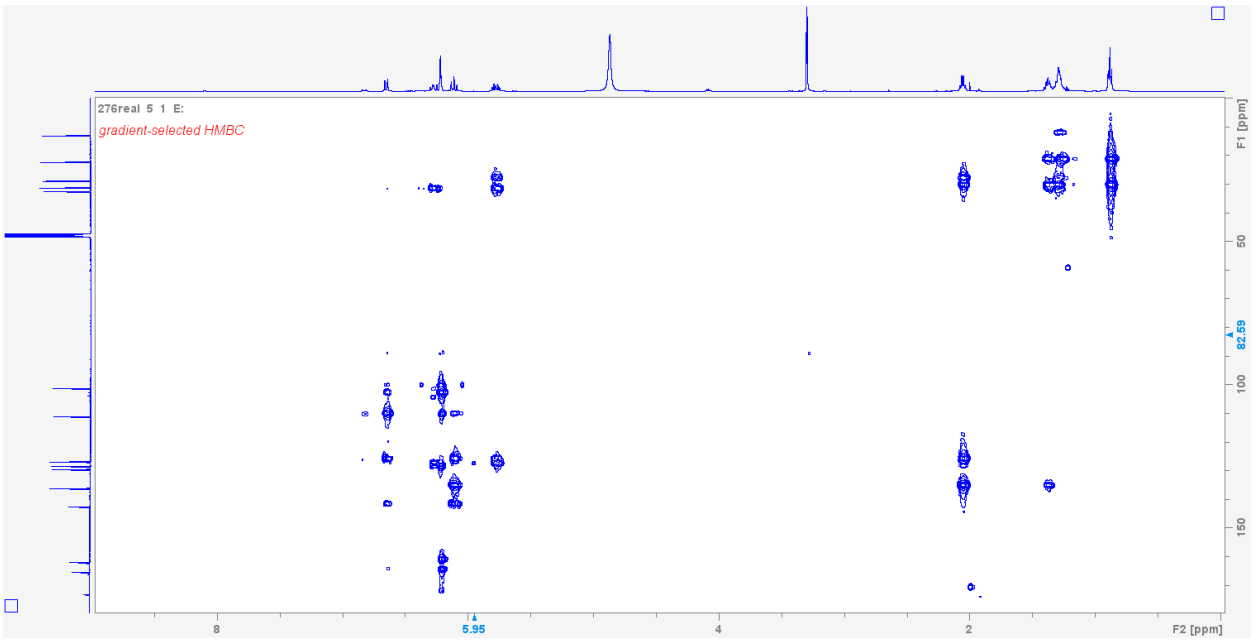

Figure S32. HMBC spectrum of compound **10** in CD_3OD

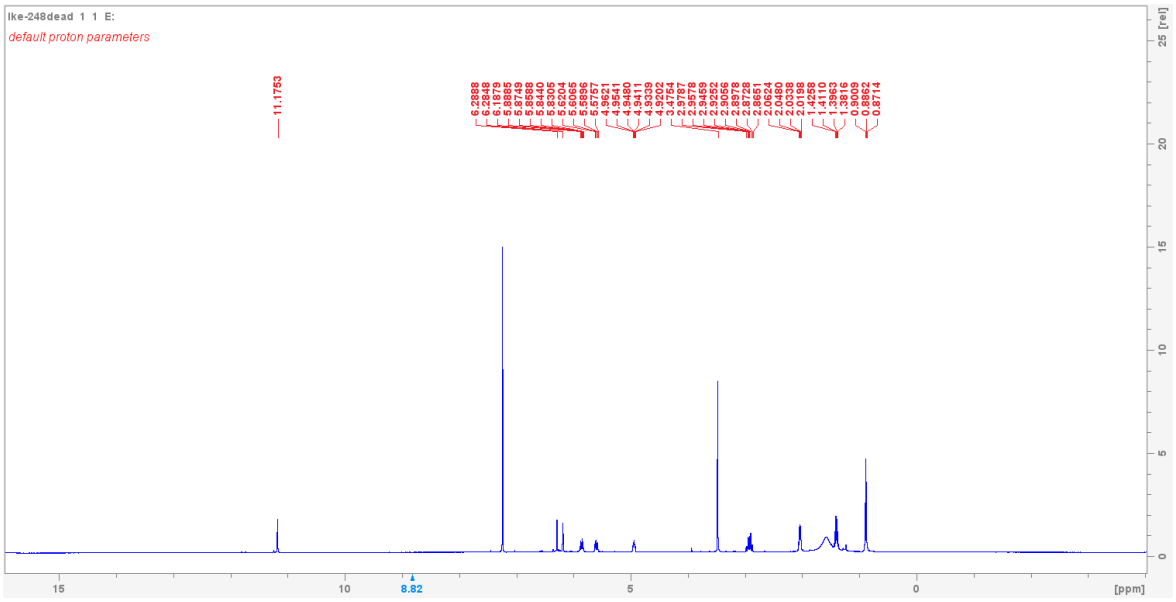

Figure S33. ^1H spectrum of **11** in $CDCl_3$ (500 MHz)

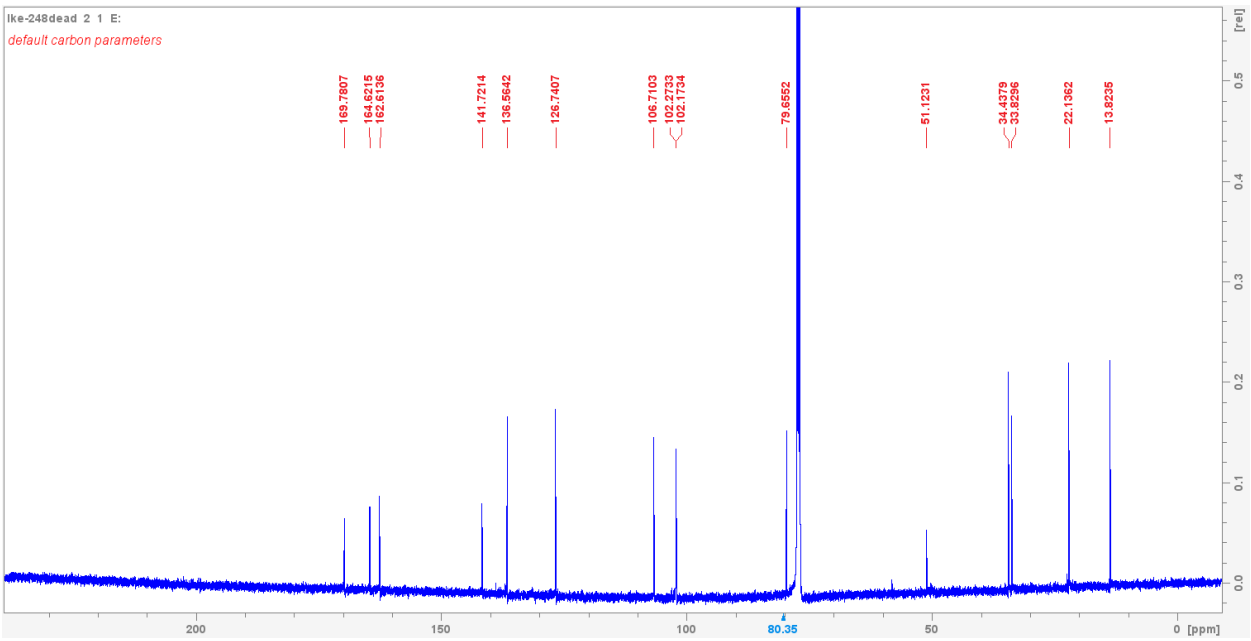

Figure S34. ^{13}C spectrum of **11** in $CDCl_3$ (500 MHz)

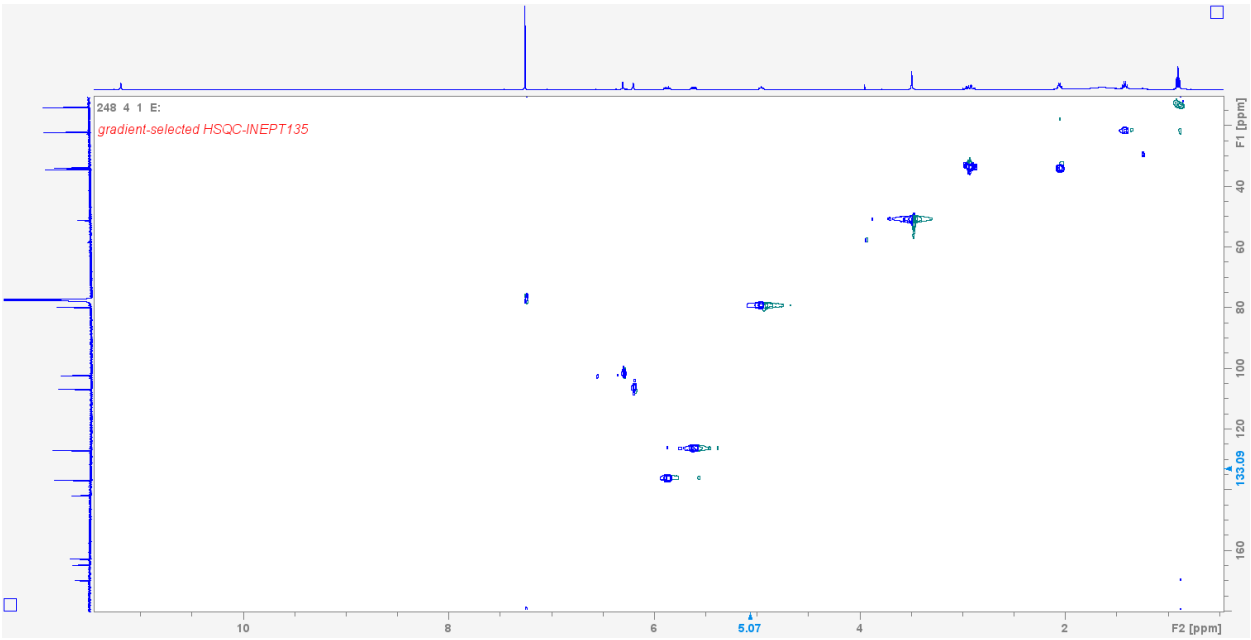

Figure S35. HSQC spectrum of compound **11** in $CDCl_3$

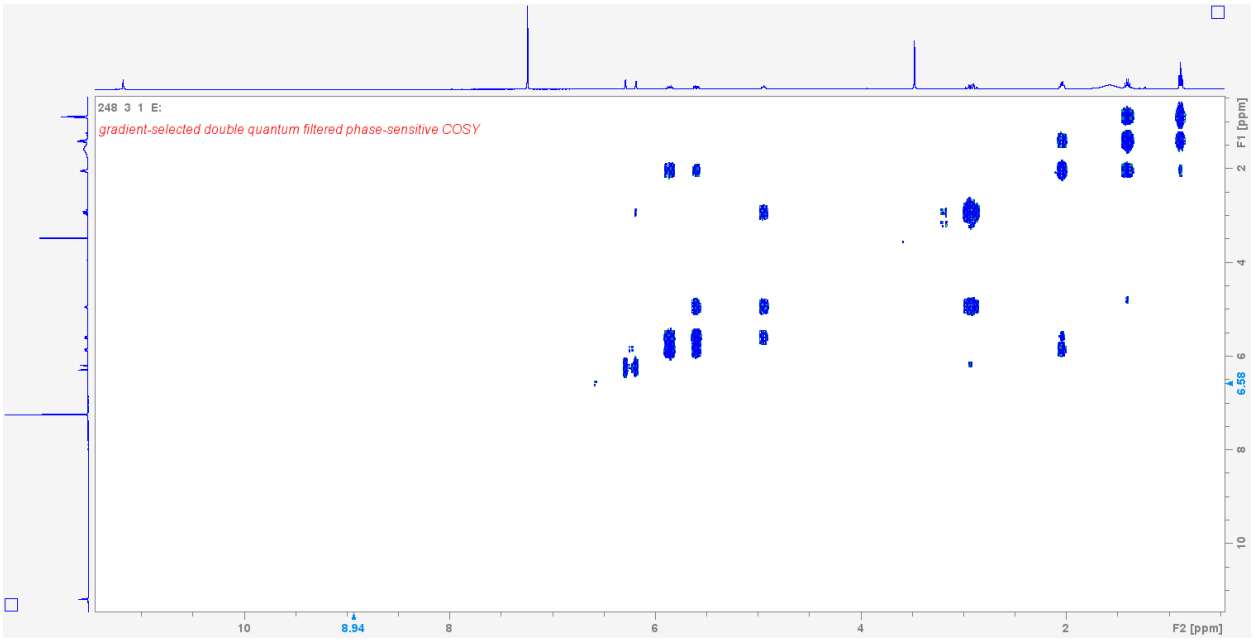

Figure S36. COSY spectrum of compound **11** in $CDCl_3$

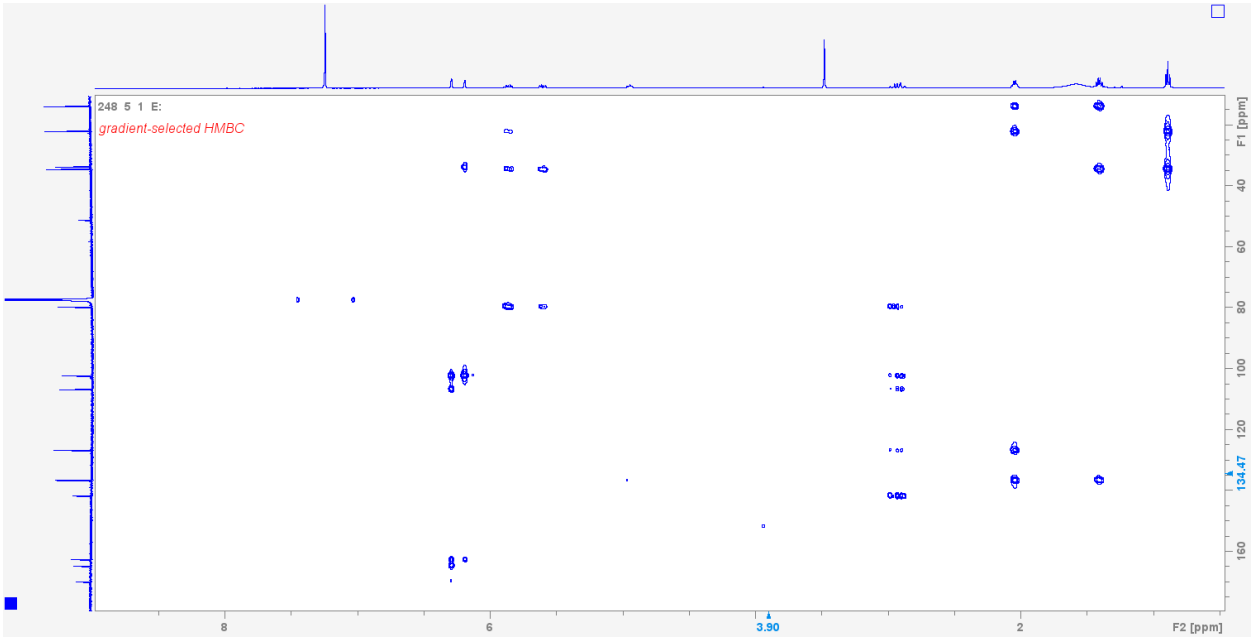

Figure S37. COSY spectrum of compound **11** in $CDCl_3$

9. References

1) Shah SA, Gupta AS, and Kumar P (2021) Emerging role of cannabinoids and synthetic cannabinoid receptor 1/cannabinoid receptor 2 receptor agonists in cancer treatment and chemotherapy-associated cancer management. *J. Cancer Res Ther* 17, 1–9.

2) Fraguas-Sánchez AI and Torres-Suárez AI (2018) Medical Use of Cannabinoids." *Drugs* 78,1665–1703.

3) Kovalchuk O and Kovalchuk I (2020) Cannabinoids as anticancer therapeutic agents. *Cell Cycle* 19.9, 961-989.

4)National Academies of Sciences, Engineering, and Medicine (2017) The Health Effects of Cannabis and Cannabinoids: The Current State of Evidence and Recommendations for Research. *Nat. Acad. Press* 377–390.

5) Warf B (2014) High points: An historical geography of cannabis. *Geographical Review* 104, 414-438.

6) Mikuriya TH (1969) Marijuana in medicine: past, present and future. *Calif Med* 110(1), 34-40.

7) Touwn M (1981) The religious and medicinal uses of Cannabis in China, India and Tibet. *J Psychoactive Drugs* 13(1), 23-34.

8) Li HL (1978) Hallucinogenic plants in Chinese herbals. *J Psychodelic Drugs* 10(1), 17-26.

9) O'Shaugnessy WB (1840) New remedy for tetanus and other convulsive disorders. *The Boston Medical and Surgical Journal* 23, 153–155.

10) ElSohly MA, Gul W (2014) Constituents of cannabis sativa, *Handbook of Cannabis*, 20

11) Pertwee, RG (2008) The diverse CB1 and CB2 receptor pharmacology of three plant cannanbinoids: Δ9-tetrahydrocannabinol, cannabidiol and Δ9-tetrahydrocannabivarin. *Br. J. Pharmacol.* 153, 199-215.

12) Grotenhermen F (2003) Pharmacokinetics and pharmacodynamics of cannabinoids. *Clinical Pharmacokinetics* 42(4), 327–360.

13) National Academies of Sciences, Engineering, and Medicine; Health and Medicine Division; Board on Population Health and Public Health Practice; Committee on the Health Effects of Marijuana: An Evidence Review and Research Agenda (2017) The Health Effects of Cannabis and Cannabinoids: The Current State of Evidence and Recommendations for Research. *National Academies Press.*

14) Chandra S, Lata H, Khan IA, ElSohly MA (2013) The role of biotechnology in Cannabis sativa propagation for the production of phytocannabinoid. *Biotechnology for medicinal plants* 2013, 123–148.

15) Devane WA, Dysarz FA 3rd, Johnson MR, Melvin LS, Howlett AC (1988) Determination and characterization of a cannabinoid receptor in rat brain. *Molecular Pharmacology* 34(5),605–613.

16) Fredriksson R, Lagerström MC, Lundin LG, Schiöth HB (2003) The G-protein-coupled receptors in the human genome form five main families. Phylogenetic analysis, paralogon groups, and fingerprints. *Mol Pharmacol.* 63(6), 1256–72.

17) Bow EW, Rimoldi JM (2016) The Structure–Function Relationships of Classical Cannabinoids: CB1/CB2 Modulation. *Perspectives in Medicinal Chemistry* 8.

18) Gragg, M and Park PSH (2019) Detection of misfolded rhodopsin aggregates in cells by Förster resonance energy transfer. *Methods in Cell Biology* 149, 87-105.

19) Ghosh E, Kumari P, Jaiman D, Shukla AK (2015) Methodological advances: the unsung heroes of the GPCR structural revolution. *Nat Rev Mol Cell Biol.* 16, 69–81.

20) Stevens RC, Cherezov V, Katritch V et al. (2013) The GPCR network: a large-scale collaboration to determine human GPCR structure and function. *Nat Rev Drug Discov.* 12(1), 25–34.

21) Howlett AC, Fleming RM (1984) Cannabinoid inhibition of adenylate cyclase. Pharmacology of the response in neuroblastoma cell membranes. *Mol Pharmacol.* 26(3), 532–8.

22) Howlett AC, Qualy JM, Khachatrian LL (1986) Involvement of Gi in the inhibition of adenylate cyclase by cannabimimetic drugs. *Mol Pharmacol.* 29(3), 307–13.

23) Matsuda LA, Lolait SJ, Brownstein MJ, Young AC, Bonner TI (1990) Structure of a cannabinoid receptor and functional expression of the cloned cDNA. *Nature* 346(6284), 561–4.

24) Herkenham M, Lynn AB, Johnson MR, Melvin LS, de Costa BR, Rice KC (1991) Characterization and localization of cannabinoid receptors in rat brain: a quantitative in vitro autoradiographic study. *J Neurosci.* 11(2), 563–83.

25) Demuth DG and Molleman A (2006) Cannabinoid signalling. *Life Sci* 78(6), 549–63.

26) Munro S, Thomas KL, Abu-Shaar M (1993) Molecular characterization of a peripheral receptor for cannabinoids. *Nature* 365(6441), 61–5.

27) Di Marzo V, Stella N, Zimmer A (2015) Endocannabinoid signalling and the deteriorating brain. *Nat Rev Neurosci.* 16(1), 30–42.

28) Savonenko AV, Melnikova T, Wang Y et al (2015) Cannabinoid CB2 receptors in a mouse model of Aβ amyloidosis: immunohistochemical analysis and suitability as a PET biomarker of neuroinflammation. *PLoS One.* 10(6).

29) Derkinderen P, Valjent E, Toutant M.et al (2003). Regulation of extracellular signal-regulated kinase by cannabinoids in hippocampus. *J Neurosci.* 23(6), 2371–82.

30) Turu G, Hunyady L (2010). Signal transduction of the CB1 cannabinoid receptor. *J Mol Endocrinol.* 44(2), 75–85.

31) Clister T, Mehta S, Zhang J (2015). Single-cell analysis of G-protein signal transduction. *J Biol Chem.* 290(11), 6681-8.

32) De Petrocellis L, Di Marzo V (2010). Non-CB1, Non-CB2 receptors for endocannabinoids, plant cannabinoids, and synthetic cannabimimetics: focus on G-protein-coupled receptors and transient receptor potential channels. *J Neuroimmune Pharmacol.* 5(1), 103–21.

33) De Petrocellis L. Ligresti A, Moriello AS et al (2011). Effects of cannabinoids and cannabinoid-enriched *Cannabis* extracts on TRP channels and endocannabinoid metabolic enzymes. *Br J Pharmacol.* 163(7), 1479–94.

34) Adams R, Hunt M, Clark JH (1940). Structure of cannabidiol, a product isolated form the marihuana extract of Minnesota wild hemp. *I. Journal of the American Chemical Society* 62 (1), 196-200.

35) Adams R, Pease DC, Cain CK, Baker BR, Clark JH, Wolff H, Wearn RB (1940). Conversion of cannabidiol to.a product with marihuana activity. *Journal of the American Chemical Society* 62 (8), 2245-2246.

36) Zhornitsky S, and Potvin S (2012) Cannabidiol in humans—the quest for therapeutic targets. *Pharmaceuticals* 5(5), 529-52.

37) Cannabis Pharmaceuticals Market Size, Share & Trends Analysis Report By Brand Type (Sativex, Epidiolex), By Region (North America, Europe, Asia Pacific, Latin America, MEA), And Segment Forecasts, 2023 – 2030. https://www.researchandmarkets.com/reports/5534066/cannabis-pharmaceuticals-market-size-share-and

38) Gagne SJ, Stout JM, Liu E, Boubakir Z, Clark SM, and Page JE (2012) Identification of olivetolic acid cyclase from Cannabis sativa reveals a unique catalytic route to plant polyketides. *Proceedings of the National Academy of Sciences* 109(31), 12811-6.

39) Fellermeier M and Zenk MH (1998) Prenylation of olivetolate by a hemp transferase yields cannabigerolic acid, the precursor of tetrahydrocannabinol. *FEBS Letters* 427, 283-285.

40) Tan Z, Clomburg JM, and Gonzalez R (2018) Synthetic Pathway for the Production of Olivetolic Acid in *Escherichia coli*. *ACS Synth. Biol* 7, 1886–1896.

41) Luo X, Reiter MA, d'Espaux L, Wong J, Denby CM, Lechner A, Zhang Y, Grzybowski AT, Harth S, Lin W, Lee H, Yu C, Shin J, Deng K, Benites VT, Wang G, Baidoo EEK, Chen Y, Dev I, Petzold CJ, and Keasling J (2019) Complete biosynthesis of cannabinoids and their unnatural analogues in yeast. *Nature* 567, 123–126.

42) Valliere MA, Korman TP, Woodall NB, Khitrov GA, Taylor RE, Baker D, and Bowie JU (2019) A cell-free platform for the prenylation of natural products and application to cannabinoid production. *Nat Commun* 10, 565

43) Ma J, Gu Y, and Xu P (2022) Biosynthesis of cannabinoid precursor olivetolic acid in genetically engineered *Yarrowia lipolytica*. *Commun Biol* 5, 1239

44) Reimer C, Kufs JE, Rautschek J, Regestein L, Valiante V, and Hillman F (2022) Engineering the amoeba *Dictyostelium discoideum* for biosynthesis of a cannabinoid precursor and other polyketides. *Nat Biotechnol* 40, 751–758.

45) Kufs JE, Reimer C, Steyer E, Valiante, V,Hillman F, and Regestein L (2022) Scale-up of an amoeba-based process for the production of the cannabinoid precursor olivetolic acid. *Microb Cell Fact* 21, 217.

46) Hyde K et al. (2019) The amazing potential of fungi: 50 ways we can exploit fungi industrially. *Fungal Diversity* 97, 1-136.

47) Cragg GM and Newman DJ (2018) Natural Products as Sources of Anticancer Agents: Current Approaches and Perspectives. *Natural Products as Source of Molecules with Therapeutic Potential* 309-331.

48)Barrett David (2002) From natural products to clinically useful antifungals. *Biochimica et Biophysica Acta (BBA) – Molecular Basis of Disease* 1587.2-3, 224-233

49) Long J (2003) New Antifungal Agent Additions to the Existing Armamentarium. *Pharmacotherapy Update* 6.3.

50)World Health Organization (2019) World Health Organization model list of essential medicines: 21st list 2019.

51) Demain AL and Fang A (2000) The natural functions of secondary metabolites. *History of modern biotechnology I*. 1-39.

52) Singh AK, Rana HK, and Pandey AK (2019) Fungal-Derived Natural Product: Synthesis, Function, and Applications. *Recent Advancement in White Biotechnology through Fungi- Fungal Biology.*229-248

53) Schueffler A and Anke, T (2014) Fungal Natural Products in Research and Development. *Natural Product Reports* 31,1425-1448.

54) Skellam, E (2019) Strategies for Engineering Natural Product Biosynthesis in Fungi. *Trends in Biotechnology* 37(4), 416-427.

55) Corre C and Challis, GL (2010) Exploiting Genomics for New Natural Product Discovery in Prokaryotes. *Reference Module in Chemistry, Molecular Sciences and Chemical Engineering - Comprehensive Natural Products II* 2, 429-453

56) Ziemert N and Alanjary M, and Weber T (2016) The evolution of genome mining in microbes- a review. *Natural Product Reports* 33(8), 988-1005.

57) Fischbach MA, Walsh CT, and Clardy, J (2008) The evolution of gene collectives: How natural selection drives chemical innovation. *Proceedings of the National Academy of Sciences of the United States of America* 105(12), 4601-4608.

58) Ziemert N, Podell S, Penn K, Badger JH, Allen E, and Jensen PR (2012) The Natural Product Domain Seeker NaPDoS: A Phylogeny Based Bioinformatic Tool to Classify Secondary Metabolite Gene Diversity. *PLoS ONE* 7(3), e34064.

59) Bingle LE, Simpson TJ, and Lazarus CM (1999) Ketosynthase Domain Probes Identify Two Subclasses of Fungal Polyketide Synthase Genes. *Fungal Genetics and Biology* 26(3), 209-223

60) Rausch C, Hoof I, Weber T, Wohlleben W, and Huson DH (2007) Phylogenetic analysis of condensation domains in NRPS sheds light on their functional evolution. *BMC Evolutionary Biology* 7(78).

61) D'Costa VM, King CE, Kalan L, Morar M, Sung WWL, Schwarz C, Froese D, Zazula G, Calmels F, Debruyne R, Golding GB, Poinar HN, and Wright GD (2011) Antibiotic resistance is ancient. *Nature* 477, 457-461

62) Cox G and Wright GG (2013) Intrinsic antibiotic resistance: Mechanisms, origins, challenges and solutions. *International Journal of Medical Microbiology* 303.6-7, 287-292

63) Almabruk K, Dinh LK, and Philmus B (2018) Self-Resistance of Natural Product Producers: Past, Present, and Future Focusing on Self-Resistant Protein Variants. *ACS Chemical Biology* 13(6), 1426-1437.

64) Tang X, Li J, Millán-Aguiñaga N, Zhang JJ, O'Neill EC, Ugalde JA, Jensen PR, Mantovani SM, and Moore BM (2015) Identification of Thiotetronic Acid Antibiotic Biosynthetic Pathways by Target-directed Genome Mining. *ACS Chemical Biology* 10(12):2841-2849.

65) Lin HC, Chooi YH, Dhingra S, Xu W, Calvo AN, and Tang Y (2013) The Fumagillin Biosynthetic Gene Cluster in *Aspergillus fumigatus* Encodes a Cryptic Terpene Cyclase Involved in the Formation of βtrans-Bergamotene. *Journal of the American Chemical Society* 135(12):4616-4619.

66) Yeh HH, Ahuja M, Chiang YM, Oakley CE, Moore S, Yoon O, Hajovsky H, Book JW, Keller NP, Wang CCC, and Oakley BR (2016) Resistance Gene-Guided Genome Mining: Serial Promoter Exchanges in *Aspergillus nidulans* Reveal the Biosynthetic Pathway for Fellutamide B, a Proteasome Inhibitor. *ACS Chemical Biology* 11(8), 2275-2284

67) Kling A, Lukat P, Almeida DV, Bauer A, Muller R et al. (2015) Targeting DnaN for tuberculosis therapy using novel griselimycins. *Science* 348 (6239),1106-1112

68) Medema MH, Blin K, Cimermancic P, de Jager V, Zakrzewki P, Fischbach MA, Weber T, Takano E, and Breitling R (2011) antiSMASH: rapid identification, annotation and analysis of secondary metabolite biosynthesis gene clusters in bacterial and fungal genome sequences." *Nucleic Acids Research* 39,W339-W346

69) Khaldi N, Seifuddin FT, Turner G, Haft N, Nierman WC, Wolfe KH, and Fedorova ND (2010) SMURF: genomic mapping of fungal secondary metabolite clusters. *Fungal Genetics and Biology* 47(9), 736-741

70) Alanjary M, Kronmiller B, Adamek M, Blin K, Weber T, Huson D, Philmus B, and Ziermert N (2017) The Antibiotic Resistant Target Seeker (ARTS), an exploration engine for antibiotic cluster prioritization and novel drug target discovery. *Nucleic Acids Research* 45, W42-W48.

71) Zhou H, Zhan J, Watanabe K, Xie X, and Tang Y (2008) A polyketide macrolactone synthase from the filamentous fungus Gibberella zeae. *Proc Natl Acad Sci U S A* 105(17), 6249-54

72) Kuttikrishnan S, Prabhu KS, Sharie AHA, Al Zu'bi YO, Alali FQ, Oberlies NH,Ahmad A, El-Elimat T, and Uddin S (2022) Natural resorcylic acid lactones: A chemical biology approach for anticancer activity.

Drug Discovery Today 27(2),547-557

73) DELMOTTE P and DELMOTTE-PLAQUEE J (1953) A New Antifungal Substance of Fungal Origin. *Nature* 171, 344

74) Shen W, Mao H, Huang Q, and Dong J (2015) Benzenediol lactones: a class of fungal metabolites with diverse structural features and biological activities.

European Journal of Medicinal Chemistry 97, 747-777

75) Bang S, Shim SH (2020) Beta resorcylic acid lactones (RALs) from fungi: chemistry, biology, and biosynthesis. *Arch. Pharm. Res.* 43, 1093–1113

76) Wang M, Zhou H, Wirz M, Tang Y, and Boddy CN (2009) A Thioesterase from an Iterative Fungal Polyketide Synthase Shows Macrocyclization and Cross Coupling Activity and May Play a Role in Controlling Iterative Cycling through Product Offloading. *Biochemistry* 48, 6288–6290

77) Heberlig GW, Wirz M, Weng M, and Boddy CN (2014) Resorcylic Acid Lactone Biosynthesis Relies on a Stereotolerant Macrocyclizing Thioesterase. *Org. Lett* 16, 5858–5861.

78) Okorafor IC, Chen M, and Tang Y (2021) High-Titer Production of Olivetolic Acid and Analogs in Engineered Fungal Host Using a Nonplant Biosynthetic Pathway. *ACS Synth Biol.* 10(9), 2159-2166

79) Zabala AO, Chooi YH, Choi MS, Lin HC, and Tang Y (2014) Fungal polyketide synthase product chain-length control by partnering thiohydrolase. *ACS Chem Biol.* 9(7),1576-86

80) Cheng YQ, Coughlin JM, Lim SK, and Shen B (2009) Type I polyketide synthases that require discrete acyltransferases. *Methods Enzymol.* 459,165-86.

81) Chen H, and Du L (2016) Iterative polyketide biosynthesis by modular polyketide synthases in bacteria. *Appl Microbiol Biotechnol.* 100(2),541-57.

82) Grininger M (2020) The role of the iterative modules in polyketide synthase evolution. *Proc Natl Acad Sci U S A.* 117(16), 8680-8682

83) Meurer G, Gerlitz M, Wendt-Pienkowski E, Vining LC, Rohr J, and Hutchinson CR (1997) Iterative type II polyketide synthases, cyclases and ketoreductases exhibit context-dependent behavior in the biosynthesis of linear and angular decapolyketides. *Chem Biol.* 4(6), 433-43.

84) Seow KT, Meurer GU, Gerlitz MA, Wendt-Pienkowski EV, Hutchinson CR, and Davies JU (1997) A study of iterative type II polyketide synthases, using bacterial genes cloned from soil DNA: a means to access and use genes from uncultured microorganisms. *Journal of Bacteriology* 179(23),7360-8.

85) Katsuyama Y and Ohnishi Y (2012) Type III polyketide synthases in microorganisms. *Methods Enzymol.* 515, 359-77

86) Yu D, Xu F, Zeng J, and Zhan J (2012) Type III polyketide synthases in natural product biosynthesis. *IUBMB life* 64(4),285-95.

87) Hayashi T, Kitamura Y, Funa N, Ohnishi Y, and Horinouchi S (2011) Fatty Acyl-AMP Ligase Involvement in the Production of Alkylresorcylic Acid by a *Myxococcus xanthus* Type III Polyketide Synthase. *ChemBioChem* 12(14), 2166-76.

88) Cox RJ (2007) Polyketides, proteins and genes in fungi: Programmed nano-machines begin to reveal their secrets *Org Biomol Chem* 5, 2010–2026

89) Crawford JM, Dancy BC, Hill EA, Udwary DW, and Townsend CA (2006) Identification of a starter unit acyl-carrier protein transacylase domain in an iterative type I polyketide synthase. *Proc Natl Acad Sci USA* 103, 16728–16733

90) Fujii I, Watanabe A, Sankawa U, and Ebizuka Y (2001) Identification of Claisen cyclase domain in fungal polyketide synthase WA, a naphthopyrone synthase of *Aspergillus nidulans*. *Chem Biol* 8, 189–197

91) Ma SM, Zhan J, Xie X, Watanabe K, Tang Y, and Zhang W (2008) Redirecting the cyclization steps of fungal polyketide synthase. *J Am Chem Soc* 130, 38–39

92) Ma SM, Zhan J, Watanabe K, Xie X, Zhang W, Wang CC, and Tang Y (2007) Enzymatic synthesis of aromatic polyketides using PKS4 from Gibberella fujikuroi. *J Am Chem Soc*. 129(35),10642-3

93) Soehano I, Yang L, Ding F, Sun H, Low ZJ, Liu X, and Liang ZX (2014) Insights into the programmed ketoreduction of partially reducing polyketide synthases: stereo- and substrate-specificity of the ketoreductase domain. *Org Biomol Chem* 12(42),:8542-9.

94) Moriguchi T, Ebizuka Y, and Fujii I (2008). Domain-Domain Interactions in the Iterative Type I Polyketide Synthase ATX from Aspergillus terreus. *Chembiochem : a European journal of chemical biology* 9,1207-12

95) Liu T, Sanchez JF, Chiang YM, Oakley BR, and Wang CC (2014) Rational domain swaps reveal insights about chain length control by ketosynthase domains in fungal nonreducing polyketide synthases. *Organic letters* 16(6),1676-9.

96) Ismed F, Farhan A, Bakhtiar A, Zaini E, Nugraha YP, Dwichandra PO, and Uekusa H (2016) Crystal structure of olivetolic acid: a natural product from *Cetrelia sanguinea (Schaer.). Acta Crystallographica Section E: Crystallographic Communications* 72(11),1587-9.

97) Xu W, Chooi YH, Choi JW, Li S, Vederas JC, Da Silva NA, and Tang Y (2013) LovG: the thioesterase required for dihydromonacolin L release and lovastatin nonaketide synthase turnover in lovastatin biosynthesis. *Angew. Chem. Int. Ed. Engl* 52, 6472–6475.

98) Weber T, Blin K, Duddela S, Krug D, Kim HU, Bruccoleri R, Lee SY, Fischbach MA, Müller R, Wohlleben W, Breitling R, Takano E, and Medema MH (2015) antiSMASH 3.0-a comprehensive resource for the genome mining of biosynthetic gene clusters. *Nucl. Acids Res* 43, W237–243

99) Keating DH, Carey MR, and Cronan JE Jr (1995) The unmodified (apo) form of Escherichia *coli* acyl carrier protein is a potent inhibitor of cell growth. *J. Biol. Chem* 270, 22229–22235

100) Flugel RS, Hwangbo Y, Labalot RH, Cronan JE Jr., and Walsh CT (2000) Holo-(acyl carrier protein) synthase and phosphopantetheinyl transfer in *Escherichia coli*. *J. Biol. Chem* 275, 959–968.

101) Crawford JM, Vagstad AL, Ehrlich KC, Udwary DW, and Townsend CA (2008) Acyl-carrier protein-phosphopantetheinyltransferase partnerships in fungal fatty acid synthases. *ChemBioChem* 9, 1559–1563.

102) Chen M, Liu Q, Gao SS, Young AE, Jacobsen SE, and Tang Y (2019) Genome mining and biosynthesis of a polyketide from a biofertilizer fungus that can facilitate reductive iron assimilation in plant. *Proc. Natl. Acad. Sci. U S A* 116, 5499–5504.

103) Liu N, Hung YS, Gao SS, Hang L, Zou Y, Chooi YH, and Tang Y (2017) Identification and Heterologous Production of a Benzoyl-Primed Tricarboxylic Acid Polyketide Intermediate from the Zaragozic Acid A Biosynthetic Pathway. *Org. Lett* 19, 3560–3563.

104) Papagianni M (2007) Advances in citric acid fermentation by Aspergillus niger: Biochemical aspects, membrane transport and modeling. *Biotechnol. Adv* 25, 244–263.

105) Citti C, Linciano P, Russo F, Luongo L, Iannotta M, Maione S, Laganà A, Capriotti AL, Forni F, Vandelli MA, Gigli G, and Cannazza G (2019) A novel phytocannabinoid isolated from *Cannabis sativa* L. with an *in vivo* cannabimimetic activity higher than Δ9-tetrahydrocannabinol: Δ9-Tetrahydrocannabiphorol." *Scientific Reports* 9, 20355.

106) Hitchman TS, Schmidt EW, Trail F, Rarick MD, Linz JE, and Townsend CA (2001) Hexanoate Synthase, a Specialized Type I Fatty Acid Synthase in Aflatoxin B1 Biosynthesis." *Bioorg. Chem* 29, 293–307.

107) Brown BW, Yu JH, Kelkar HS, Fernandes M, Nesbitt TC, Keller NP, Adams TH, and Leonard TJ (1996) Twenty-five coregulated transcripts define a sterigmatocystin gene cluster in *Aspergillus nidulans*. *Proc. Natl. Acad. Sci. U S A* 93, 1418–1422.

108) Liu T, Chiang YM, Somoza AD, Oakley BR, and Wang CCC (2011) Engineering of an "Unnatural" Natural Product by Swapping Polyketide Synthase Domains in *Aspergillus nidulans*. *J. Am. Chem. Soc* 133, 13314–13316.

109) Zhang W and Tang Y (2008) Combinatorial Biosynthesis of Natural Products. *J. Med. Chem* 51, 2629–2633.

110) Crawford JM, Dancy BCR, Hill EA, Udwary DW, and Townsend CA (2006) Identification of a starter unit acyl-carrier protein transacylase domain in an iterative type I polyketide synthase. *Proc. Natl. Acad. Sci. U S A* 103, 16728–16733.

111) Xu Y, Zhou T, Zhang S, Espinosa-Artiles P, Wang L, Zhang W, Lin M, Gunatilaka AAL, Zhan J, and Molnár I (2014) Diversity-oriented combinatorial biosynthesis of benzenediol lactone scaffolds by subunit shuffling of fungal polyketide synthases. *Proc. Natl. Acad. Sci. U S A* 111, 12354–12359.

112) Bai J, Lu Y, Xu YM, Zhang W, Chen M, Lin M, Gunatilaka AAL, Xu Y, and Molnár I (2016). Diversity-Oriented Combinatorial Biosynthesis of Hybrid Polyketide Scaffolds from Azaphilone and Benzenediol Lactone Biosynthons. *Org. Lett* 18, 1262–1265.

113) Lussier FX, Colatriano D, Wiltshire Z, Page JE, and Martin VJ (2012) Engineering microbes for plant polyketide biosynthesis. *Computational and Structural Biotechnology Journal* 3(4)

114) Ahsan T, Chen J, Wu Y, and Irfan M (2017) Application of response surface methodology for optimization of medium components for the production of secondary metabolites by *Streptomyces diastatochromogenes KX852460*. *AMB Express* 7,1-10.

115) Colla LM, Primaz AL, Benedetti S, Loss RA, Lima MD, Reinehr CO, Bertolin TE, and Costa JA (2016) Surface response methodology for the optimization of lipase production under submerged fermentation by filamentous fungi. *Brazilian Journal of Microbiology* 47,461-7.

116) Su Y, Zhang X, Hou Z, Zhu X, Guo X, and Ling P (2011) Improvement of xylanase production by thermophilic fungus Thermomyces lanuginosus SDYKY-1 using response surface methodology. *New biotechnology* 28(1),40-6.

117) Levin L, Herrmann C, and Papinutti VL (2008) Optimization of lignocellulolytic enzyme production by the white-rot fungus Trametes trogii in solid-state fermentation using response surface methodology. *Biochemical Engineering Journal.* 39(1), 207-14.

118) Weissman SA and Anderson NG (2015) Design of experiments (DoE) and process optimization. A review of recent publications. *Organic Process Research & Development*. 19(11),1605-33.

119) Anderson MJ and Whitcomb PJ (200) Design of experiments. *Kirk-Othmer Encyclopedia of Chemical Technology* 4, 1-22.

120) Vazquez AR, Schoen ED, and Goos P (2022 Two-level orthogonal screening designs with 80, 96, and 112 runs, and up to 29 factors. *Journal of Quality Technology* 54(3),338-58.

121) Sibanda W and Pretorius P (2011) Application of two-level fractional factorial design to determine and optimize the effect of demographic characteristics on HIV prevalence using the 2006 South African annual antenatal HIV and syphilis seroprevalence data. *International Journal of Computer Applications*. 35(12),15-20.

122) Cotter SC (1979) A screening design for factorial experiments with interactions. *Biometrika* 66(2),317-20.

123) Pantoja YV, Ríos AJ, and Tapia Esquivias M (2019) A method for construction of mixed-level fractional designs. *Quality and Reliability Engineering International* 35(6),1646-65.

124) Vanaja K and Shobha Rani RH (2007) Design of experiments: concept and applications of Plackett Burman design. *Clinical research and regulatory affairs*. 24(1),1-23.

125) St L and Wold S (1989) Analysis of variance (ANOVA). *Chemometrics and intelligent laboratory systems* 6(4),259-72.

126) Livingston EH (2004) Who was student and why do we care so much about his t-test? *Journal of Surgical Research* 118(1),58-65.

127) Dong C, Davies IJ, Fornari Junior CC, and Scaffaro R (2017) Mechanical properties of Macadamia nutshell powder and PLA bio-composites. *Australian Journal of Mechanical Engineering*. 2017 Sep 2;15(3):150-6.

128) Li A, Pfelzer N, Zuijderwijk R, and Punt P (2012) Enhanced itaconic acid production in Aspergillus niger using genetic modification and medium optimization. *BMC biotechnology* 12,1-9.

129) Bezerra MA, Santelli RE, Oliveira EP, Villar LS, and Escaleira LA (2008) Response surface methodology (RSM) as a tool for optimization in analytical chemistry. *Talanta* 76(5),965-77.

130) Rakić T, Kasagić-Vujanović I, Jovanović M, Jančić-Stojanović B, and Ivanović D (2014) Comparison of full factorial design, central composite design, and box-behnken design in chromatographic method development for the determination of fluconazole and its impurities. *Analytical Letters* 47(8),1334-47.

131) Talukdar S, Talukdar M, Buragohain M, Yadav A, Yadav RN, and Bora TC (2016) Enhanced candicidal compound production by a new soil isolate Penicillium verruculosum MKH7 under submerged fermentation. *BMC microbiology* 16(1), 1-2.

132) Chaichanan J, Wiyakrutta S, Pongtharangkul T, Isarangkul D, and Meevootisom V (2014) Optimization of zofimarin production by an endophytic fungus, Xylaria sp. Acra L38. *Brazilian Journal of Microbiology* 45,287-93.

133) Bhattacharya S (2021) Central composite design for response surface methodology and its application in pharmacy. *Response surface methodology in engineering science*.

134) Ngan CL, Basri M, Lye FF, Masoumi HR, Tripathy M, Karjiban RA, and Abdul-Malek E (2014) Comparison of Box–Behnken and central composite designs in optimization of fullerene loaded palm-based nano-emulsions for cosmeceutical application. *Industrial Crops and Products* 59,309-17.

135) Shi S, Chen Y, Siewers V, and Nielsen J (2014) Improving production of malonyl coenzyme A-derived metabolites by abolishing Snf1-dependent regulation of Acc1. *MBio* 5(3), e01130-14.

136) Hubbard RD and Fidanze S (2007) Therapeutic areas II: cancer, infectious diseases, inflammation and immunology and dermatology. *Comprehensive Medicinal Chemistry II*

137) Anderson LL, Udoh M, Everett-Morgan D, Heblinski M, McGregor IS, Banister SD, and Arnold JC (2022) Olivetolic acid, a cannabinoid precursor in Cannabis sativa, but not CBGA methyl ester exhibits a modest anticonvulsant effect in a mouse model of Dravet syndrome. *Journal of Cannabis Research*. 4(1),1-9.

138) Lee YE, Kodama T, and Morita H (2023) Novel insights into the antibacterial activities of cannabinoid biosynthetic intermediate, olivetolic acid, and its alkyl-chain derivatives. *Journal of Natural Medicines* 77(2),298-305.

139) Citti C, Linciano P, Russo F, Luongo L, Iannotta M, Maione S, Laganà A, Capriotti AL, Forni F, Vandelli MA, and Gigli G (2019) A novel phytocannabinoid isolated from Cannabis sativa L. with an in vivo cannabimimetic activity higher than Δ9-tetrahydrocannabinol: Δ9-Tetrahydrocannabiphorol. *Scientific reports* 9(1), 1-3.

140) Sherman DH (2005) The Lego-ization of polyketide biosynthesis. *Nature biotechnology* 23(9),1083-4.

141) Johansson P, Wiltschi B, Kumari P, Kessler B, Vonrhein C, Vonck J, Oesterhelt D, and Grininger M (2008) Inhibition of the fungal fatty acid synthase type I multienzyme complex. *Proceedings of the National Academy of Sciences* 105(35),12803-8.

142) Zhu Z, Zhou YJ, Krivoruchko A, Grininger M, Zhao ZK, and Nielsen J (2017) Expanding the product portfolio of fungal type I fatty acid synthases. *Nature chemical biology* 13(4),360-2.

143) Gajewski J, Buelens F, Serdjukow S, Janßen M, Cortina N, Grubmüller H, and Grininger M (2017) Engineering fatty acid synthases for directed polyketide production. *Nature Chemical Biology* 13(4),363-5.

144) Living Biofoundry. Biopacificmip.org. https://biopacificmip.org/platform/instrumentation/living-biofoundry

145) NSF Pacific MIP. https://biopacificmip.org/

146) Russo EB, Cuttler C, Cooper ZD, Stueber A, Whiteley VL, and Sexton M (2022) Survey of patients employing cannabigerol-predominant cannabis preparations: Perceived medical effects, adverse events, and withdrawal symptoms. *Cannabis and Cannabinoid Research* 7(5),706-16.

147) Anokwuru CP, Makolo FL, Sandasi M, Tankeu SY, Elisha IL, Agoni C, Combrinck S, and Viljoen A (2022) Cannabigerol: a bibliometric overview and review of research on an important phytocannabinoid. *Phytochemistry Reviews* 21(5), 1523-47.

148) Navarro G, Varani K, Reyes-Resina I, Sanchez de Medina V, Rivas-Santisteban R, Sanchez-Carnerero Callado C, Vincenzi F, Casano S, Ferreiro-Vera C, Canela EI, and Borea PA (2018) 9,632 Cannabigerol action at cannabinoid CB1 and CB2 receptors and at CB1–CB2 heteroreceptor complexes. *Frontiers in pharmacology*

149) Mechoulam R (1970) Marihuana Chemistry: Recent advances in cannabinoid chemistry open the area to more sophisticated biological research. Science 168(3936),1159-66.

150) Kuzuyama T, Noel JP, and Richard SB (2005) Structural basis for the promiscuous biosynthetic prenylation of aromatic natural products. *Nature* 435(7044),983-7.

151) Cheng W, and Li W (2014) Structural insights into ubiquinone biosynthesis in membranes. *Science* 343(6173), 878-81.

152) Huang H, Levin EJ, Liu S, Bai Y, Lockless SW, and Zhou M (2014) Structure of a membrane-embedded prenyltransferase homologous to UBIAD1. *PLoS biology* 12(7),e1001911.

153) Yu X and Li SM (2012) Prenyltransferases of the dimethylallyltryptophan synthase superfamily. *Methods in Enzymology* 516,259-278.

154) Yu X, Liu Y, Xie X, Zheng XD, and Li SM (2012) Biochemical characterization of indole prenyltransferases: filling the last gap of prenylation positions by a 5-dimethylallyltryptophan synthase from Aspergillus clavatus. *Journal of Biological Chemistry*. 287(2),1371-80.

155) Winkelblech J, Fan A, and Li SM (2015)/ Prenyltransferases as key enzymes in primary and secondary metabolism. *Applied microbiology and biotechnology* 99, 7379-97.

156) Tello M, Kuzuyama T, Heide L, Noel JP, and Richard S (2008) The ABBA family of aromatic prenyltransferases: broadening natural product diversity. Cellular and molecular life sciences 65(10),1459.

157) Zirpel B, Degenhardt F, Martin C, Kayser O, and Stehle F (2017) Engineering yeasts as platform organisms for cannabinoid biosynthesis. *Journal of biotechnology* 259, 204-12.

158) Chooi YH, Wang P, Fang J, Li Y, Wu K, Wang P, and Tang Y (2012) Discovery and characterization of a group of fungal polycyclic polyketide prenyltransferases. Journal of the American Chemical Society. 134(22):9428-37.

159) Blatt-Janmaat K and Qu Y (2021) The biochemistry of phytocannabinoids and metabolic engineering of their production in heterologous systems. *International Journal of Molecular Sciences* 22(5), 2454.

160) Araki Y, Awakawa T, Matsuzaki M, Cho R, Matsuda Y, Hoshino S, Shinohara Y, Yamamoto M, Kido Y, Inaoka DK, and Nagamune K (2019) Complete biosynthetic pathways of ascofuranone and ascochlorin in Acremonium egyptiacum. *Proceedings of the National Academy of Sciences* 116(17),8269-74.

161) Sanchez JF, Chiang YM, Szewczyk E, Davidson AD, Ahuja M, Oakley CE, Bok JW, Keller N, Oakley BR, and Wang CC (2010) Molecular genetic analysis of the orsellinic acid/F9775 gene cluster of Aspergillus nidulans. *Molecular Biosystems* 6(3),587-93.

162) Krogh A, Larsson B, Von Heijne G, and Sonnhammer EL (2001) Predicting transmembrane protein topology with a hidden Markov model: application to complete genomes. *Journal of molecular biology* 305(3),567-80.

163) Goldstein JL and Brown MS (1990) Regulation of the mevalonate pathway. *Nature* 343(6257),425-30.

164) Dimou S, Georgiou X, Sarantidi E, Diallinas G, and Anagnostopoulos AK (2021) Profile of membrane cargo trafficking proteins and transporters expressed under N source derepressing conditions in *Aspergillus nidulans*. *Journal of Fungi* 7(7),560.

165) Feldheim D, Rothblatt J, and Schekman R (1992) Topology and functional domains of Sec63p, an endoplasmic reticulum membrane protein required for secretory protein translocation. *Molecular and cellular biology* 12(7), 3288-96.

166) van der Klei IJ and Veenhuis M (2006) PTS1-independent sorting of peroxisomal matrix proteins by Pex5p. *Biochimica et Biophysica Acta (BBA)-Molecular Cell Research*. 1763(12),1794-800.

167) Cokol M, Nair R, and Rost B (2000) Finding nuclear localization signals. *EMBO reports* 1(5),411-5.

168) Da Silva Ferreira ME, Colombo AL, Paulsen I, Ren Q, Wortman J, Huang J, Goldman MH, and Goldman GH (2005) The ergosterol biosynthesis pathway, transporter genes, and azole resistance in *Aspergillus fumigatus*. *Medical Mycology* 43,S313-9.

169) Soid-Raggi G, Sánchez O, Aguirre J (2006) TmpA, a member of a novel family of putative membrane flavoproteins, regulates asexual development in *Aspergillus nidulans*. *Molecular microbiology* 59(3),854-69.

170) Sirikantaramas S, Morimoto S, Shoyama Y, Ishikawa Y, Wada Y, Shoyama Y, and Taura F (2004) The gene controlling marijuana psychoactivity: molecular cloning and heterologous expression of Δ1-tetrahydrocannabinolic acid synthase from Cannabis sativa L. *Journal of Biological Chemistry* 279(38),39767-74.

171) van Velzen R and Schranz ME (2021) Origin and evolution of the cannabinoid oxidocyclase gene family. *Genome Biology and Evolution* 13(8), evab130.

172) Sirikantaramas S, Taura F, Tanaka Y, Ishikawa Y, Morimoto S, and Shoyama Y (2005) Tetrahydrocannabinolic acid synthase, the enzyme controlling marijuana psychoactivity, is secreted into the storage cavity of the glandular trichomes. *Plant and Cell Physiology* 46(9),1578-82.

173) Rodziewicz P, Loroch S, Marczak Ł, Sickmann A, and Kayser O (2019) Cannabinoid synthases and osmoprotective metabolites accumulate in the exudates of Cannabis sativa L. glandular trichomes. *Plant Science* 284,108-16.

174) Morimoto S, Komatsu K, Taura F, and Shoyama Y (1998) Purification and characterization of cannabichromenic acid synthase from Cannabis sativa. *Phytochemistry* 49(6),1525-9.

175) Tahir MN, Shahbazi F, Rondeau-Gagné S, and Trant JF (2021) The biosynthesis of the cannabinoids. *Journal of cannabis research* 3(1),1-2.

176) Thakkar K, Ruan CH, and Ruan KH (2021) Recent advances of cannabidiol studies in medicinal chemistry, pharmacology and therapeutics. *Future Medicinal Chemistry* 13(22),1935-7.

177) Zirpel B, Degenhardt F, Zammarelli C, Wibberg D, Kalinowski J, Stehle F, and Kayser O (2018) Optimization of Δ9-tetrahydrocannabinolic acid synthase production in Komagataella phaffii via post-translational bottleneck identification. *Journal of biotechnology* 272, 40-7.